1957

Relative apparent molal heat contents of some rare-earth chlorides and nitrates in aqueous solutions

Robert Eugene Eberts
Iowa State College

RELATIVE APPARENT MOLAL HEAT CONTENTS OF SOME RARE-EARTH CHLORIDES AND NITRATES IN AQUEOUS SOLUTIONS

by

Robert Eugene Eberts

A Dissertation Submitted to the
Graduate Faculty in Partial Fulfillment of
The Requirements for the Degree of
DOCTOR OF PHILOSOPHY

Major Subject: Physical Chemistry

Approved:

Signature was redacted for privacy.
In Charge of Major Work

Signature was redacted for privacy.
Head of Major Department

Signature was redacted for privacy.
Dean of Graduate College

Iowa State College
1957

TABLE OF CONTENTS

I. INTRODUCTION

Thermodynamics is the science which concerns itself with temperature and heat. It furnishes the laws governing changes of energy from one form to another and from one system to another. Likewise, these laws govern the chemical and physical transformations of matter. Thermochemistry is the study of the thermal effects which accompany chemical reactions, changes of state and the formation of solutions. This study will be concerned with the thermal effects accompanying changes in aqueous solutions.

Solutions of electrolytes in water are the most common type of solution found in nature. Moreover, due to the wide use of water as a reaction and purification media, they are frequently encountered in industry. Thus, they are of great interest to the chemist in the laboratory from a practical, as well as theoretical, standpoint.

In studying electrolytic solutions, one makes measurements of the solution as a whole. From these macroscopic measurements, one tries to deduce the microscopic properties of the solution. One would particularly like to determine the species present in solution, the effect ions have on one another, and the effect they have on solvent molecules.

Various theories have been proposed which attempt to predict the properties of solutions. While some success has been achieved for very dilute solutions, deviations from

these theoretical predictions manifest themselves as the concentration is increased, especially for the higher charged ions. These theories take into account such variables as the charge on the ions, the size of the ions, the dielectric constant of the solvent, the degree of solvation of the ions, the amount of association of the ions and the temperature and pressure.

Ideally, one would like to hold all of the variables constant, save one. Specifically, one would vary the size of one ion, i.e., the cation, in a regular manner, while keeping the other variables constant. In this way the effect of the size of the cation on various properties could be isolated.

The lanthanide elements are the closest to an idealized system of varying ionic size that nature has provided. The chemical properties of the fifteen elements from lanthanum to lutetium are quite similar; their usual valence state is three; and they form soluble salts with strong acids. As the atomic number increases down the series, the additional electrons fall into the 4f orbital. Since this orbital is well shielded, these electrons contribute little to the chemical properties of the rare earths. The increasing nuclear charge tends to pull the electronic cloud inward, resulting in a gradual decrease in ionic size. The rare earths are usually present in solution as tripositive ions. Thus, they also provide a strenuous test to theoretical predictions

of charge effects, which are usually based on a charge-squared term.

Besides these theoretical considerations, it is desirable to study the properties of rare earth salt solutions for practical reasons. Commercial interest in the rare earths is increasing now that the rare earths are becoming available in large quantities and in high purity. A knowledge of their fundamental chemical and physical properties will be required to utilize these elements industrially. The lanthanides also appear as fission products of nuclear reactions. With the advent of nuclear power reactors, a knowledge of the properties of these elements in solution is needed. There seems little doubt that the rare earth elements will assume greater commercial importance in the future.

Because of the similarity of their aqueous chemistry, the individual elements were not, until the past ten years, available in the amounts and purity required for extensive experimental study. The separation of the individual elements on a large scale has been accomplished mainly through the ion exchange techniques developed at the Ames Laboratory (1, 2, 3, 4, 5, 6, 7, 8, 9, 10, 11, 12). An extensive program was initiated at this laboratory for the study of the physical and chemical properties of the rare earth metals and their compounds. A part of this program was a study of the properties of aqueous solutions of the soluble rare earth salts.

Data have been collected by the Ames Laboratory on the

conductances, transference numbers, and activity coefficients (13, 14, 15, 16, 17, 18, 19, 20, 21) of a large number of rare-earth salts; heats of solution (22, 23) of eight rare-earth chlorides have been reported. Work has also been done on partial molal volumes (24) and partial molal compressibilities (25) of some chlorides and nitrates, and on the heats of dilution (26) of two chlorides. This work has recently been reviewed by Spedding and Atkinson (27).

The values for the activity coefficients, conductances and partial molal volumes are in agreement with the theoretical limiting values predicted by the Debye-Huckel theory. Deviations from theoretical values occurred as low as 0.01 molal in the case of the latter two. The transference numbers and partial molal compressibilities are linear functions of the square root of the concentration, but the slopes in the range measured are considerably different from those predicted by theory for infinitely dilute solutions.

The above measurements also seem to indicate that the rare earths, in solution, may consist of two distinct groups. The difference between the lighter and heavier rare earths appears to be caused by a change in the degree of hydration of the ions, or by the formation of some species due to hydrolysis. This point is somewhat disconcerting, since our "ideal" series of elements of changing ionic size has broken into two shorter series. On the other hand, this phenomenon may show how and why similar ions differ in solution.

for lanthanum chloride, neodymium chloride and erbium chloride solutions, from heat of dilution measurements, were very nearly the same for concentrations above 0.2 molal. However, the results below 4×10^{-4} molal were quite different for the four salts.

In the light of the differences in the very dilute range, it was deemed advisable to extend the heat of dilution measurements to other 3-1 salts. This report gives data for four salts: lanthanum chloride, ytterbium chloride, lanthanum nitrate, and ytterbium nitrate. The data for lanthanum chloride and lanthanum nitrate were run both as a check on the data obtained in this laboratory and to extend the data to higher concentrations. Ytterbium chloride was chosen to determine whether its limiting behavior would resemble that of erbium chloride. The nitrates were run to see if the data for these salts would show a greater degree of specificity than the chlorides, as has been observed in the case of lower valence type salts.

There is a drastic disagreement in the $\underline{\phi_L}$ values for neodymium chloride. Spedding and Miller (22) calculated their $\underline{\phi_L}$'s from the integral heat of solution of anhydrous $NdCl_3$; Naumann (26) derived his values from the heats of dilution of $NdCl_3$ solutions. Measurements are reported here on the heat of solution of $NdCl_3 \cdot 6H_2O$. This work was done in an attempt to explain the discrepancy between the two sets of data.

II. HISTORICAL BACKGROUND

A. Calorimetric Methods

1. General

Calorimetric determinations of quantities of heat are very often based on the measurement of temperature or temperature differences. In the past hundred years, calorimetry has progressed from rather crude measurements to a very exacting science. This progress has followed improvements in thermometry, temperature control, measurement of electrical energy, and evaluation of corrections to the "raw" data. The great impetus for these improvements has been the far reaching developments in thermodynamics, especially the contributions of J. W. Gibbs and of G. N. Lewis and M. Randall.

Space does not permit even a moderately extensive survey of the methods and measurements in the widely diversified field of calorimetry. For more complete treatments of the subject, the reader is referred to White (31), particularly for the theory, Sturtevant (32), especially as applied to organic chemistry, Swietoslawski (33) for microcalorimetry, and to Rossini (34) for bomb calorimetry. A general review of the methods and measurements will be limited to those applying to the present work.

2. Types of calorimeters

The calorimeters used for measurements of heats of solution and heats of dilution can be divided into three groups: the isothermally jacketed, the adiabatically jacketed, and the twin or differential types.

An isothermally jacketed calorimeter is one surrounded by a constant temperature "jacket", which is usually a large reservoir of water. The apparatus is fairly simple to construct. However, the heat leakage into and out from the calorimeter must be accurately measured; and the calculation of such heat leakage corrections becomes an involved and tedious task. Accurate methods for the calculation of these corrections have been developed by several authors (31, 35, 36, 37). Isothermally jacketed calorimeters are best suited for reactions liberating large quantities of heat in relatively short periods of time.

The adiabatically jacketed calorimeter is surrounded by a "jacket" which is maintained at the same temperature as the calorimeter. This type has several advantages, all involving the heat leakage. By keeping the thermal head between the jacket and calorimeter as small as possible, one reduces any heat leakage corrections to a minimum. The disadvantage arises in the mechanics of keeping the system truly adiabatic. The adiabatic method is preferred for the measurement of small quantities of heat and for processes of long duration.

The advantage of using twin calorimeters depends upon

keeping the two "halves" at the same temperature. They are usually placed side by side in the same jacket so that the heat leakage into each will be identical. Here it is possible to make maximum use of thermocouples to determine the temperature differential between the containers. This type has been particularly adapted to short duration processes involving small quantities of heat.

By employing a system of twin calorimeters in an adiabatic jacket, one hopes to eliminate the need for any heat leakage correction. The big disadvantage to such a method is the need for a rather complicated and carefully designed apparatus.

The apparatus used in this work for measuring heats of solution was an isothermally jacketed calorimeter. The heats of dilution were measured in an adiabatically jacketed, differential calorimeter. Such small quantities of heat were involved that it was also practically an isothermal calorimeter.

B. Electrolytic Solutions

The modern idea of the nature of electrolytic solutions had its conception in the ionization theory of Arrhenius (38). His idea of the electrolytic dissociation of solute molecules into ions was confirmed by the contemporary work of van't Hoff (39). From this beginning, explanations of the behavior of electrolytic solutions have relied upon the consideration

of the forces of attraction between the ions present in the solution. Harned and Owen (40, p. 17) have aptly summarized the early development of the modern theory of ionic solutions:

> ....It has been suspected for a long time that the behavior of strong electrolytes in dilute solution could be accounted for by the hypothesis of complete dissociation and an adequate consideration of the effects of interionic attraction. Sutherland, Noyes, and particularly Bjerrum were among the first to adopt this point of view. Before this van Laar had emphasized the importance of electrostatic forces in explaining the characteristics of ionic solutions. Hertz and Ghosh attempted to give the effects of interionic attraction mathematical expression, but the basis of their treatments proved to be inadequate. Milner successfully analyzed the problem, but his mathematical treatment was exceedingly involved and did not yield an entirely satisfactory result.

Since 1923, the field of electrolytic solutions has been dominated by the interionic attraction theory of Debye and Huckel (28). The basic assumptions inherent in their theory have been critically analyzed by Kirkwood (41) and by Fowler and Guggenheim (42). These assumptions can be summarized as follows:

(a) The electrolyte is completely dissociated into ions.

(b) Deviations from ideality are due entirely to coulombic interactions between ions.

(c) The solvent is a continuous medium of dielectric constant, D, which is independent of the solute present.

(d) The ions are rigid spheres, having a mean distance of closest approach; they occupy a negligible volume

of space in the solvent.

(e) The electrical potential, ψ, at a point in the solution can be calculated by a combination of Poisson's equation and the Boltzmann distribution function.

(f) The Poisson-Boltzmann differential equation converges such that terms higher than the second can be neglected.

(g) The principle of the linear superposition of fields is valid.

Using these assumptions Debye and Hückel developed a mathematical expression for the rational activity coefficient. In the limit of infinite dilution, this results in the logarithum of the activity coefficient being proportional to the square root of the concentration, that is,

$$\log f_{\pm} = -S_{(f)}\Gamma^{\frac{1}{2}} \quad . \tag{1}$$

When the theory is extended to take in the effect of the apparent diameters of the ions, the limiting law becomes

$$\log f_{\pm} = \frac{-S_{(f)}\Gamma^{\frac{1}{2}}}{1 + A\Gamma^{\frac{1}{2}}} \quad . \tag{2}$$

In the above expressions,

$f_{\pm}$ = the mean rational activity coefficient;

$$S_{(f)} = \frac{1}{\nu} \sum_{i=1}^{n} \frac{\nu_j z_j^2}{2.303} \left[\frac{\pi N \epsilon^6}{1000\,(DkT)^3}\right]^{\frac{1}{2}} ;$$

$$\Gamma = \sum_{i=1}^{n} c_i z_i^2 = \text{ional concentration} ;$$

$$A = \frac{a^{\circ} K}{\Gamma^{\frac{1}{2}}} \quad ;$$

$$K = \left[\frac{4\pi \epsilon^2 N}{1000\, DkT}\right]^{\frac{1}{2}} \Gamma^{\frac{1}{2}} \quad ;$$

where ν is the number of ions into which the electrolyte dissociates; ν_j, the number of j-ions produced in the dissociation; z_j, the charge on the jth species; N, Avogadro's number; ϵ, the electronic charge; k, Boltzmann's constant; D, the dielectric constant of the solvent; c_i, the concentration of the ith species in moles per liter; and a°, the mean distance of closest approach. It should be noted that a° is the only adjustable parameter present in the original theory. A derivation of this theory is reserved for a later section.

The Debye-Hückel theory has been used as a cornerstone for most of the developments made since its publication. Since the theory is successful only for very dilute solutions, many attempts have been made to extend it to higher concentrations. These extensions of the theory usually attempt to modify, circumvent, or eliminate one or more of the basic assumptions. When these simplifying assumptions are changed, the mathematical procedures often become discouragingly involved. Another disappointing factor in the extensions is that they often lead to extra adjustable parameters, which are incapable of independent evaluation. A brief summary of some of these modifications is given here.

Bjerrum (43) has proposed a theory of ion pair formation,

which in essence modifies assumption (a). Fuoss and Kraus (44) have extended the theory to triple ions and quadrupoles. Bjerrum's theory is based on replacing the potential energy function in the Maxwell-Boltzmann distribution law by the simple Coulomb law. The resulting probability that an i-ion is at a distance r from a j-ion has a minimum at r = q. It is assumed that two ions within a distance q of each other are associated. The unassociated ions then obey the Debye-Hückel predictions. This treatment has been applied mainly to mixed solvents having low dielectric constants.

Robinson and Stokes (45, 46) have modified assumption (b) by taking into account ion-solvent interactions. They suggest that the Debye-Huckel theory actually predicts the mean rational activity coefficient of solvated ions. In considering the solution to consist of solvated ions dissolved in solvent, they differentiate between "free" and "solvated" solvent molecules. Glueckauf (47) has modified this treatment by using volume-fraction (instead of mole fraction) statistics. While these equations are capable of predicting values for much higher concentrations, they likewise contain another adjustable parameter, the "hydration number".

Bjerrum (48) has pointed out that certain anamolies can be explained by assuming that the dielectric constant decreases in the immediate neighborhood of ions. Debye and Pauling (49) have shown that variations of the dielectric

constant do not effect the limiting law for very dilute solutions of strong electrolytes. Hückel (50) has proposed that a term, linear with concentration, be added to the limiting law to take into account the variations of the dielectric constant with concentration. Since no experimental method of determining the dielectric constants of solutions was available, this treatment (and others adding such linear terms) has been considered an empirical extension, which gives a better fit to the data due to the extra adjustable parameter. Using high frequency techniques, a group of English workers (51, 52, 53) has recently measured the dielectric constants of solutions of strong electrolytes. They point out that the linear term should be the summation of several effects, i.e., the variation of the dielectric constant, ion-pair formation, co-volume effects, and the breaking down of the water structure.

Assumptions (d) and (e) have recently been modified by Dutta and Bagchi (54, 55, 56) and by Eigen and Wicke (57, 58, 59, 60, 61). Both derive their statistics by considering the distribution of ions and possible ion sites around the central ion. Dutta and Bagchi obtain essentially a Fermi-Dirac distribution function. Eigen and Wicke compute the available ion sites on the basis of the volume required by a hydrated ion. The possible equivalence of these two treatments has been argued by the authors. Eigen and Wicke (61) have extended their treatment to include incomplete dissocia-

tion. Lange and Möhring (62) have derived the expression for the relative apparent heat content from this theory. Good agreement is obtained between theory and experiment for activity coefficients, heats of dilution, and apparent molal heat capacities. The theory loses a great deal of its luster, however, when one considers the large number of unevaluated, and hence adjustable, parameters available for curve fitting.

Assumption (f), dropping terms higher than the second in the expansion of the Poisson-Boltzmann equation, can be eliminated by carrying through the involved mathematics of evaluating higher terms. Müller (63) used a graphical integration instead of expanding the Poisson-Boltzmann equation. Gronwall, LaMer and Sandved (64) carried out a complex mathematical integration, retaining six terms of the expansion, for symmetrical type electrolytes; LaMer, Gronwall and Greiff (65) obtained the equation for the unsymmetrical case. Fowler and Güggenheim (42) have pointed out that these extensions of the Debye-Hückel theory lead to a mathematical inconsistency. They show this by the fact that the Debye and the Guntelberg (66) charging processes lead to different results. Onsager (67) has concluded that the Poisson-Boltzmann equation cannot be expected to hold at higher concentrations, since the potentials are no longer additive in this range. Thus, if one intends to use higher terms of the expansion, one should simultaneously consider deviations from the linear superposition principle.

Mayer (68) has recently developed a theory of electrolytic solutions based on an entirely different viewpoint than that of Debye and Hückel. His derivation is similar to the statistical mechanical evaluation of virial coefficients of real gases. Poirier (69), using Mayer's rather complicated expression for the activity coefficient, derived expressions for the partial molal volume, the apparent molal volume, the relative partial molal heat content, the relative apparent molal heat content, and the stoichiometric mean ionic activity coefficient. He calculated numerical values for the activity coefficients of four salts and tabulated the quantities needed to compute the above thermodynamic functions.

While the above summary does not exhaust the number of different approaches to the theory of electrolytic solutions, it does present some of the more fruitful attempts. With all the work done on this problem in the last 24 years, the Debye-Hückel theory remains the most reliable treatment.

C. Comparison of Experimental and Theoretical Values for Relative Apparent Molal Heat Contents

Bjerrum (70) pointed out in 1926 that an expression for the heat of dilution could be derived from the Debye-Hückel interionic attraction theory. This predicted that the heat of dilution of electrolytes should be positive and that salts of the same valence type should give the same limiting value. Scatchard (71) pointed out that the differentiation should

have been made at constant pressure (instead of constant volume); however, this did not alter the conclusions. Comparing predictions to the data of Richards and Rowe (72, 73), Bjerrum found wide differences for different salts, some giving positive and others negative heats of dilution. Richards and Rowe used an adiabatic calorimeter, whose jacket was maintained to within a few hundredths of a degree. The temperature was read to 0.0005 degrees with a mercury-in-glass thermometer. They measured the heats of dilution of several 1-1 salts; the lowest concentration reached was 0.139 molal, a range where deviations from the theory might well be expected.

In 1926 Nernst and Orthmann (74) measured heats of dilution down to concentrations of 0.1 and 0.03 molar. Their calorimeter employed a 20 junction iron-constantan thermopile, which had a sensitivity of 0.121 calories per mm deflection of a galvanometer. This data still did not agree with the theoretical predictions. They repeated this work in 1927 (75), lowering the concentration range to 0.004 molar and increasing the sensitivity to 3.18×10^{-3} calories per mm galvanometer deflection by using a 100 junction thermopile. Nernst's data (76), and that of Naude (77), were in qualitative agreement with the predictions of the Debye-Hückel theory. Nernst (78) and a group of followers preferred to attribute deviations from the theory to heat adsorbed when the electrolyte dissociated in the process of dilution.

Gulbransen and Robinson's (83) data for sodium chloride. They obtained the first really satisfactory (better than 5 per cent) agreement with the theoretical limiting slopes. Young and Seligmann (84) extended the calculations to other 1-1 and 1-2 salts, also obtaining good agreement. This method of calculation will be described in the treatment of data section.

The only really new type solution calorimeter designed since 1927 is that of Gucker, Pickard and Planck (85). Their apparatus essentially consists of two separate containers, connected by a 60 junction copper-constantan thermopile, enclosed in a jacket and submerged in an automatically controlled adiabatic bath. A sensitivity of about 6×10^{-4} calories per mm deflection of a very sensitive Paschen galvanometer was obtained. The improvement of their apparatus was in reducing the heat exchange between the two "sides" of the differential calorimeter and between the calorimeter proper and the jacket. The apparatus has been used mainly for heats of dilution of nonelectrolytic solutes.

Wallace and Robinson (86) have used a modification of the chord-area method to evaluate their data on alkaline earth sulfates. They found what appears to be a maximum in their "short chord" data between $c^{\frac{1}{2}} = 0.02$ and 0.03. Young (87) has attributed this, at least for sulfuric acid, to the dissociation of the bisulfate ion.

Lange and Miederer (30) have recently summarized the

limiting slopes for the heats of dilution of ten different valence type electrolytes. They compare this data to the experimentally determined slope for a 1-1 salt. While the majority are in agreement with theory, the 2-2, 2-3, and 2-4 salts gave values two to three times as large as predicted, and the 3-3 salt gave a value about eight times too small.

III. THEORY

A. General Thermodynamics

The first law of thermodynamics requires that the change in energy of a system equals the heat adsorbed, δq, minus the work done by the system on the surroundings, δw. Limiting the process to a reversible one, in which only mechanical work is done, the energy change may be written

$$dE = \delta q - \delta w = TdS - PdV \quad , \tag{3}$$

where T is the absolute temperature, S the entropy, P the pressure and V the volume.

The thermodynamic function H, the enthalpy or heat content of the system, is defined as

$$H = E + PV \tag{4}$$

and is also a state function. The enthalpy change may be written

$$dH = TdS + VdP \quad . \tag{5}$$

It is seen that for a reversible process at constant pressure

$$dH = \delta q \quad . \tag{6}$$

The utility of defining a state function in the way that the enthalpy has been defined is immediately evident to the thermochemist. Many chemical reactions are carried out under conditions of constant pressure, and in these cases the enthalpy change is simply the heat of the reaction.

For a two component system (a solution), the enthalpy

can be expressed as

$$H = n_1\bar{H}_1 + n_2\bar{H}_2 \tag{7}$$

or

$$H = n_1\bar{H}_1^{\circ} + n_2\phi_H \tag{8}$$

where n_1 and n_2 = the moles of solvent and solute respectively,

$\bar{H}_1$ and $\bar{H}_2$ = the partial molal enthalpy of solvent and solute respectively,[1]

$\bar{H}_1^{\circ}$ = the partial molal enthalpy of solvent in its reference state (pure solvent),

and ϕ_H = the apparent partial molal enthalpy of solute.

The equations for the reference state (an infinitely dilute solution) can be expressed as

$$H^{\circ} = n_1\bar{H}_1^{\circ} + n_2\bar{H}_2^{\circ} \tag{9}$$

or

$$H^{\circ} = n_1\bar{H}_1^{\circ} + n_2\phi_H^{\circ} \quad . \tag{10}$$

The various relative molal quantities are defined by

$$H - H^{\circ} = L = \text{relative heat content,} \tag{11}$$

$$\bar{H}_1 - \bar{H}_1^{\circ} = \bar{L}_1 = \text{relative partial molal heat content of solvent,} \tag{12}$$

$$\bar{H}_2 - \bar{H}_2^{\circ} = \bar{L}_2 = \text{relative partial molal heat content of solute,} \tag{13}$$

$$\phi_H - \phi_H^{\circ} = \phi_L = \text{relative apparent molal heat content of solute.} \tag{14}$$

---

[1] If G is any extensive quantity of the system, the partial molal quantity is defined by $\bar{G}_i = \left(\frac{\partial G}{\partial n_i}\right)_{T,P,n_j}$.

B. Evaluation of Partial Molal Heat Contents

1. General

Partial molal heat contents can be determined calorimetrically from measurements of heats of dilution or from measurements of heats of solution. The data are analyzed in terms of the relative apparent molal enthalpy, $\underline{\phi_H}$. From equations (7) and (8) we see that

$$n_2\phi_H = n_1\bar{H}_1 + n_2\bar{H}_2 - n_1\bar{H}_1^\circ \quad . \tag{15}$$

And it is obvious from equations (9) and (10) that

$$\phi_H^\circ = \bar{H}_2^\circ \quad . \tag{16}$$

Then,

$$n_2\phi_H - n_2\phi_H^\circ = n_1\bar{H}_1 + n_2\bar{H}_2 - n_1\bar{H}_1^\circ - n_2\bar{H}_2^\circ \tag{17}$$

and

$$n_2\phi_L = n_1\bar{L}_1 + n_2\bar{L}_2 = L \quad . \tag{18}$$

The relative partial molal heat content of the solute is defined by

$$\bar{L}_2 = \left(\frac{\partial L}{\partial n_2}\right)_{n_1} \quad . \tag{19}$$

Hence, from equations (18) and (19)

$$\bar{L}_2 = \phi_L + n_2 \left(\frac{\partial \phi_L}{\partial n_2}\right)_{n_1} \quad . \tag{20}$$

And from equation (18)

$$\bar{L}_1 = \frac{n_2}{n_1}(\phi_L - \bar{L}_2) \quad . \tag{21}$$

Alternate ways of expressing equations (20) and (21) are

$$\bar{L}_2 = \phi_L + \frac{m^{\frac{1}{2}}}{2} \frac{\partial \phi_L}{\partial m^{\frac{1}{2}}} \qquad (22)$$

and

$$\bar{L}_1 = \frac{mM_1}{1000} (\phi_L - \bar{L}_2) \quad , \qquad (23)$$

where m = the molality of the solute

and M_1 = the molecular weight of the solvent.

2. From heats of dilution

In a dilution experiment, the change in the total heat content in going from the initial to the final solution can be expressed as

$$\Delta H_{dilution} = L' - L$$
$$= (n_1 + \Delta n_1) \bar{L}_1' \quad n_2\bar{L}_2' - n_1\bar{L}_1 - n_2\bar{L}_2 \quad , \qquad (24)$$

where the primed quantities refer to the final solution, the unprimed to the initial solution, and Δn_1 is the water added in the dilution. From equation (18)

$$\Delta H_{dilution} = n_2(\phi_L' - \phi_L) \quad , \qquad (25)$$

and for a solution containing one mole of solute

$$\Delta H_{\substack{dilution \\ n_2 = 1}} = \phi_L' - \phi_L \quad . \qquad (26)$$

From equation (14), ϕ_L' must approach zero at infinite dilution. It then follows that

$$\lim_{m \to 0} \left(\Delta H_{\substack{dilution \\ n_2 = 1}} \right) = - \phi_L \, . \qquad (27)$$

Thus, we recognize that $\underline{\phi_L}$ is the negative of the heat of dilution to infinite dilution.

The method for determining absolute values of $\underline{\phi_L}$ from heats of dilution will be given in a later section.

3. From heats of solution

In a solution experiment, the change in the total heat content can be expressed as

$$\Delta H_{solution} = n_1\bar{H}_1 + n_2\bar{H}_2 - n_1H_1^\bullet - n_2H_2^\bullet \quad , \tag{28}$$

or

$$\Delta H_{solution} = n_1\bar{H}_1^\circ + n_2\phi_H - n_1H_1^\bullet - n_2H_2^\bullet \quad , \tag{29}$$

where $H_1^\bullet$ and $H_2^\bullet$ = the enthalpy of pure solvent and pure solute respectively.

Recognizing the equivalence of $\underline{H_1^\bullet}$ and $\underline{\bar{H}_1^\circ}$ and of $\underline{\phi_H^\circ}$ and $\underline{\bar{H}_2^\circ}$, we may write equation (28) as

$$\begin{aligned}\Delta H_{solution} &= n_1(\bar{H}_1 - \bar{H}_1^\circ) + n_2(\bar{H}_2 - \bar{H}_2^\circ) - n_2(H_2^\bullet - \bar{H}_2^\circ) \\ &= n_1\bar{L}_1 + n_2\bar{L}_2 - n_2L_2^\bullet \quad ,\end{aligned} \tag{30}$$

or equation (29) as

$$\begin{aligned}\Delta H_{solution} &= n_2(\phi_H - \phi_H^\circ) - n_2(H_2^\bullet - \bar{H}_2^\circ) \\ &= n_2\phi_L - n_2L_2^\bullet \quad .\end{aligned} \tag{31}$$

From equation (31), it can be seen that the difference between any two heats of solution will give the heat of dilution as defined by equation (25).

Differentiating equations (30) and (31) with respect to

n_2,

$$\left(\frac{\partial \Delta H}{\partial n_2}\right)_{n_1} = \bar{L}_2 - L_2^{\bullet} \tag{32}$$

and

$$\left(\frac{\partial \Delta H}{\partial n_2}\right)_{n_1} = \phi_L + n_2 \frac{\partial \phi_L}{\partial n_2} - L_2^{\bullet} \quad . \tag{33}$$

Subtracting equation (32) from equation (33), one obtains equation (20) for $\bar{L}_2$.

The quantity $L_2^{\bullet}$ is evaluated by extrapolating to infinite dilution, i.e.,

$$L_2^{\bullet} = - \lim_{n_2 \to 0} \left(\frac{\partial \Delta H}{\partial n_2}\right)_{n_1} \quad , \tag{34}$$

and is recognized as the heat of solution at infinite dilution.

Relative apparent molal heat contents can be obtained by subtracting the heat of solution at infinite dilution from the heats of solution giving final solutions of different molalities.

C. Activities

For an ideal solution, the chemical potential of an electrolyte is given by

$$\mu_j = \mu_j^{\circ} + \nu RT \ln N_{\pm} \quad , \tag{35}$$

where μ_j° = the chemical potential in the standard state,

R = the gas constant,

T = the absolute temperature,

$$\nu = \nu_+ + \nu_- ,$$

ν_+ and ν_- = the number of positive and negative ions in the electrolyte respectively,

$$N_\pm = N\left[\nu_+^{\nu_+} + \nu_-^{\nu_-}\right]^{\frac{1}{\nu}} ,$$

$N_\pm$ = the mean ionic mole fraction

N = the mole fraction of electrolyte

and j refers to the jth species present in a system of n components.

The activity, a_j, of a chemical species is defined by

$$\mu_j = \mu_j^\circ + RT \ln a_j \quad . \tag{36}$$

If the species under consideration is an electrolyte, then its activity may be written

$$a_j = a_\pm^\nu \quad , \tag{37}$$

where $a_\pm$ = the mean ionic activity.

To describe departures from ideality, it is convenient to define an activity coefficient by

$$a_\pm = f_\pm N_\pm \quad , \tag{38}$$

where $f_\pm$ = the mean rational activity coefficient.

From a combination of equations (36), (37) and (38), we have

$$\mu_j = \mu_j^\circ + \nu RT \ln f_\pm + \nu RT \ln N_\pm \quad . \tag{39}$$

It can be shown that

$$\frac{\partial}{\partial T}\left[\frac{\mu}{T}\right]_P = -\frac{\bar{H}}{T^2} \quad . \tag{40}$$

Differentiating equation (39) with respect to T at constant P and N gives

$$\nu RT^2 \left[\frac{\partial \ln f_\pm}{\partial T}\right]_{P,N} = \bar{H}_2 - \bar{H}_2^\circ = \bar{L}_2 \quad . \tag{41}$$

We thus see that the relative partial molal heat content is related to the change in activity of the solute with temperature.

The comparison of experimental values with theoretical predictions is usually made on a combination of equations (22) and (41). The Debye-Hückel expression for the rational activity coefficient is given by equation (2),

$$\ln f_\pm = \frac{-2.303\, S_{(f)} \Gamma^{\frac{1}{2}}}{1 + A\Gamma^{\frac{1}{2}}} \quad . \tag{2}$$

Differentiating equation (2) with respect to $\underline{T}$ at constant $\underline{P}$ and $\underline{n_j}$ gives

$$\bar{L}_2 = \frac{S_{(H)}\Gamma^{\frac{1}{2}}}{1 + A\Gamma^{\frac{1}{2}}} + \frac{W_{(H)}\Gamma}{\left[1 + A\Gamma^{\frac{1}{2}}\right]^2} \quad , \tag{42}$$

where $S_{(H)} = -2.303\, \nu RT^2\, S_{(f)} \cdot \frac{3}{2}\left[\frac{1}{T} + \frac{\partial \ln D}{\partial T} + \frac{\alpha}{3}\right]$,

$W_{(H)} = 2.303 \nu RT^2\, S_{(f)}\, A \cdot \frac{1}{2}\left[\frac{1}{T} + \frac{\partial \ln D}{\partial T} + \alpha - \frac{2\,\partial \ln a^\circ}{\partial T}\right]$,

α = the coefficient of thermal expansion of the solution.

When applied to extremely dilute solutions, the equation reduces to

$$\bar{L}_2 = S_{(H)}\Gamma^{\frac{1}{2}} \quad . \tag{43}$$

D. Debye-Hückel Theory

Since a complete treatment of the Debye-Hückel inter-ionic attraction theory is presented by Harned and Owen (40), the derivation of the limiting law will merely be outlined here.

The primary task is to calculate the electrical potential at a point in the solution. Then the extra energy required to charge the ion due to the ionic atmosphere can be calculated.

Poisson's equation, which relates the electrical potential, ψ, and the charge density, ρ, is

$$\nabla^2\psi = \frac{4\pi\rho}{D} \quad . \tag{44}$$

Choosing the origin of the coordinate system as a particular ion, the j-ion, the charge density at a distance r from the ion is given by

$$\rho = \sum_{i=1}^{s} n_i e_i = \sum_{i=1}^{s} n_i z_i \epsilon \quad , \tag{45}$$

where n_i is the concentration of i-ions per cubic centimeter and where the summation is over all the ions in the solution.

The Boltzmann distribution gives for n_i', the concentration of i-ions at a point,

$$n_i' = n_i \exp(-\frac{U_j}{kT}) = n_i \exp(-\frac{z_i \epsilon \psi_j}{kT}) \quad , \tag{46}$$

where U_j = the potential energy of the i-ion with respect to the j-ion.

Setting $U_j = z_i \epsilon \psi_j$ is equivalent to the assumption of the linear superposition of fields. Using the condition of electroneutrality of the solution $\sum_{i=1}^{s} n_i z_i \epsilon = 0$, and assuming $z_i \epsilon \psi_j \ll kT$, the Boltzmann distribution can be expressed in the simple form

$$n_i' = - \frac{n_i z_i \epsilon \psi_j}{kT} \quad . \tag{47}$$

Combining equations (44), (45) and (47) yields the Poisson-Boltzmann differential equation

$$\nabla^2 \psi_j = \frac{4 \pi \epsilon^2}{DkT} \sum_{i=1}^{s} n_i z_i^2 \psi_j =$$

$$\frac{4 \pi \epsilon^2}{DkT} \frac{N}{1000} \sum_{i=1}^{s} c_i z_i^2 \psi_j = \kappa^2 \psi_j \quad , \tag{48}$$

where c_i = molar concentration of the i-ion.

This has the general solution

$$\psi_j = A \frac{e^{-\kappa r}}{r} + B \frac{e^{\kappa r}}{r} \quad , \tag{49}$$

where A and B are constants of integration.

Since $\psi_j(\infty) = 0$, $B = 0$, and

$$\psi_j = A \frac{e^{-\kappa r}}{r} \quad . \tag{50}$$

The constant A can be evaluated from the fact that when $\kappa = 0$, the concentration is zero and the potential is that of the j-ion alone, namely

$$\psi_j(0) = \frac{z_j \epsilon}{Dr} \quad . \tag{51}$$

The final solution is then

$$\psi_j = \frac{z_j \epsilon}{Dr} e^{-\kappa r} \quad . \tag{52}$$

This can be expanded to give

$$\psi_j = \frac{z_j \epsilon}{Dr} - \frac{z_j \epsilon \kappa}{D} \quad . \tag{53}$$

The first term is simply the potential of the isolated ion (see equation 51); the second is the potential of the ionic atmosphere, $\underline{\psi'_j}$.

The electrical energy required to charge an ion in the presence of the potential of its atmosphere is given by

$$\Delta\mu(el) = - \frac{(z_j \epsilon)^2 \kappa}{2D} \quad . \tag{54}$$

If deviations of electrolytic solutions from ideality are attributed entirely to the electrostatic forces between ions,

$$\Delta\mu(el) = kT \ln f_j = - \frac{(z_j \epsilon)^2 \kappa}{2D} \quad , \tag{55}$$

where f_j = the rational activity coefficient.

The mean rational activity coefficient of an electrolyte which dissociates into $\underline{p}$ kinds of ions is defined by

$$\ln f_{\pm} = \frac{1}{\nu} \sum_{j=1}^{s} \nu_j \ln f_j \quad . \tag{56}$$

If one now substitutes equations (48) and (55) into equation (56), one obtains the Debye-Hückel limiting law for the rational activity coefficient,

$$\log f_{\pm} = - S_{(f)} \Gamma^{\frac{1}{2}} \quad . \qquad (1)$$

IV. EXPERIMENTAL: HEATS OF DILUTION

A. Apparatus

The calorimeter used in this work was very similar to that of Gucker, Pickard and Planck (85), which has been characterized previously. The only major differences were in the sample holders and the method of measuring the potential of the thermel. A general idea of the apparatus can be obtained from the schematic diagram given in Figure 1. Schematic diagrams of the electrical circuits are given in Figures 2 and 3. References to figures will be designated by (i-X), where i refers to the figure and X to the alphabetically labeled parts.

1. Water bath

The large water bath which served as the adiabatic jacket had a capacity of about 22 gallons. The bath consisted of an inner copper tank, a galvanized iron casing, and a plywood base. The inner tank was supported above the base by two boards; a copper collar served as a lid between the inner and outer walls. The three inch space between the tank and the casing and base was filled with exploded mica insulation. The lid for the water bath consisted of a 1/4 inch aluminum plate with a plywood top held two inches above the plate by a galvanized iron casing. The area between the top and the plate was packed with hair felt insulation.

If one now substitutes equations (48) and (55) into equation (56), one obtains the Debye-Hückel limiting law for the rational activity coefficient,

$$\log f_{\pm} = - S_{(f)} \Gamma^{\frac{1}{2}} \quad . \qquad (1)$$

IV. EXPERIMENTAL: HEATS OF DILUTION

A. Apparatus

The calorimeter used in this work was very similar to that of Gucker, Pickard and Planck (85), which has been characterized previously. The only major differences were in the sample holders and the method of measuring the potential of the thermel. A general idea of the apparatus can be obtained from the schematic diagram given in Figure 1. Schematic diagrams of the electrical circuits are given in Figures 2 and 3. References to figures will be designated by (i-X), where i refers to the figure and X to the alphabetically labeled parts.

1. Water bath

The large water bath which served as the adiabatic jacket had a capacity of about 22 gallons. The bath consisted of an inner copper tank, a galvanized iron casing, and a plywood base. The inner tank was supported above the base by two boards; a copper collar served as a lid between the inner and outer walls. The three inch space between the tank and the casing and base was filled with exploded mica insulation. The lid for the water bath consisted of a 1/4 inch aluminum plate with a plywood top held two inches above the plate by a galvanized iron casing. The area between the top and the plate was packed with hair felt insulation.

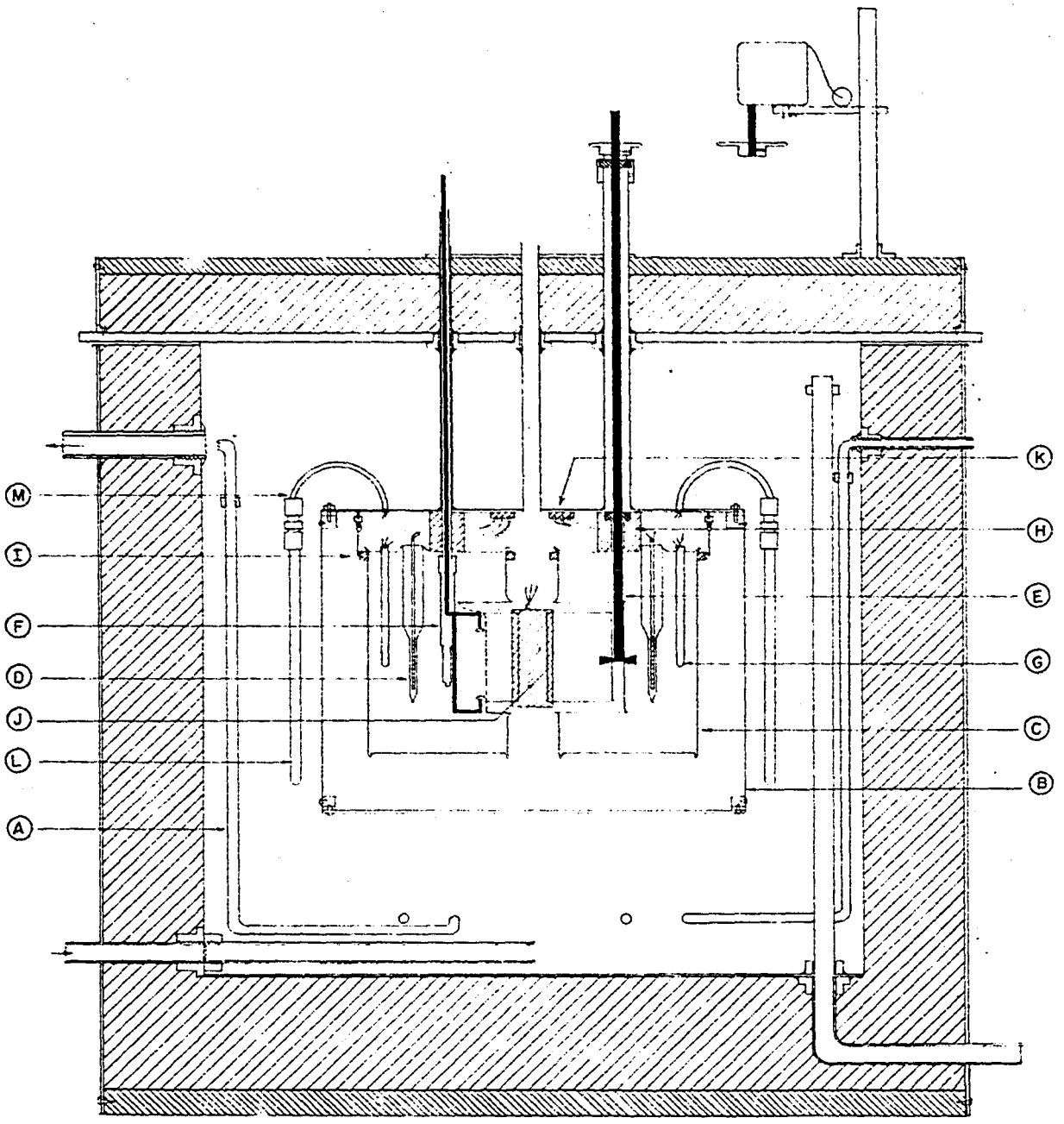

Figure 1. Adiabatically jacketed differential calorimeter for measuring heats of dilution.

The water bath lid was suspended 54 inches above the floor by an angle iron frame. The water bath and its circulating pump rested on a movable angle iron platform which could be rolled under the lid. The bath was raised and lowered by a hydraulic bumper jack mounted on the platform.

The bath was stirred by a centrifugal pump which was driven by a 1/4 horsepower motor. Water was removed at an opening three inches from the top of the tank and was returned through a tube at the bottom. The bath was also provided with an overflow tube one inch from the top.

The bath was cooled by water flowing through a length of 1/4 inch copper tubing (1-A). The cooling coil consisted of 1½ turns at the bottom of the bath and two lengths from the bottom to its outlets, which were three inches below the top and on opposite sides of the bath. The bath was heated by two 500 watt knife heaters, which hung from the lid. The power supplied the heaters could be varied, as will be described later.

2. Submarine jacket

The submarine jacket (1-B) was constructed of 1/20 inch thick monel sheet. Its horizontal cross section had straight, parallel sides, terminating in semicircular ends. Brass flanges were soldered inside the upper and lower rims of the wall. The bottom of 1/8 inch chromium plated copper was fastened permanently to the bottom flange. Studs were

threaded into the upper flange and were used to fasten the jacket to its lid. A 1/4 inch soft rubber gasket fitted between the jacket and lid. The 1/4 inch chromium plated copper lid was suspended five inches below the aluminum lid of the water bath by eight brass tubes. The tubes acted as water tight passages for various rods and wires entering the calorimeter. The tubes for the stirrers rose above the top of the bath lid and were capped with brass holders, which accommodated bearings for the stirrer shafts.

3. Calorimeter containers

The calorimeter containers (1-C) were fabricated from 15 mil tantalum. Tantalum was used because of its chemical inertness and its structural strength. The containers were 4 inches in diameter and 6 inches deep. The thermel wells in the side of each container were formed by flattening tantalum tubing over a brass form; boat shaped bottoms of sheet tantalum were welded to the ends of the wells. The lids had a 1/4 inch 45 degree flange turned up around their preiphery to match a similar flange around the rim of the containers. Each lid contained a heater well (1-D) and three 1/4 inch holes for the stirrer (1-E), sample holder (1-F) and control thermels (1-G). The container lids were mounted permanently to the under side of the submarine jacket lid by four 3 cm long lucite spacers (1-H).

In assembling the apparatus, the two containers were

raised to their lids by means of a small jack. When the lid and container flanges fitted snugly together, strips of Scotch electrical tape were wrapped tightly around the rims; brass snap rings were then slipped over the Scotch tape to insure a good seal. The containers were held in place by lucite rings (1-I) suspended from the submarine jacket lid by three strands of 30 pound test nylon fish line. The lines were tied to the bottom of ballbearing swivels; the swivels were soldered to large brass nuts, which were threaded onto studs projecting downward from the jacket lid.

4. Calorimeter heaters and circuits

Each calorimeter heater (1-D, 2-A, 2-A') consisted of a main heater to supply the heat necessary for calorimetric measurements and an auxiliary trickle heater to compensate for temperature drifts in the containers. The main heater was a 50 ohm winding of 38 B and S gauge manganin wire; the auxiliary heater was a 1.5 ohm winding of 30 B and S gauge constantan wire. The wires were wound around the bottom of a thin mica strip, which were fitted into the heater wells; the remaining space was filled with naphthalene.

Two 30 B and S gauge copper lead wires were attached to each end of the manganin winding; one lead wire to the ends of the constantan winding. The six leads from each heater were connected to the wires of a six conductor shielded cable at a junction block. The junction block, attached to the

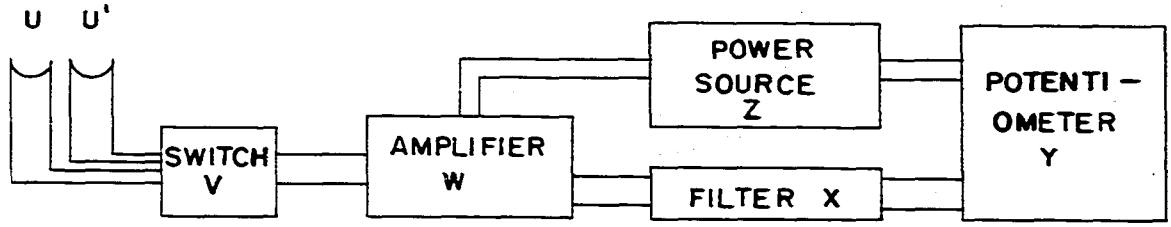

CIRCUIT FOR MAIN THERMEL

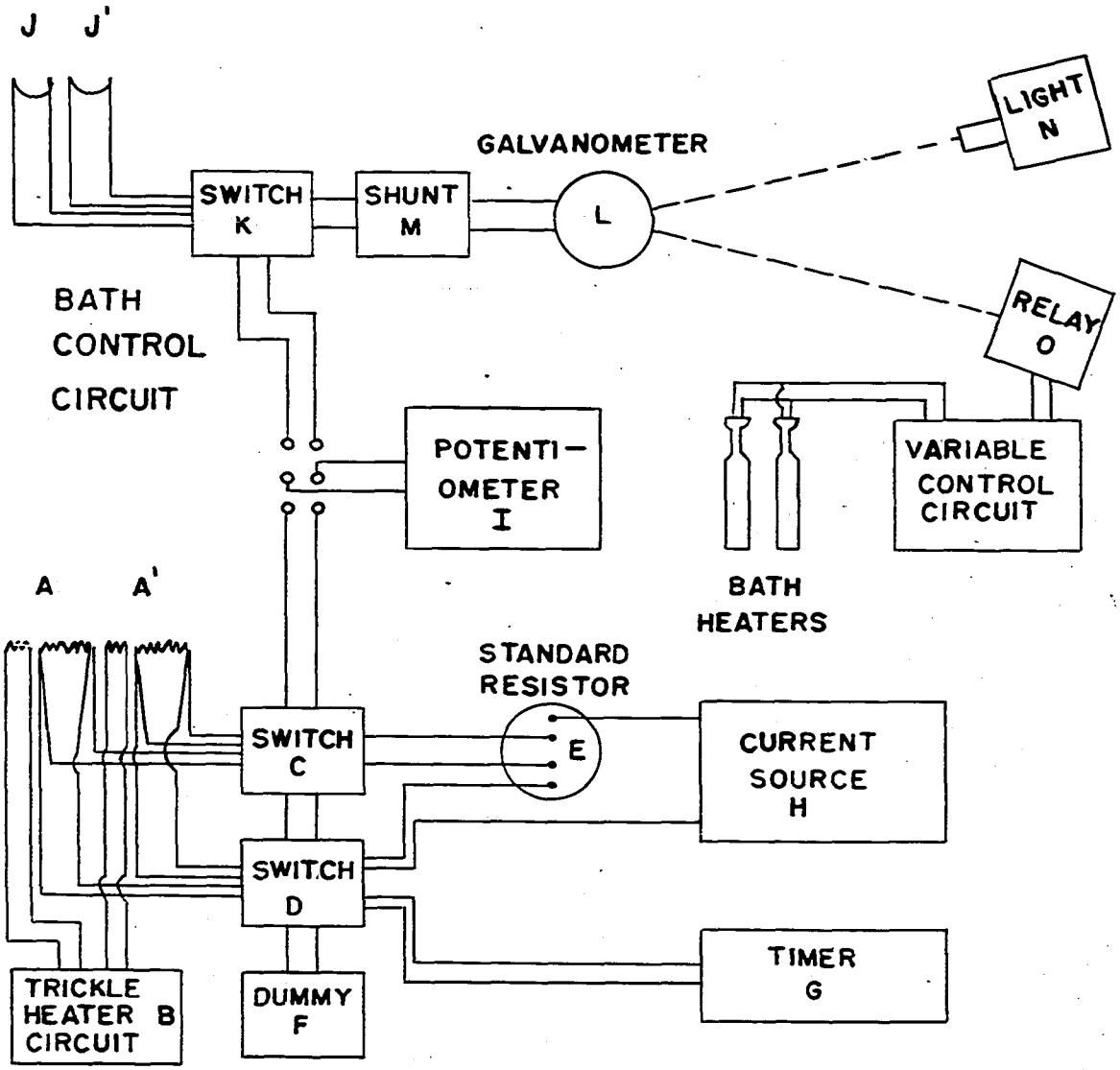

CIRCUIT FOR CALORIMETER AND BATH HEATERS

Figure 2. Schematic diagrams of circuits for differential calorimeter.

under side of the submarine jacket, consisted of brass screws and nuts mounted on a lucite strip.

The leads from the trickle heaters were connected to the current source (2-B) as shown in Figure 3. One lead from each end of the main heaters was connected to a three gang, ceramic based rotary switch (2-C); the other two leads to an identical switch (2-D). Switch (2-C) was wired so that one could measure the potential drop across either heater, across the two heaters in series, across the standard resistor (2-E), or across the dummy heater (2-F). Switch (2-D) was wired so that current could be passed through either manganin heater, through the two heaters in series, or through the dummy heater. When switch (2-D) was set to pass current through the manganin heaters, it also turned on the electronic timer (2-G). The current source (2-H) for the manganin heaters was a Willard, low discharge, six volt storage battery with a variable resistor in series.

The potential measurements were made with a Leeds and Northrup, Type K-2, potentiometer (2-I). The standard resistor and the standard cell used in conjunction with the potentiometer were calibrated by the National Bureau of Standards and were checked with other more recently calibrated instruments. The electronic timer was calibrated with the National Bureau of Standards station WWV and measured time intervals to 0.01 seconds.

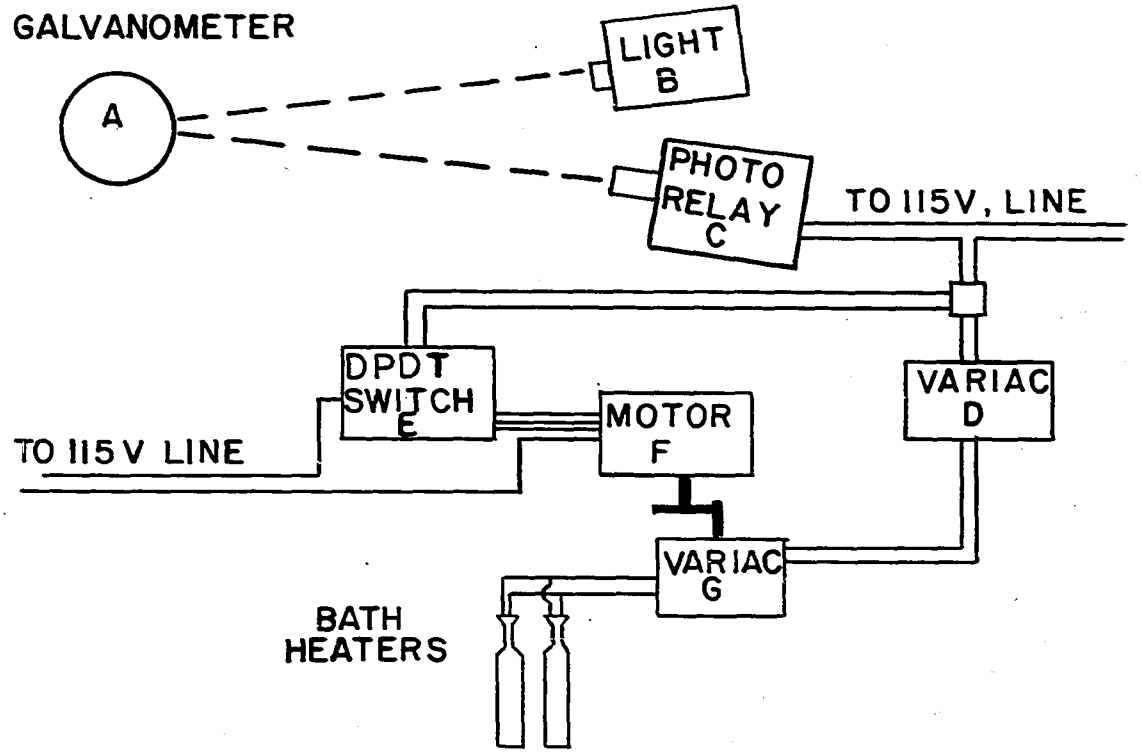

VARIABLE BATH CONTROL CIRCUIT

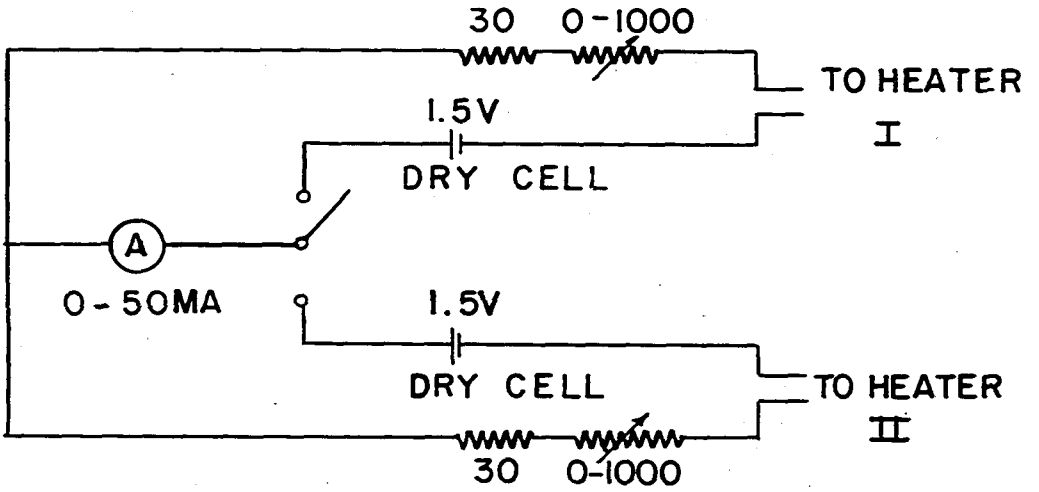

CURRENT SOURCE FOR TRICKLE HEATERS

Figure 3. Schematic diagrams of the current source for trickle heaters and of the bath control circuit.

5. Calorimeter stirrers

The liquid in the calorimeter containers was stirred by vane type stainless steel stirrers (1-E). The stirrer shafts were suspended by two stainless steel, ball bearings: one at the top of the brass tube and the other in the lucite spacer beneath the jacket lid. The stirrers were rotated at a speed of 282 rpm by a sprocket and chain drive, which was powered by a 150 rpm synchronous motor. The propellers and the chain drive were arranged so that the two containers were stirred in opposite directions.

6. Sample holders

An exploded view of the stainless steel sample holders is shown in Figure 4. The barrels were two cm in diameter and four cm long. The screw-on caps held 0.5 mil platinum disks against the rims of the barrels. Vapor tight seals were obtained by applying a thin coating of silicon grease to the rims and placing Teflon gaskets behind the disks. The samples were opened by punching holes into the disks with a breaker rod having crown shaped tips. The lower portion of the breaker was stainless steel; the rod extending out of the calorimeter was polyethylene to reduce thermal conduction.

7. Thermopile and circuit

The temperature difference between the two calorimeter containers was measured by a 60 junction copper-constantan thermopile (1-J, 2-U, 2-U'). The thermopile was constructed

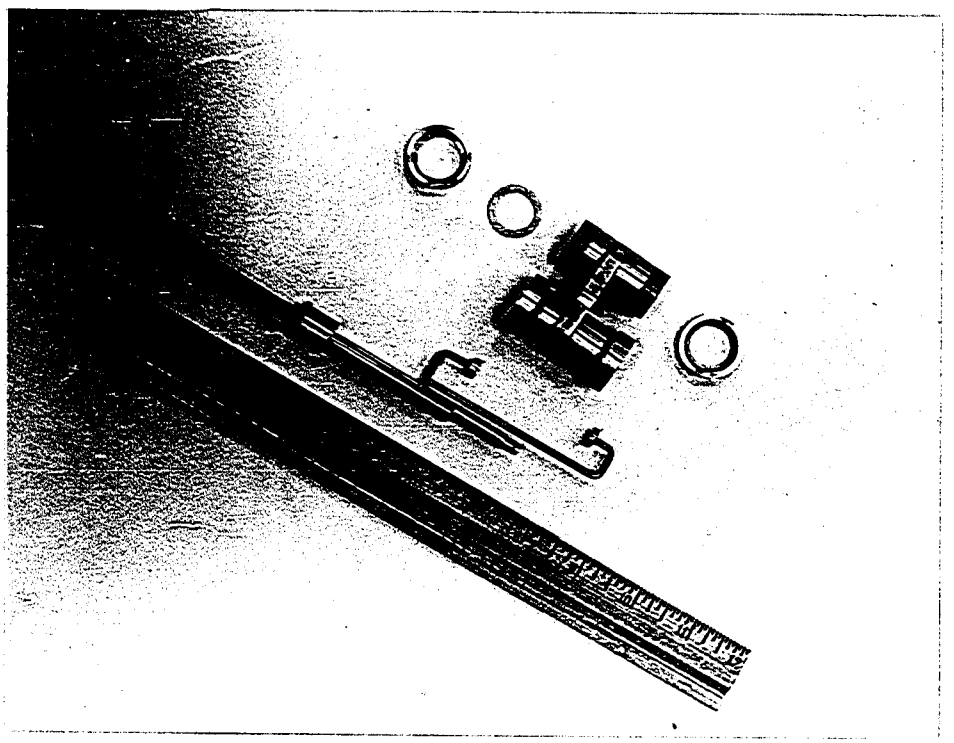

Figure 4. Sample holders for dilution experiments.

of 32 B and S gauge copper wire and 24 B and S gauge constantan wire; 30 B and S gauge copper wire was used for leads. The wires were mounted on two thin mica sheets, giving two 30 junction thermopiles having resistances of 10 ohms. The junctions were made by wrapping the ends of the copper wire around the ends of the heavier constantan wire; the junctions were dipped into a rosin in ethyl alcohol flux; and finally they were dipped into molten solder. The solder was supplied by the Liston-Becker Instrument Company for use in the input circuits of their D.C. breaker amplifiers. Two thin copper shields covered the ends of the thermopile and were separated by a lucite collar. The two thermopiles were insulated from each other and from the walls of the case by thin mica sheets. The space within the case was filled with naphthalene to improve thermal conduction and for stability.

The lead wires, attached to the ends of each half of the thermopile, were joined to the wires of a four conductor shielded cable at a junction block (1-K) consisting of pure copper screws and nuts mounted on a lucite strip. Before the connections were made, the screws, nuts and wires were cleaned with a solution of hydrochloric and nitric acids, then with a mixture of nitric, phosphoric and acetic acids, and finally with several water rinses.

The four conductor cable led out of the calorimeter to a Leeds and Northrup, number 31-3-0-3, 12 position, silver contact rotary selector switch (2-V). This switch was wired

so that the potential across the two 30 junction sections of the thermopile could be measured separately, in series, or in opposition and with either direct or reversed polarities. The switch could also be set to place 0, 10, and 20 ohm shunts in the input circuit; these were used to test the circuit. The switch was mounted in a steel casing to which the braided shieldings of the incoming and outgoing cables were grounded. The case was placed in a large, covered Dewar flask and surrounded with blown mica insulation.

A two conductor shielded cable connected the selector switch to a model 14 Liston-Becker D.C. breaker amplifier (2-W). The output of the amplifier was fed into a filter circuit (2-X) which attenuated the signal slightly and reduced the noise level considerably. The signal was then recorded on a Brown recording potentiometer (2-Y) with a 0 to 60 millivolt range. A type IE 5101 Stabiline voltage regulator (2-Z) supplied the power for the amplifier and potentiometer.

8. Adiabatic control

Two 10 junction copper-constantan thermopiles (2-J, 2-J') were used as sensing elements to control the water bath at the same temperature as the calorimeter containers. They were constructed of 36 B and S gauge constantan wire and 30 B and S gauge copper wire. The junctions immersed in the water bath were spaced at two cm intervals; at the container

end, five were located at the bottom and the other five two cm above. The junctions were made in the same way as the main thermopile; the wires were tied together in a long bundle and painted with clear Corex insulating varnish. The bath ends were placed in copper tubes (1-L), the calorimeter ends in glass tubes (1-G); the tubes were filled with naphthalene. The copper tubes were connected to semi-circular sections of copper tubing (1-M) which lead into the submarine jacket; the glass tubes were attached to the container lids with paraffin.

The lead wires from the thermopile were joined to the wires of a four conductor shielded cable at the same junction block as the main thermel. The cable was connected to another Leeds and Northrup 31-3-0-3 selector switch (2-K). One section of this switch was wired to connect either thermopile separately or the two in series (as was used during a run) to the bath control circuit. The other section placed the thermopiles in the circuit of the potentiometer (2-I) to permit testing of the thermopile circuits.

For bath control, switch (2-K) connected the thermopiles to a Leeds and Northrup, Type HS, reflecting galvanometer (2-L, 3-A) through an Aryton shunt (2-M). A Warner model 62L light source (2-N, 3-B) was focused to reflect light from the galvanometer to a Warner model 62R photoelectric receiver and relay (2-O, 3-C) three meters away. The galvanometer zero was set so that the light was reflected

onto the photocell when the temperature of the bath fell below that of the containers. This activated the relay to close the input circuits of a type 116 Powerstat (3-D) and of a 115V A.C. double-pull-double-throw switch (3-E). The DPDT switch controlled the direction of a four lead, 20 rpm synchronous reversible motor (3-F), which was geared down to drive a second Powerstat (3-G) at 0.11 rpm. The output of the first variac was fed to the second variable one, which was connected to the bath heaters.

When light fell on the photocell, current was passed through the heaters and the motor drove the variac to increase the voltage to the heaters. When the light moved off the photocell, the current to the heaters was cut and the variac was driven back. The flow rate of the cooling water and the setting of the primary variac were controlled so that equal periods of heating and cooling were obtained every 30 to 40 seconds. In this way the bath was controlled to $\pm 0.003^{\circ}$ C of the containers. The bath temperature was measured with a platinum resistance thermometer and Müeller temperature bridge.

B. Preparation of Solutions

The rare-earth oxides used in preparing the solutions were obtained from the rare earth separation group of the Ames Laboratory of the Atomic Energy Commission. Table 1 gives the spectrographic analysis of the oxides. The oxides

Table 1. Spectrographic analysis of rare-earth oxides.

La_2O_3 for $LaCl_3$ solution:	Ca	<
	Other impurities	< 0.04%
La_2O_3 for $La(NO_3)_3$ solution:	Ca	< 0.10%
	Fe	< 0.05%
	Ce	≲ 0.03%
	Nd	≲ 0.02%
	Pr	≲ 0.03%
	Other impurities	< 0.01%
Yb_2O_3 for $YbCl_3$ solutions:	Ca	< 0.03%
	Sm	≲ 0.06%
	Pr	≲ 0.08%
	Other impurities	< 0.02%
Yb_2O_3 for $Yb(NO_3)_3$ solutions:	Ca	~ 0.04%
	Fe	< 0.02%
	Y	~ 0.01%
	La	~ 0.09%
	Other impurities	< 0.01%
Nd_2O_3 for $NdCl_3 \cdot 6H_2O$ preparation:	Ca	< 0.03%
	Fe	< 0.01%
	Pr	≲ 0.08%
	Sm	≲ 0.06%

were dissolved with C. P. Baker and Adamson hydrochloric and nitric acids. Conductivity water having a specific conductivity of 1.5×10^{-6} mhos or less was used in the preparations and for dilutions of the stock solutions.

The stock solutions for this work were made by an "excess oxide" method. An amount of rare-earth oxide was added to a deficiency of acid and the mixture brought to a boil. After dissolution had occurred, the excess oxide was filtered off. A 25 ml. aliquot of the filtrate was titrated with dilute acid, yielding a strong acid-weak base titration curve. The bulk

solution was then titrated to the pH of the inflection point of the curve. It was brought to a boil and then diluted back to its original volume. Another aliquot was taken and the procedure repeated. When the bulk solution remained at the equivalence pH after boiling, it was placed in a volumetric flask and diluted to one liter.

In the case of the chlorides, the stock solution was analyzed for both rare-earth and chloride content; for the nitrates, only a rare-earth analysis was made. Chlorides were determined gravimetrically as described by Willard and Furman (88). For the rare-earth analysis, a weighed amount of solution was precipitated with a slight excess of recrystallized oxalic acid in a weighed crucible. This was evaporated to dryness and then fired to the oxide in a muffle furnace at 1000° C. The precision obtained for the analyses was better than one part per thousand.

The solutions used in the experiments were prepared by dilution of the stock solution. These dilutions were made by weight and the final concentrations were calculated by means of the formulas

$$P = \frac{wP_o}{W+w} \tag{57}$$

and

$$m = \frac{P \times 10^3}{1000 - M_2 P} \tag{58}$$

where P = moles of solute per 1000 grams of final solution,

P_o = moles of solute per 1000 grams of stock solution,

w = weight of stock solution,

W = weight of water,

m = molality of final solution,

and M_2 = molecular weight of solute.

Vacuum corrections were calculated from the data of Ayers (24).

pH data for the stock solutions, for the experimental solutions, and for the final solutions resulting from the dilution experiments, are given in Table 2. In the case of the $LaCl_3$ data, sufficient quantities of all the solutions were not available at the time these measurements were made. The significance of this set of data will be discussed later.

C. Experimental Procedure

In preparation for a run, the calorimeter containers and inner parts of the calorimeter were rinsed with conductivity water. The sample holders were soaked in the water for at least five hours and then air dried. The solution to be used was placed in a water bath at 25° C.

Solution was transferred to the sample holder, with bottom caps in place, with a 10 ml. pipet. The upper cap was screwed onto the barrel and the sample holder weighed. By repeating this for each barrel of the sample holders, the

Table 2. pH data for solutions.

Salt	Soln. no.	m	pH of solution	Dilution Experiment	
				pH of water	pH of final solution
$LaCl_3$	2	0.01977	5.92	5.41	5.68
	4	0.06017	5.31	5.52	5.72
	5	0.1358	5.31	5.48	5.68
	stock	0.1811	5.02		
$YbCl_3$	1	0.01117	5.17	5.52	5.45
	2	0.02341	5.16	5.51	5.48
	3	0.03562	4.92	5.42	5.43
	4	0.06036	4.92	5.44	5.40
	5	0.1203	4.67	5.41	5.34
	7	0.1641	4.59	5.42	5.36
	6	0.2029	4.52	5.53	5.30
	stock	0.3551	4.26		
$La(NO_3)_3$	1	0.01125	5.63	5.58	5.75
	2	0.02087	5.59	5.58	5.79
	3	0.04945	5.40	5.49	5.74
	4	0.07200	5.43	5.56	5.70
	5	0.1447	5.39	5.59	5.70
	6	0.2052	5.19	5.46	5.64
	stock	0.3009	5.09	5.49	5.60
$Yb(NO_3)_3$	1	0.02428	5.22	5.54	5.84
	2	0.04680	5.21	5.50	5.77
	3	0.09137	5.02	5.44	5.67
	4	0.1763	4.87	5.48	5.60
	5	0.2538	4.68	5.67	5.63
	stock	0.5621	4.20	5.60	5.38

weight of the samples were obtained. The four samples were always within 0.01 gram of their mean weight. The sample holders were reweighed after several hours to insure that leak tight seals had been obtained. The sample holders were then mounted on their supporting rods.

Sufficient water was weighed into each calorimeter con-

tainer to give a total liquid content, water plus sample solution, of 900 grams. The weighings were made to the nearest drop on a two kilogram balance.

With the main thermel in place, the containers were raised to their lids, the seal about their rims was made and the nylon line tightened to support their weight. The submarine jacket was fastened to its lid and the bath raised into place. Stirring was then begun and the switch was set to pass current through the dummy heater.

The bath was brought to the same temperature as the containers and the equilibrium temperature of the system noted. To bring the system to within 0.02° of 25° C, a thermal head was maintained between the bath and the calorimeter. The bath was heated (or cooled) to a certain point, predetermined through experience, and then returned to equilibrium with the containers. Usually only one such cycle was required to obtain the desired temperature. At this point the bath began to control automatically.

Next the temperature difference between the two containers was reduced to the microdegree range. When this was obtained, the potential of the main thermopile could be recorded with the amplifier on gain 18. Finally, the appropriate trickle heater was then turned on and adjusted to maintain a steady temperature difference between the two containers. The amount of current needed through the heater to compensate for drifts seldom exceeded 15 milliamperes. Al-

though the temperature drift could rarely be completely eliminated, it was usually reduced to a few microdegrees per hour.

Three types of experiments were run: electrical calibrations, blank experiments, and dilution experiments. The general procedure was similar in each case. During the fore period of 15 to 30 minutes, the temperature difference between the calorimeter containers was recorded. Then the given experiment was made and the recording potentiometer traced the change in the temperature difference during and after the experiment. When the system had come to equilibrium, which was realized when a linear tracing was again obtained, the temperature difference was recorded for a 15 to 30 minute after period.

In general, the fore and after drifts were not parallel. To evaluate the deflection of the potentiometer pen, straight lines were drawn through the tracings of the fore and after periods. The distance between the lines was measured perpendicular to the fore drift at the point where the experiment was begun and perpendicular to the after drift at the point where equilibrium was first obtained. In the case of the blank and the dilution experiments, the average of the two measurements was used. Two separate values were obtained for the calibrations. The change in the drift was attributed to a lag in thermal conductivity between the heater, the liquid in the container and the thermopile, to slight changes

in stirring, to differing evaporation losses, and to fluctuations of the bath temperature. The first cause predominated for the calibrations, but was probably canceled out for the dilution experiments.

For a calibration experiment, one of the heaters was switched on for a period of 15 to 40 seconds. The current of approximately 15 milliamperes was determined exactly by measuring the potential across the standard resistor. The length of the heating period was obtained from the electronic timer. The amount of heat liberated was calculated by the formula

$$q_{el} = \frac{1}{4.184} \frac{R_h}{R_s^2} E_s^2 t \quad , \tag{59}$$

where q_{el} = heat liberated in defined calories,

R_h = heater resistance,

R_s = standard resistance,

E_s = potential across the standard resistor,

and t = time in seconds.

The heater resistances were determined by passing current through the heater and measuring the potential across it and the standard resistor. The sensitivity was calculated in calories per mm pen displacement.

Blank experiments, with 10 ml of water as the sample, were made to determine the heat of opening of the sample holders. The heat evolved in opening a sample was quite small and was determined from the pen displacement.

A dilution experiment was a combination of the previous

two. A sample in one of the containers was opened and then heating was begun in the opposite container. The length of the heating period ranged from 20 seconds to five minutes, depending upon the concentration of the sample solution. The amount of electrical heating was chosen to balance as nearly as possible the heat liberated in the dilution. In a few experiments, especially when the more concentrated solutions were used for the first time, a second heating in one of the containers was required to realize this balance. For sample solutions below 0.1 molal a current of 15 milliamperes was us3d, for those above this concentration a current of 25 milliamperes. The current was stable during the heating periods to better than 10 microamperes at 15 milliamperes and 20 microamperes at 25 milliamperes. The heat liberated in the dilution was calculated from the electrical heat and the amount of the pen displacement, that is,

$$q_{dil} = q_{el} + q_{dis} \quad . \tag{60}$$

D. Treatment of Data

Since in each container, two samples could be opened one after the other, the experiments were of two types. In the first, $\underline{q_1}$ calories of heat were evolved when a sample of molality $\underline{m_1}$, containing $\underline{n_2'}$ moles of salt, was diluted into water to give a final solution of molality $\underline{m_2}$. In the second type, $\underline{q_2}$ calories of heat were evolved when a sample of

molality m_1, containing n_2'' moles of salt, was diluted into a solution of molality m_2 to give a final solution of molality m_3. From equation (25), the heats given off for the two cases are

$$q_1 = n_2' \left[\phi_{L(m_1)} - \phi_{L(m_2)}\right] + q_o \tag{61}$$

and

$$q_2 = n_2'' \left[\phi_{L(m_1)} - \phi_{L(m_3)}\right] + n_2' \left[\phi_{L(m_2)} - \phi_{L(m_3)}\right] + q_o \tag{62}$$

where q_o is the heat of opening of the sample holder.

The heats of dilution per mole as given in equation (26) are

$$\Delta H_{1,2} = \phi_{L(m_2)} - \phi_{L(m_1)} \quad , \tag{63}$$

$$\Delta H_{1,3} = \phi_{L(m_3)} - \phi_{L(m_1)} \quad , \tag{64}$$

$$\Delta H_{3,2} = \phi_{L(m_2)} - \phi_{L(m_3)} \quad , \tag{65}$$

where $\Delta H_{i,k}$ is the heat adsorbed when a solution of concentration m_i is diluted to concentration m_k. The quantities $\Delta H_{1,2}$ and $\Delta H_{1,3}$ are referred to as "long chord dilutions" and $\Delta H_{3,2}$ as a "short chord dilution". These terms arise from the plot of heat of dilution versus concentration. When equations (61) and (62) are combined with equations (63), (64) and (65), one obtains for the heats of dilution

$$\Delta H_{1,2} = - \frac{q_1 - q_o}{n_2'} \quad , \tag{66}$$

$$\Delta H_{1,3} = - \frac{q_1 + q_2 - 2q_o}{n_2' + n_2''} \quad , \tag{67}$$

and

$$\Delta H_{3,2} = - \frac{(q_1 - q_o) - \frac{n_2''}{n_2'} (q_2 - q_o)}{(n_2' + n_2'')} \quad . \qquad (68)$$

When $n_2' \approx n_2''$, which was the case in these experiments, equation (68) reduces to

$$\Delta H_{3,2} = - \frac{q_1 - q_2}{n_2' + n_2''} \quad . \qquad (69)$$

To establish the concentration dependence of ϕ_L, experiments were run at various concentrations. Several runs were made at each concentration, giving an average value for the $\Delta H_{i,k}$'s for each concentration.

Absolute values of ϕ_L cannot be calculated directly from heats of dilution. The data treatment used to determine ϕ_L followed that of Young and co-workers (81, 82). The modification of Wallace and Robinson (86) was particularly applicable to this work since a short chord could be obtained without dismantling the apparatus. In this treatment, the slope of ϕ_L versus $m^{\frac{1}{2}}$ is determined for the very dilute concentration range from the values of $\Delta H_{3,2}$. The equation corresponding to the slope is integrated to give an equation for ϕ_L applicable over this concentration range. By adding the heat of dilution to the ϕ_L for the very dilute solution resulting from the experiment, absolute values of ϕ_L for the sample solution can be calculated.

The average slope of the ϕ_L versus $m^{\frac{1}{2}}$ plot for solution

$\underline{i}$ over the concentration range $\underline{m_3^{\frac{1}{2}}}$ to $\underline{m_2^{\frac{1}{2}}}$ is

$$\overline{P}_i = \frac{-\Delta H_{3,2\,(i)}}{m_3^{\frac{1}{2}} - m_2^{\frac{1}{2}}} \quad . \tag{70}$$

It is assumed that the slope, $\underline{S}$, of $\underline{\phi_L}$ versus $\underline{m^{\frac{1}{2}}}$ has the form

$$S = S^o + Bm^{\frac{1}{2}} + Cm + \ldots\ldots \tag{71}$$

and that no more than three terms are needed for this very dilute range. Because only the average slopes can be determined experimentally equation (71) is written in the form

$$P_i = S^o + Bx_i + Cx_i^2 \quad , \tag{72}$$

where P_i = the true slope of the ϕ_L versus $m^{\frac{1}{2}}$ plot at x_i, the midpoint of the concentration range,

and $x_i = \frac{1}{2}\left[m_3^{\frac{1}{2}} \quad m_2^{\frac{1}{2}}\right]$.

Since $\overline{P}_i$ is the average value of S for the given concentration range,

$$\overline{P}_i = \frac{\int_{m_2^{\frac{1}{2}}}^{m_3^{\frac{1}{2}}} S\,dm^{\frac{1}{2}}}{m_3^{\frac{1}{2}} - m_2^{\frac{1}{2}}} \quad , \tag{73}$$

or

$$\overline{P}_i = S^o + Bx_i + \frac{C}{3}\left(4x_i^2 - m_3^{\frac{1}{2}} - m_2^{\frac{1}{2}}\right) \quad . \tag{74}$$

The difference between the true slope and the average slope is

$$P_i - \overline{P}_i = -C\,\frac{\delta_i^2}{12} \quad , \tag{75}$$

where $\delta_i = m_3^{\frac{1}{2}} - m_2^{\frac{1}{2}}$.

When equations (72) and (75) are combined,

$$\overline{P}_i = S^o + Bx_i + C(x_i^2 + \frac{\delta_i^2}{12}) \quad . \tag{76}$$

If only a two parameter equation is needed to represent the slope, $\underline{S}$, equation (71) becomes

$$S = S^o + Bx_i \quad . \tag{77}$$

Then $\overline{P}_i = P_i$, and

$$\overline{P}_i = S^o + Bx_i \quad . \tag{78}$$

The constants for equations (76) and (78) were obtained by a method of least squares in which the values were weighted by the inverse square of the probable errors in $\underline{\overline{P}_i}$. The constants were substituted in equation (71) or (77), which was integrated to yield

$$\underline{\phi_L} = S^o m^{\frac{1}{2}} + \frac{B}{2} m + \frac{C}{3} m^{3/2} \quad , \tag{79}$$

which gives $\underline{\phi_L}$ for the very dilute range.

The absolute value of the apparent molal heat content, $\underline{\phi_L}$, for the sample solution under study was obtained by combining equations (63) and (64) with equation (79).

To obtain relative partial molal heat contents, it was necessary to have an analytic function to represent the concentration dependence of $\underline{\phi_L}$. This function was obtained by applying an unweighted least squares treatment to the $\underline{\phi_L}$ data. After a suitable empirical equation was obtained for $\underline{\phi_L}$ versus $\underline{m^{\frac{1}{2}}}$, $\underline{\overline{L}_2}$ and $\underline{\overline{L}_1}$ were calculated by equations (22) and (23) re-

spectively.

E. Electrical Calibrations

The differential calorimeter was calibrated in terms of the deflection of the potentiometer pen caused by liberating a given amount of heat in one of the containers. The sensitivity was defined as calories per mm pen displacement. By calibrating the system in this way, it was not necessary to determine the water equivalents of the two sides. Nevertheless, the two sides were constructed so that the heat capacities of the two were very nearly identical.

Each time the thermopile or any part of its amplification or recording circuit was changed, the sensitivity of the system changed and a new series of calibrations was needed. Four different series of calibrations were made. The first series corresponds to the original system. The second calibration was necessary after the tubes in the amplifier and recorder were replaced. The last two changes in sensitivity resulted when lead wires from the thermopile broke; in each case all the lead wires were cut back and extensions soldered to the leads. The results of the four series of calibrations are summarized in Table 3. The sensitivities of the various series applied to the determinations as follows: series A to the $LaCl_3$ data, the blank experiments and the first eight $YbCl_3$ runs, series B to the last ten $YbCl_3$ runs, series C to the $La(NO_3)_3$ runs, and series

Table 3. Summary of electrical calibrations.

Series	Container	No. of detn.	Displacement measured perpendicular to the	Average sensitivity[a]	σ[a]	Average sensitivity for container	Average sensitivity for system	σ
A	I	35[b]	fore drift	5.24	0.24	5.28		
			after drift	5.32	0.27			
							5.27	0.23
	II	36[c]	fore drift	5.22	0.19	5.26		
			after drift	5.30	0.22			
B	I	26[b]	fore drift	4.70	0.28	4.71		
			after drift	4.71	0.20			
							4.72	0.27
	II	27	fore drift	4.71	0.31	4.73		
			after drift	4.76	0.30			
C	I	43	fore drift	4.95	0.25	4.98		
			after drift	5.00	0.26			
							4.97	0.24
	II	41[b]	fore drift	4.91	0.20	4.97		
			after drift	5.03	0.23			
D	I	31	fore drift	4.85	0.25	4.88		
			after drift	4.91	0.25			
							4.91	0.29
	II	33	fore drift	4.89	0.20	4.94		
			after drift	5.00	0.19			

[a]The sensitivity and the standard deviations are given in cal/mm x 10^4.

[b]One value not used.

[c]Two values not used.

D to the $Yb(NO_3)_3$ data.

The number of determinations made by heating in each container for the specific series is given in column three. A few values have not been used in calculating the average sensitivities either because the specific value was higher or lower than the average by four times the standard deviation or because a drastic change in drift occurred during the experiment.

Columns four and five give the values obtained for the sensitivity depending on how the displacement was measured. As can be seen, the distance measured perpendicular to the after drift was smaller on the average for all series. This was interpreted to mean that true equilibrium was reached only after some length of time. Unfortunately, the drifts were usually only stable for about an hour. Rather than arbitrarily decide whether a slight change in drift was due to the attainment of true equilibrium or to some slight fluctuation in bath temperature, the procedure outlined previously was followed.

Column two gives the container in which the electrical heating was made and column seven the average sensitivity for each container. No reproducible difference was noted between containers. The average sensitivity for the system is given in column eight. This value was used to evaluate the $q_{displacement}$ in the blank and dilution experiments.

The standard deviation, $\underline{\sigma}$, which is listed for the data

is defined by

$$\sigma = \left[\frac{\sum_{i=1}^{n} (X_i - \bar{X})}{n-1}\right]^{\frac{1}{2}} , \qquad (80)$$

where X_i = value obtained for measurement $\underline{i}$,

$\bar{X}$ = average value,

and n = number of determinations.

From the high values for the standard deviation of the calibrations, it is to be expected that larger deviations will be obtained for experiments in which $q_{displacement}$ contributes heavily to the total heat. This will be seen in the data for the blank experiments and for dilutions involving sample solutions of low concentration.

F. Blank Experiments

The heat of opening the sample holders, $\underline{q_o}$, was determined by running a series of blank experiments using water as the sample. The results are listed in Table 4. The probable error, $\underline{E}$, of the arithmetic mean is defined as

$$E = \frac{0.6745\sigma}{n^{\frac{1}{2}}} . \qquad (81)$$

The large deviations in these measurements resulted from (a) evaluating the heat evolved solely from the pen displacement, (b) opening the samples manually, and (c) the platinum disks not puncturing exactly the same each time.

Table 4. Heat of opening sample holders.

Number of determinations	23 samples opened
Average heat of opening	12.3×10^{-3} calories
Standard deviation,	2.5×10^{-3} calories
Probable error, E	3.5×10^{-4} calories

G. Dilution Experiments

Heats of dilution were measured for several solutions each of lanthanum chloride, ytterbium chloride, lanthanum nitrate and ytterbium nitrate. The experimental data and the various thermodynamic properties from the measurements are presented in Tables 5 through 16 and in Figures 5 through 12. The erbium chloride data of Naumann (26) have also been recalculated and the results are given in the Appendix. All heat quantities listed in the tables and figures are given in defined calories. Since the data for all the salts were treated similarly, a general explanation of the tables and figures will be given here to prevent needless repetition.

Tables 5, 8, 11 and 14 list the experimental data and the heats of dilution. The molalities of solutions, numbered in the order in which they were made up, are given. The data are grouped into runs. In some cases different solutions were used in the two containers; thus several groupings of two, instead of four, samples are listed. In these tables, $\underline{q_E}$, is the electrical heat calculated by equation (59);

q_{dis} is the heat evaluated from the displacement of the potentiometer pen and the sensitivity of the system; $q - q_o$ is the total heat evolved in the dilution experiment minus the heat of opening the sample holder; and n_2' and n_2'' are the moles of salt present in the first and second samples respectively. $\Delta H_{1,2}$ was calculated by equation (66), $\Delta H_{1,3}$ by equation (67), and $\overline{P}_i$ by equation (69) and (70). The averages of these three quantities are given for each solution.

Tables 6, 9, 12 and 15 give the short chord data and the evaluation of the relative apparent molal heat contents. In these tables, m_1 is the concentration of the sample solution; the m_k's are the average concentrations of the very dilute solutions resulting from the dilution experiments; $\overline{P}_i$ is the average $\overline{P}_i$ for a given sample solution; and $E_{\overline{P}_i}$ is the probable error of the average $\overline{P}_i$. Five figures are given for the concentrations and four for the average $\overline{P}_i$. While it is recognized that the last figures are not significant, they were used in applying the least squares treatment to this data. Three types of equations were used in least squares treatments to determine the concentration dependence of $\overline{P}_i$. The first type of equation contained two free parameters,

$$\overline{P}_i = a + bx_i^{\frac{1}{2}} \quad . \tag{82}$$

The second treatment used an equation with one free parameter and the Debye-Hückel limiting law value of 6925,

$$\overline{P}_i = 6925 + bx_i \quad . \tag{83}$$

The third type of treatment employed a three parameter

equation,

$$\overline{P}_i = a + bx_i + c(x_i^2 + \frac{\delta^2}{12}) \quad . \tag{84}$$

These equations correspond to equations (76) and (78) in the treatment of data section. The short chord data was used to calculate $\underline{\phi_L}$'s for the very dilute solutions. These are listed in column seven of the tables as $\underline{\phi_{L(m_k)}}$. The absolute values of $\underline{\phi_L}$ were obtained by rearranging equations (63) and (64) to give

$$\phi_{L(m_1)} = \phi_{L(m_k)} - \Delta H_{1,k} \quad . \tag{85}$$

In this way two values for the relative apparent molal heat content were obtained for each solution. The two $\underline{\phi_{L(m_1)}}$'s were averaged to give a final absolute value of $\underline{\phi_L}$. This last quantity was used in a least squares treatment to find an empirical expression for $\underline{\phi_L}$ versus $\underline{m^{\frac{1}{2}}}$. These least squares treatments were applied to an equation of the type

$$\phi_L = am^{\frac{1}{2}} + bm + cm^{3/2} \quad . \tag{86}$$

It should be remembered that while the empirical equations for the concentration dependence of $\underline{\overline{P}_i}$ and $\underline{\phi_L}$ give good representations of the data presented, they are probably unsuitable for extrapolations to higher concentrations.

Tables 7, 10, 13 and 16 list the thermodynamic properties for the various solutions. Both the derived values and the values calculated from the empirical equations are listed for $\underline{\phi_L}$, the relative apparent molal heat content. The relative partial molal heat contents of solvent and solute, $\underline{\overline{L}_1}$

and $\overline{L}_2$, were calculated by equations (22) and (23) from the empirical expressions for ϕ_L versus $m^{\frac{1}{2}}$.

The short chord data are plotted in Figures 5, 7, 9 and 11. When two values for P_i were obtained within 0.1 x 10^3, only one chord was drawn. It is immediately apparent that the uncertainty in $\overline{P}_i$ increases rapidly with decreasing concentration. This is as expected since for the lower concentration sample solutions a relatively larger proportion of the heat is measured from the pen displacement. Another reason for this can be seen from equations (69) and (70). Even if the heat evolved could be measured to the same precision, $\Delta H_{3,2}$ decreases with decreasing concentration and the relative error in $\Delta H_{3,2}$ thus increases. Furthermore, the denominators in these equations are decreasing and the uncertainty in $\overline{P}_i$ is further increased.

Figures 6, 8, 10 and 12 show the concentration dependence of the relative apparent molal heat contents. Curves representing the empirical equation are drawn through the experimentally derived points for ϕ_L .

1. Lanthanum chloride

The data for the lanthanum chloride solutions are tabulated in Tables 5, 6 and 7 and are plotted in Figures 5 and 6.

Two least squares treatments were run to determine the concentration dependence of $\overline{P}_i$. The first, corresponding to equation (82), yielded the expression

$$\overline{P}_i = 6630 - 24650x_i \quad , \qquad (87)$$

Table 5. Heats of dilution of lanthanum chloride solutions at 25° C.

Soln. No. m	Run	Sample	$q_E \cdot 10^3$	$q_D \cdot 10^3$	$q-q_\delta \cdot 10^3$	$n_2' \cdot 10^3$ $(n_2'+n_2'') \cdot 10^3$	$-\Delta H_{1,2}$	$-\Delta H_{1,3}$	$\bar{F}_i \cdot 10^3$
1	3	Outer I	96.0	-29.9	53.8	0.09601	560.4		
		Inner I	56.2	- 5.5	38.4	0.1922		479.6	18.75
0.009645		Outer II	50.3	10.4	48.4	0.09624	502.9		
		Inner II	56.9	5.4	50.0	0.1924		511.3	-1.95
	5	Outer II	71.6	-10.7	48.6	0.09622	505.1		
		Inner II	(Breaker rod broke)						
		Outer I	64.8	- 2.4	50.1	0.09622	520.7		
		Inner I	55.9	1.2	44.8	0.1924		493.2	6.51
	6	Outer II	66.9	- 9.1	45.5	0.09620	473.0		
		Inner II	75.1	-19.1	43.7	0.1925		463.5	2.22
	16	Inner II	67.7	- 0.1	55.3	0.09622	574.7		
		Outer II	60.6	- 4.6	43.7	0.1925		514.4	14.27
		Outer I	67.1	- 5.5	49.3	0.09620	512.5		
		Inner I	66.7	-17.4	37.0	0.1925		448.4	15.13
	17	Outer I	64.7	- 2.3	50.1	0.09623	520.7		
		Inner I	52.5	3.0	43.2	0.1924		485.0	8.50
		Outer II	61.1	0.3	49.1	0.09618	510.5		
		Inner II	56.4	0.5	44.6	0.1923		487.3	5.55
	18	Inner I	62.5	6.3	56.5	0.09619	587.3		
		Outer I	55.0	7.6	50.3	0.1923		555.3	7.62
						Average	526.8	493.1	8.53
						Standard Deviation	35.8	31.9	6.60

Table 5. (Continued).

Soln. No. m	Run	Sample	$q_E \cdot 10^3$	$q_D \cdot 10^3$	$q-q_D \cdot 10^3$	$n_2' \cdot 10^3$ $(n_2'+n_2'') \cdot 10^3$	$-\Delta H_{1,2}$	$-\Delta H_{1,3}$	$\bar{r}_i \cdot 10^3$
2	2	Outer II	146.8	- 0.9	133.6	0.1972	677.5		
		Inner II	123.2	3.3	114.2	0.3943		628.4	8.14
0.01975		Outer I	160.7	-37.3	111.1	0.1971	563.7		
		Inner I	65.2	53.6	106.5	0.3942		552.0	1.94
	6	Outer I	152.6	-15.7	124.6	0.1970	632.5		
		Inner I	135.0	-14.4	118.3	0.3941		590.9	6.85
	12	Outer II	141.6	- 2.0	127.3	0.1970	646.1		
		Inner II	121.2	6.3	115.2	0.3938		615.7	5.09
		Outer I	141.7	-11.9	117.5	0.1969	596.6		
		Inner I	119.5	- 2.1	105.1	0.3938		565.2	5.22
	13	Outer I	141.8	-10.4	119.1	0.1970	604.5		
		Inner I	119.5	- 0.5	106.7	0.3940		573.1	5.21
		Outer II	140.4	- 1.5	126.6	0.1971	642.2		
		Inner II	119.2	5.0	111.9	0.3943		604.9	6.17
	18	Inner II	139.5	0.2	127.4	0.1970	646.8		
		Outer II	119.5	0.8	108.0	0.3939		597.6	8.14
						Average	626.2	591.0	5.85
					Standard	Deviation	35.9	26.1	2.01

Table 5. (Continued).

Soln. No. m	Run	Sample	$q_E \cdot 10^3$	$q_D \cdot 10^3$	$q-q_o \cdot 10^3$	$n_2' \cdot 10^3$ $(n_2'+n_2'') \cdot 10^3$	$-\Delta H_{1,2}$	$-\Delta H_{1,3}$	$\bar{P}_i \cdot 10^3$
3	1	Outer II	293.9	-23.3	258.3	0.3399	759.8		
		Inner II	267.6	-24.3	231.0	0.6798		719.8	5.07
0.03410		Outer I	286.8	-25.9	248.6	0.3398	731.6		
		Inner I	277.5	-34.8	230.4	0.6799		704.6	3.38
	7	Outer II	318.4	-45.3	260.8	0.3401	766.9		
		Inner II	(Leak developed in submarine jacket)						
	8	Outer II	305.3	-30.3	262.7	0.3400	772.6		
		Inner II	276.7	-44.3	220.1	0.6801		709.9	7.88
		Outer I	296.4	-28.9	255.2	0.3400	750.5		
		Inner I	269.8	-38.2	219.3	0.6800		697.8	6.65
	11	Outer I	269.4	-14.1	243.0	0.3394	716.0		
		Inner I	220.2	5.7	213.6	0.6795		671.9	5.45
		Outer II	261.5	0.1	249.3	0.3389	735.7		
		Inner II	218.3	8.3	214.3	0.6786		683.2	6.50
	15	Inner I	260.3	- 1.6	246.4	0.3400	724.8		
		Outer I	217.2	- 6.6	198.3	0.6798		654.2	8.91
						Average	744.7	691.6	6.26
						Standard Deviation	20.7	23.0	1.84

Table 5. (Continued).

Soln. No. m	Run	Sample	$q_E \cdot 10^3$	$q_D \cdot 10^3$	$q-q_o \cdot 10^3$	$n_2^I \cdot 10^3$ $(n_2^I+n_2^{II}) \cdot 10^3$	$-\Delta H_{1,2}$	$-\Delta H_{1,3}$	$\bar{P}_i \cdot 10^3$
4	4	Outer II	527.7	- 1.9	513.5	0.5992	857.0		
		Inner II	421.7	26.1	435.5	1.199		791.7	6.19
0.06012		Outer I	528.7	-13.1	503.3	0.5991	840.0		
		Inner I	443.9	- 2.5	429.1	1.198		778.3	5.87
	9	Outer II	524.3	0.9	512.9	0.5988	856.5		
		Inner II	448.8	7.1	443.6	1.198		798.5	5.49
		Outer I	519.5	- 8.0	499.2	0.5990	833.7		
		Inner I	434.2	8.0	429.9	1.198		775.5	5.48
						Average	846.7	786.1	5.76
					Standard	Deviation	11.9	10.9	.34
5	10	Outer I	1410.9	- 2.4	1396.2	1.349	1034.8		
		Inner I	1189.5	-22.8	1154.4	2.697		945.6	5.67
0.1357		Outer II	1422.5	8.4	1418.6	1.349	1051.5		
		Inner II	1170.4	5.8	1163.9	2.698		957.1	5.97
	15	Inner II	1386.6	30.0	1404.3	1.349	1041.1		
		Outer II	1152.6	- 5.3	1135.0	2.698		941.3	6.31
	20	Inner I	1360.0	62.6	1410.3	1.348	1046.6		
		Outer I	1192.3	-16.3	1163.7	2.697		954.2	5.77
		Inner II	1412.5	4.9	1405.1	1.348	1042.4		
		Outer II	1172.7	22.4	1182.8	2.696		959.9	5.22
						Average	1043.3	951.6	5.79
					Standard	Deviation	6.2	7.9	.40

Table 5. (Continued).

Soln. No. m	Run	Sample	$q_E \cdot 10^3$	$q_D \cdot 10^3$	$q-q_o \cdot 10^3$	$n_2^I \cdot 10^3$ $(n_2^I+n_2^{II}) \cdot 10^3$	$-\Delta H_{1,2}$	$-\Delta H_{1,3}$	$\bar{P}_i \cdot 10^3$
6	14	Outer I	2000.3	29.9	2017.9	1.796	1123.7		
		Inner I	1665.7	16.5	1669.9	3.592		1026.6	5.31
0.1809		Outer II	1960.6	53.4	2001.7	1.798	1113.4		
		Inner II	1684.2	7.1	1679.0	3.595		1023.7	4.92
	21	Outer I	1997.7	19.5	2004.9	1.797	1115.5		
		Inner I	1661.6	12.5	1661.8	3.594		1020.2	5.23
		Outer II	1984.5	37.0	2009.2	1.797	1118.0		
		Inner II	1648.8	25.9	1662.4	3.595		1021.3	5.28
						Average	1117.6	1023.0	5.19
					Standard	Deviation	4.5	2.8	.18

Table 6. Short chord data and relative apparent molal heat content of lanthanum chloride solutions at 25° C.

Soln. No.	$m_1^{\frac{1}{2}}$	$m_k^{\frac{1}{2}} \times 10^2$	$x_i \cdot 10^2$	$\overline{P}_i$	$\frac{E}{p_i}$	$\phi_{L(m_k)}$	$-\Delta H_{1,k}$	$\phi_{L(m_1)}$	$\overline{\phi}_L$
1	0.098207	1.0391 1.4613	1.2502	8531	1480	70.3 97.9	527.8 493.1	597.1 591.0	594.1
2	0.14055	1.4873 2.0915	1.7894	5845	479	99.6 138.1	626.2 591.0	725.8 729.1	727.5
3	0.18467	1.9529 2.7468	2.3499	6262	468	129.3 178.6	744.7 691.6	874.0 870.2	872.1
4	0.24520	2.5933 3.6473	3.1203	5758	115	169.2 232.1	846.7 786.1	1015.9 1018.2	1017.1
5	0.36843	3.8915 5.4729	4.6822	5788	120	246.2 333.2	1043.3 951.6	1288.5 1284.8	1286.7
6	0.42534	4.4931 6.3193	5.4062	5185	86	280.0 376.0	1117.6 1023.0	1397.6 1399.0	1398.3

Table 7. Thermodynamic properties of lanthanum chloride solutions at 25° C.

$m^{\frac{1}{2}}$	ϕ_L		$\bar{L}_2$	$-\bar{L}_1 \times 10^3$
	Derived	Eq. 91	Eq. 92	Eq. 93
0.0100	68[a]	68	101	
0.0300	194[a]	195	286	2
0.0500	308[a]	312	451	6
0.07071	413[a]	421	601	16
0.09821	594	553	773	38
0.1406	727	725	983	73
0.1847	872	871	1148	170
0.2452	1017	1031	1317	310
0.3000		1149	1450	488
0.3684	1287	1282	1643	883
0.4253	1398	1400	1872	1540

[a]Derived from equation (89).

which is represented in Figure 5 as a solid line. The second treatment, corresponding to equation (83), gave

$$\bar{P}_i = 6925 - 30826x_i \quad . \tag{88}$$

This is represented as alternate dots and dashes. Since the two limiting slopes were well within the experimental error, equation (88), containing the theoretical limiting slope was used for subsequent calculations. Thus, equation (88) was integrated to give

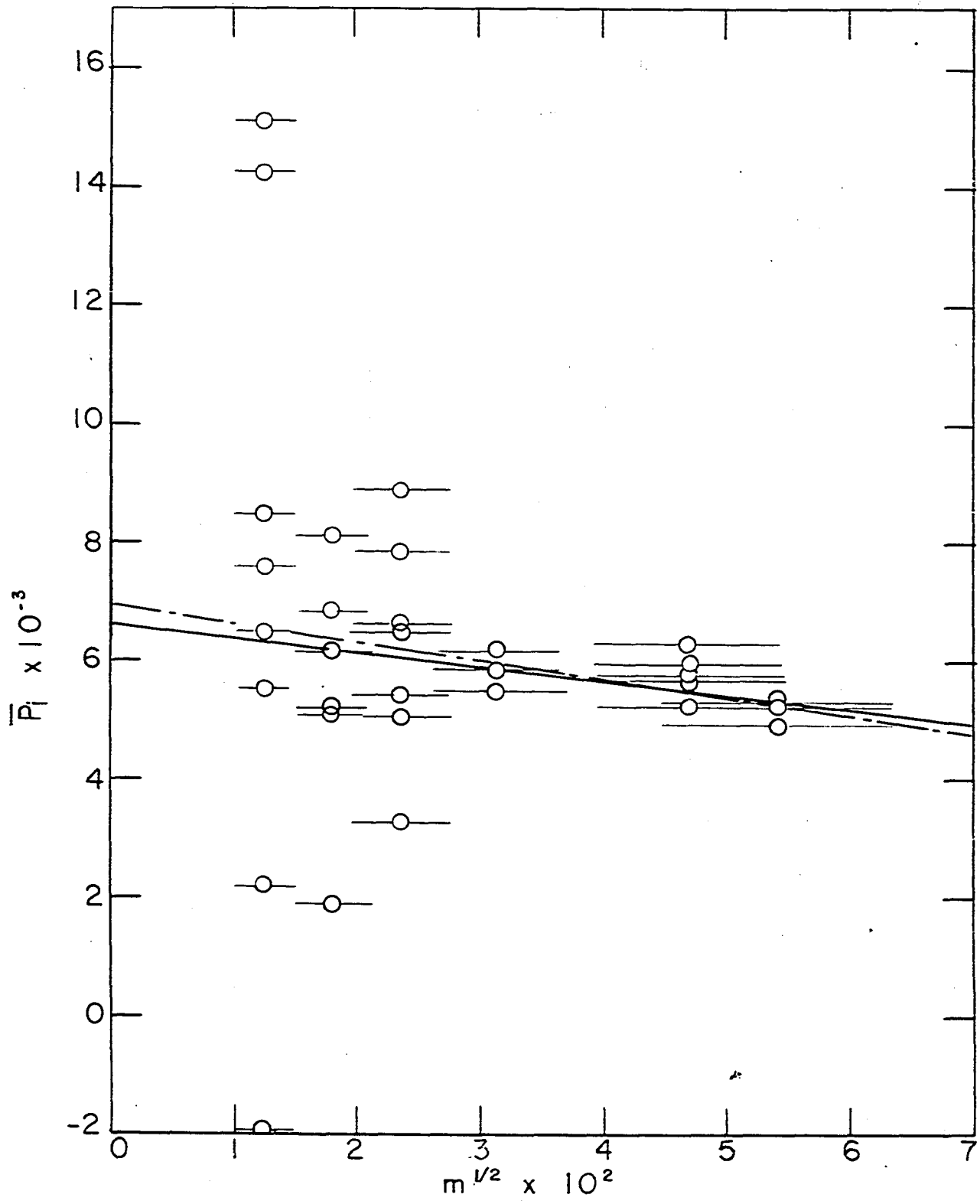

Figure 5. Short chords for lanthanum chloride solutions.

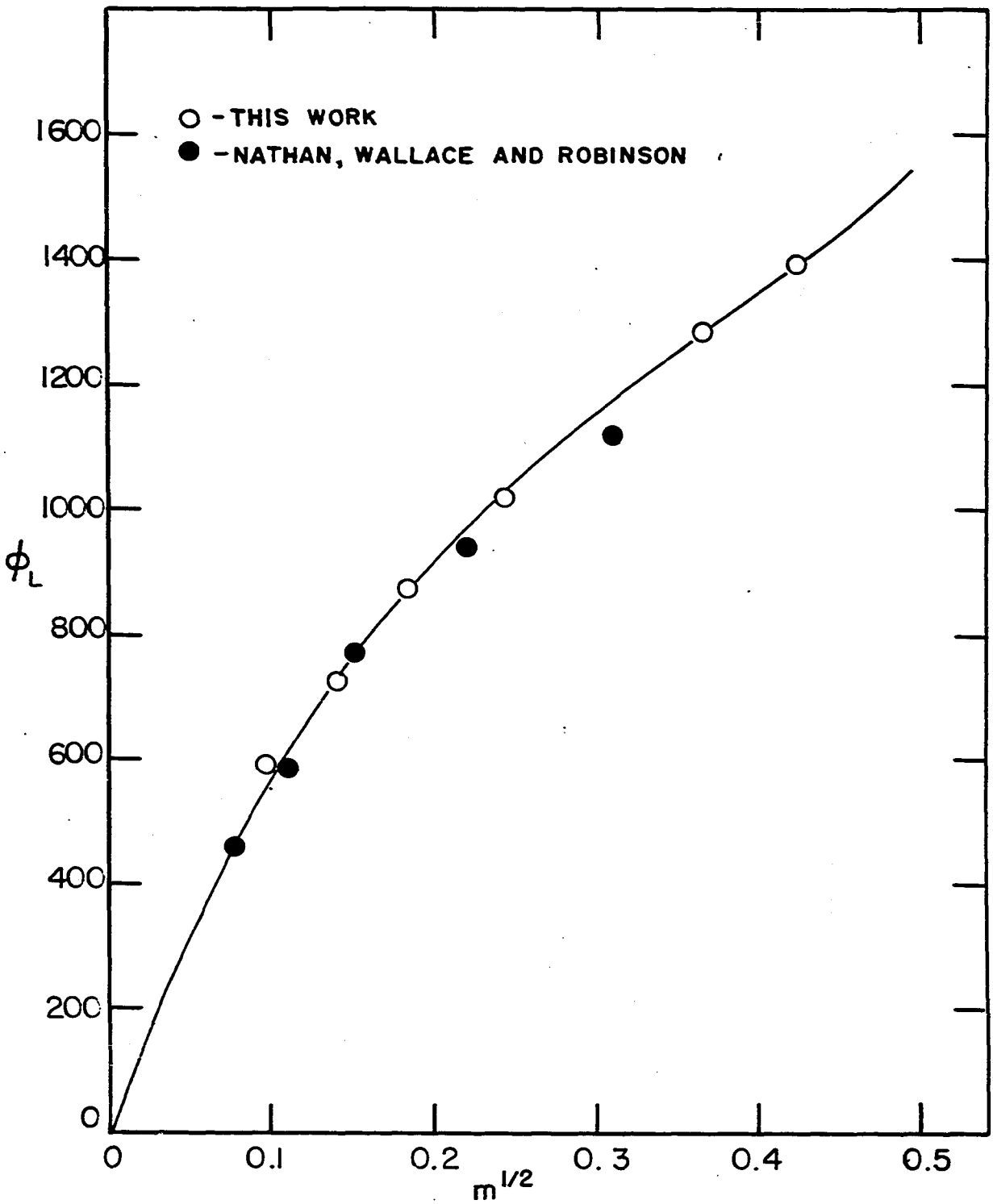

Figure 6. Relative apparent molal heat contents of lanthanum chloride solutions at 25° C.

$$\phi_L = 6925m^{\frac{1}{2}} - 1541.3m \qquad (89)$$

for the very dilute range. This equation was then used to calculate the $\underline{\phi_{L(m_k)}}$'s in Table 6.

The empirical expression for the concentration dependence of $\underline{\phi_L}$ was obtained by least squares treatments using the $\underline{\overline{\phi}_L}$'s listed in Table 6 along with the $\underline{\phi_L}$ value predicted for 0.005m by equation (89). Two such treatments were carried out. The first treatment used three free parameters in equation (86), while the second substituted the limiting law value of 6925 for the constant $\underline{a}$. These yielded the expressions

$$\phi_L = 7228m^{\frac{1}{2}} - 16773m + 17990.6m^{3/2} \qquad (90)$$

and

$$\phi_L = 6925m^{\frac{1}{2}} - 14575m + 14178m^{3/2} \quad . \qquad (91)$$

Equation (91) gave the best fit to the data and was used to evaluate $\underline{\overline{L}_1}$ and $\underline{\overline{L}_2}$. The equations for the relative partial molal heat contents are

$$\overline{L}_2 = 10388m^{\frac{1}{2}} - 29150m + 35445m^{3/2} \qquad (92)$$

and

$$\overline{L}_1 = -62.36m^{3/2} + 262.47m^2 - 382.98m^{5/2} \quad . \qquad (93)$$

The values of these properties for the solutions used are given in Table 7.

The curve defined by equation (91) has a slight inflection point at about $m^{\frac{1}{2}} = 0.4$. This inflection was not brought out in the experimental data, but is merely a property of the

curve fitting equation.

In Figure 6 the data of Nathan, Wallace and Robinson (29) are plotted along with the $\underline{\phi_L}$ values from this work. While agreement is good for the lower concentrations, a difference of about four per cent is present at their highest concentration. These workers obtained only two short chords for each concentration except the highest, where four were obtained. For the very dilute concentration range their equation for $\underline{\phi_L}$ versus $\underline{m^{\frac{1}{2}}}$ was

$$\phi_L = 3129m^{\frac{1}{2}} + 41,121m \quad . \qquad (94)$$

Their limiting slope was considerably below the value predicted by the Debye-Hückel theory. If their short chord data is superimposed upon Figure 5, their chords are effectively "lost", except for the highest concentration where their uncertainty is considerably larger than that of this work. If the short chord data from this work is applied to their heats of dilution, the $\underline{\phi_L}$ values obtained lie uniformly about 15 calories above the curve obtained from this work.

2. Ytterbium chloride

The data for the ytterbium chloride solutions are tabulated in Tables 8, 9 and 10 and are plotted in Figures 7 and 8.

All three types of least squares treatments were used to evaluate the concentration dependence of $\underline{\overline{P}_i}$ for the $YbCl_3$ solutions. They yielded the equations

Table 8. Heats of dilution of ytterbium chloride solutions at 25° C.

Soln. No. m	Run	Sample	$q_E \cdot 10^3$	$q_D \cdot 10^3$	$q-q_o \cdot 10^3$	$n_2' \cdot 10^3$ $(n_2'+n_2'') \cdot 10^3$	$-\Delta H_{1,2}$	$-\Delta H_{1,3}$	$\overline{P}_i \cdot 10^3$
1	6	Inner I	63.5	- 8.8	42.4	0.1113	380.8		
		Outer I	56.8	- 2.4	42.1	0.2227		379.5	0.30
0.01117		Outer II	62.0	7.4	57.1	0.112	513.4		
		Inner II	57.4	3.2	48.3	0.2224		473.9	8.72
	7	Outer I	65.0	-12.5	40.2	0.1113	361.1		
		Inner I	57.3	- 9.0	36.0	0.2226		342.3	4.16
		Inner II	61.4	- 5.8	43.3	0.1113	389.1		
		Outer II	57.0	0.5	44.2	0.2226		393.1	-0.89
	10	Inner I	68.6	- 3.6	52.7	0.1113	473.5		
		Outer I	60.8	3.7	52.2	0.2227		471.1	0.50
		Outer II	69.1	- 1.2	55.6	0.1113	499.8		
		Inner II	58.7	6.6	53.0	0.2225		488.0	2.57
	15	Inner I	67.4	4.9	60.0	0.1113	538.9		
		Outer I	58.0	4.0	49.7	0.2227		492.5	10.17
		Outer II	67.9	- 8.0	47.6	0.1113	427.5		
		Outer II	57.0	2.2	46.9	0.2227		424.4	0.69
	18	Inner I	67.9	- 6.1	49.5	0.1114	444.5		
		Outer I	62.3	2.6	52.6	0.2227		458.5	-3.06
						Average	447.6	435.9	2.57
					Standard	Deviation	63.1	53.6	4.15

Table 8. (Continued).

Soln.No. m	Run	Sample	$q_E \cdot 10^3$	$q_D \cdot 10^3$	$q-q_o \cdot 10^3$	$n_2' \cdot 10^3 / (n_2'+n_2'') \cdot 10^3$	$-\Delta H_{1,2}$	$-\Delta H_{1,3}$	$\bar{P}_1 \cdot 10^3$
2	3	Inner I	141.6	8.2	137.5	0.2334	589.1		
		Outer I	117.1	22.4	127.2	0.4666		567.3	3.26
0.02341		Outer II	145.9	9.9	143.5	0.2335	614.6		
		Inner II	128.6	25.8	142.1	0.4665		612.2	0.46
	11	Inner II	152.0	1.2	140.9	0.2332	604.2		
		Outer II	135.4	5.5	128.6	0.4664		577.8	4.01
		Inner I	153.8	- 6.6	134.9	0.2333	578.3		
		Outer I	127.2	11.3	126.2	0.4666		559.6	2.83
	12	Inner II	151.3	6.7	145.7	0.2337	623.5		
		Outer II	134.8	11.5	134.0	0.4672		598.6	3.80
		Inner I	153.1	2.2	143.0	0.2335	612.4		
		Outer I	129.8	8.6	126.1	0.4671		576.2	5.50
	18	Outer II	155.7	6.5	149.9	0.2334	642.4		
		Inner II	135.9	14.4	138.0	0.4667		616.9	3.88
						Average	609.2	586.9	3.39
						Standard Deviation	21.3	22.4	1.54

Table 8. (Continued).

Soln. No. m	Run	Sample	$q_E \cdot 10^3$	$q_D \cdot 10^3$	$q-q_o \cdot 10^3$	$n_2' \cdot 10^3$ $(n_2'+n_2'') \cdot 10^3$	$-\Delta H_{1,2}$	$-\Delta H_{1,3}$	$P_i \cdot 10^3$
3	2	Inner I	267.1	-15.8	239.0	0.3550	673.3		
		Outer I	219.0	16.6	223.3	0.7100		651.2	2.72
0.03562		Outer II	265.3	1.2	254.2	0.3544	717.2		
		Inner II	219.0	14.6	221.3	0.7094		670.3	5.72
	4	Inner II	262.5	- 0.9	249.3	0.3548	702.6		
		Outer II	223.4	20.0	231.1	0.7095		677.1	3.17
		Outer I	262.9	- 4.6	246.0	0.3551	692.8		
		Inner I	227.9	4.1	219.7	0.7100		655.9	4.56
	14	Inner II	273.4	- 7.2	253.5	0.3551	714.0		
		Outer II	217.8	20.8	226.3	0.7100		675.7	4.72
		Inner I	260.5	- 3.2	245.0	0.3551	690.0		
		Outer I	217.2	20.2	225.1	0.7103		661.9	3.44
	17	Inner I	264.9	- 2.6	250.0	0.3550	704.3		
		Outer I	230.5	17.9	236.1	0.7102		684.4	2.41
						Average	699.2	668.1	3.82
					Standard	Deviation	15.1	12.4	1.21

Table 8. (Continued).

Soln. No. m	Run	Sample	$q_E \cdot 10^3$	$q_D \cdot 10^3$	$q-q_\rho \cdot 10^3$	$n_2' \cdot 10^3$ $(n_2'+n_2'') \cdot 10^3$	$-\Delta H_{1,2}$	$-\Delta H_{1,3}$	$\bar{P}_i \cdot 10^3$
4	1	Outer II	481.1	49.9	518.7	0.6015	862.3		
		Inner II	434.4	40.4	462.5	1.203		815.7	4.42
0.06036		Outer I	526.4	-28.7	485.4	0.6014	807.1		
		Inner I	490.1	-29.6	448.2	1.202		776.5	2.93[a]
	5	Inner I	501.3	9.1	498.4	0.6003	830.3		
		Outer I	459.2	- 7.5	439.4	1.201		780.8	4.65
		Inner II	519.1	2.1	508.9	0.6007	847.2		
		Outer II	439.2	21.3	448.2	1.201		796.6	4.78
	17	Outer II	519.7	- 1.9	505.5	0.6007	841.6		
		Inner II	462.7	- 2.6	447.8	1.202		793.1	4.54
						Average	837.7	792.5	4.60
					Standard	Deviation	20.6	15.4	0.15
5	8	Inner II	1222.9	37.7	1248.3	1.196	1043.6		
		Outer II	1048.5	6.1	1042.3	2.393		957.1	5.78
0.1203		Inner I	1200.8	42.2	1230.7	1.196	1028.9		
		Outer I	1042.2	24.8	1054.7	2.393		955.2	4.94
	13	Inner I	1202.5	42.6	1232.8	1.198	1029.4		
		Outer I	1006.5	47.8	1042.0	2.396		949.6	5.34
		Outer II	1221.2	29.1	1238.0	1.197	1034.2		
		Inner II	1048.1	22.7	1058.5	2.395		959.1	5.03
						Average	1034.0	955.3	5.27
					Standard	Deviation	6.8	4.1	0.38

[a]This value not used in average.

Table 8. (Continued).

Soln. No. m	Run	Sample	$q_E \cdot 10^3$	$q_D \cdot 10^3$	$q-q_o \cdot 10^3$	$n_2' \cdot 10^3$ $(n_2'+n_2'') \cdot 10^3$	$-\Delta H_{1,2}$	$-\Delta H_{1,3}$	$\bar{P}_i \cdot 10^3$
7	9	Outer I	1831.7	19.5	1838.9	1.631	1127.5		
		Inner I	1539.6	30.0	1557.3	3.261		1041.3	4.96
0.1641		Outer II	1840.7	5.7	1834.1	1.631	1124.8		
		Inner II	1544.4	20.2	1552.3	3.261		1038.5	4.97
						Average	1126.2	1039.9	4.97
					Standard	Deviation	1.8	2.0	0.01
6	16	Outer I	2483.6	-73.0	2398.3	2.015	1190.2		
		Inner I	2090.0	-55.3	2022.4	4.030		1096.9	4.83
0.2029		Inner II	2344.7	71.5	2403.9	2.015	1193.0		
		Outer II	2060.1	-32.9	2014.9	4.030		1096.4	4.99
						Average	1191.6	1096.7	4.91
					Standard	Deviation	2.0	0.6	0.11

Table 9. Short chord data and relative apparent molal heat content of ytterbium chloride solutions at 25° C.

Soln. No.	$m_1^{\frac{1}{2}}$	$m_k^{\frac{1}{2}} \times 10^2$	$x_i \cdot 10^2$	$\overline{P}_i$	$E_{\overline{P}_i}$	$\phi_{L(m_k)}$	$-\Delta H_{1,k}$	$\phi_{L(m_1)}$	$\overline{\phi}_L$
1	0.10566	1.1177 1.5719	1.3448	2573	933	14.9 26.8	447.6 435.9	462.5 462.7	462.6
2	0.15299	1.6186 2.2762	1.9474	3391	393	28.3 51.0	609.2 586.9	637.5 637.9	637.7
3	0.18873	1.9960 2.8074	2.4017	3820	308	40.6 72.9	699.2 668.1	739.8 741.0	740.4
4	0.24567	2.5975 3.6532	3.1254	4598	46.5	64.0 112.4	837.7 792.5	901.7 904.9	903.3
5	0.34683	3.6663 5.1568	4.4116	5273	128	113.3 189.3	1034.0 955.3	1147.3 1144.6	1146.0
7	0.40503	4.2803 6.0195	5.1499	4965	75.0[a]	144.1 232.3	1126.2 1039.9	1270.3 1272.2	1271.3
6	0.45048	4.7586 6.6925	5.7256	4910	53.9	168.8 263.1	1191.6 1096.7	1360.4 1359.8	1360.1

[a]Assigned probable error.

Table 10. Thermodynamic properties of ytterbium chloride solutions at 25° C.

$m^{\frac{1}{2}}$	ϕ_L		$\bar{L}_2$	$-\bar{L}_1 \times 10^3$
	Derived	Eq. 98	Eq. 99	Eq. 100
0.01	12[a]	(47)	(71)	
0.03	82[a]	(139)	(206)	(1)
0.05	181[a]	(227)	(334)	(5)
0.0707	279[a]	(314)	(458)	(13)
0.1057	463	451	652	40
0.1530	638	621	882	110
0.1887	740	738	1034	190
0.2456	903	905	1242	367
0.3468	1146	1153	1532	821
0.4050	1271	1273	1665	1159
0.4505	1360	1357	1758	1465

[a]Derived from equation (97).

$$\bar{P}_i = 4100 + 15626x_i \quad , \tag{95}$$

$$\bar{P}_i = 6925 - 44530x_i \quad , \tag{96}$$

and

$$\bar{P}_i = 246.5 + 2.0289 \times 10^5 x_i - 2.2143 \times 10^6 \left(x_i^2 + \frac{\delta^2}{12}\right) . \tag{97}$$

In Figure 7, the first is represented as a solid line, the second by alternate dots and dashes and the third by a dashed line. As can be seen, equation (95) with the theoretical

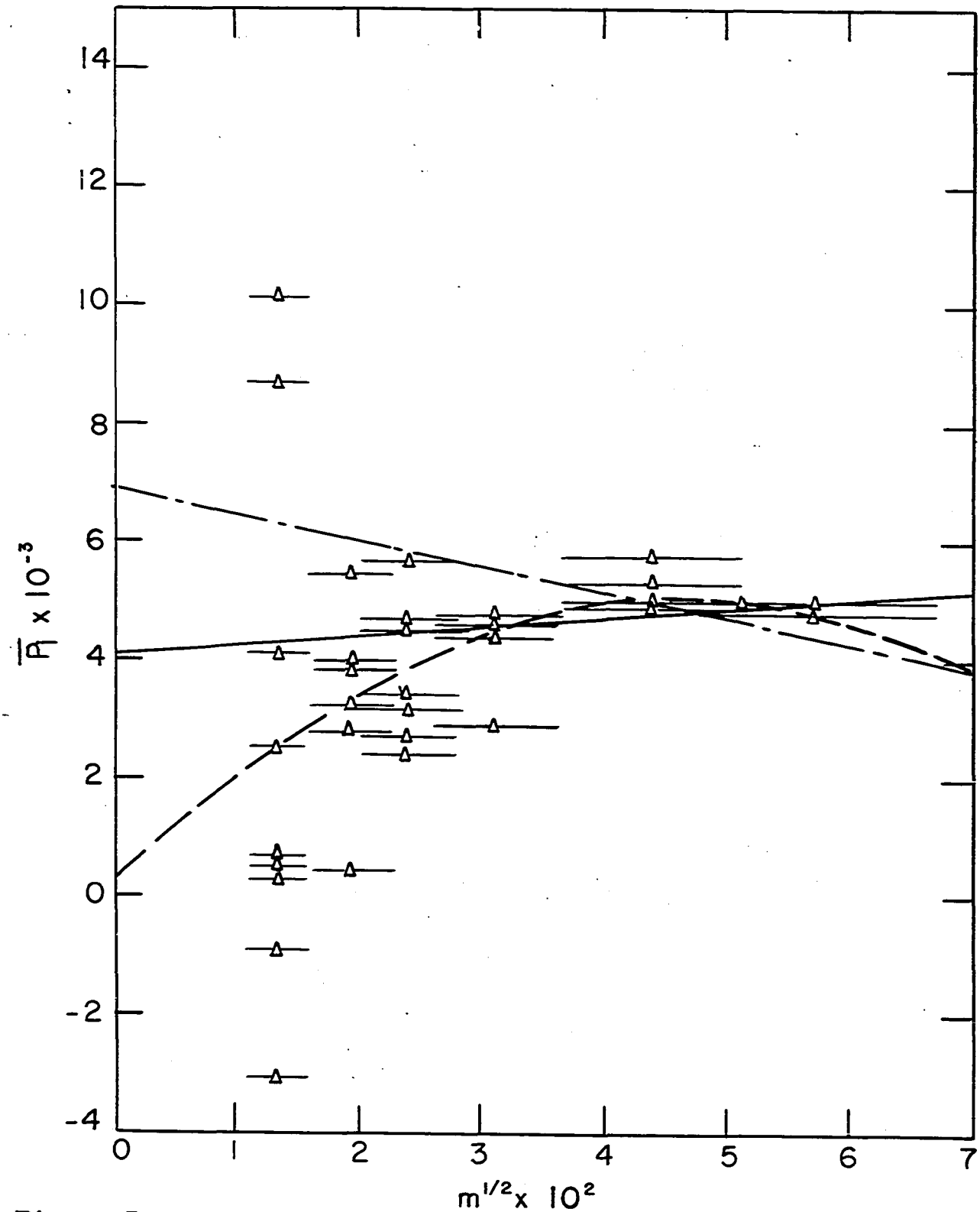

Figure 7. Short chord data for ytterbium chloride solutions.

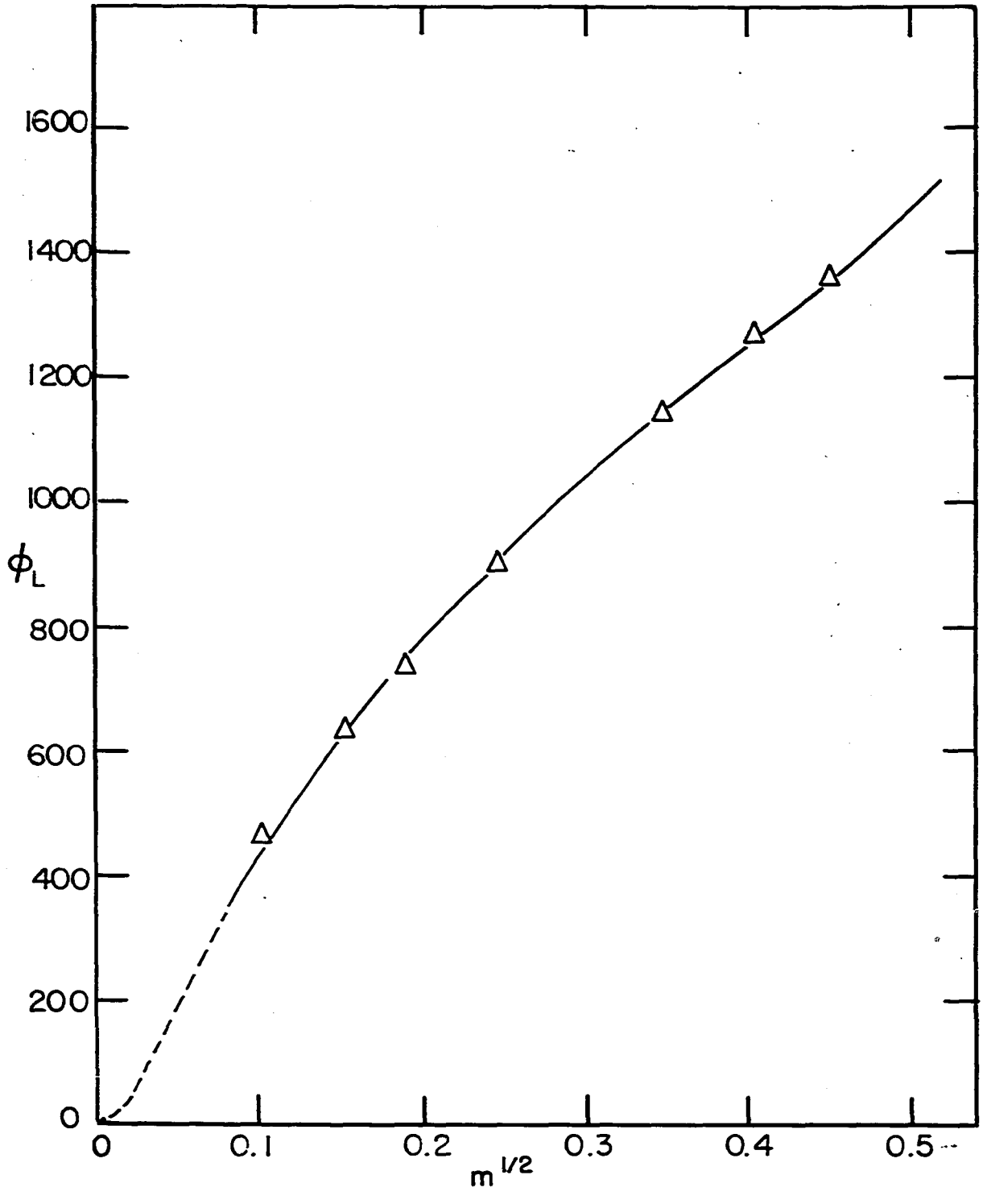

Figure 8. Relative apparent molal heat contents of ytterbium chloride solutions at 25° C.

limiting value does not fit the data and equation (96) gives only a fair representation. Therefore equation (97) was integrated to give

$$\phi_L = 246.5m^{\frac{1}{2}} + 1.045 \times 10^5 m - 0.7381 \times 10^6 m^{3/2} \qquad (98)$$

for the very dilute range. The values of $\underline{\bar{\phi}_L}$ in Table 9 along with the value for 0.005 m calculated from equation (98) were used in the least squares treatment. Since the data obviously were not approaching the theoretical limiting value, only one equation with three free parameters was derived for the concentration dependence of $\underline{\phi_L}$. The equation was

$$\phi_L = 4783m^{\frac{1}{2}} - 5122m + 2644m^{3/2} \quad . \qquad (99)$$

Equation (99) also has an inflection point at about $m^{\frac{1}{2}} = 0.4$. In this case an experimental value was obtained at this concentration and brings out the fact that the "true" expression for $\underline{\phi_L}$ versus $\underline{m^{\frac{1}{2}}}$ should continue to curve smoothly, at least in this region.

Equation (99) is represented in Figure 8 as a solid line. Equation (98) was used to calculate values of $\underline{\phi_L}$ up to $m^{\frac{1}{2}} = 0.05$. From this point to $m^{\frac{1}{2}} = 0.1$ a curve was "smoothed in" to join the curve for higher concentrations.

The equations for the relative partial molal heat contents are

$$\bar{L}_2 = 7175m^{\frac{1}{2}} - 10244m + 6610m^{3/2} \qquad (100)$$

and

$$\overline{L}_i = -43.09m^{3/2} + 92.278m^2 - 71.451m^{5/2} \quad . \qquad (101)$$

In Table 10 the thermodynamic properties for low concentrations derived from the last three equations are listed in parentheses to indicate that considerable doubt is present as to their validity.

3. Lanthanum nitrate

The data for lanthanum nitrate solutions are tabulated in Tables 11, 12 and 13 and are plotted in Figures 9 and 10. Because of the small amounts of heat liberated in diluting the nitrate solutions, measurements could not be made to as low a concentration as for the chloride solutions.

Two linear equations were derived for the concentration dependence of $\underline{\overline{P}_i}$. They were

$$\overline{P}_i = 6230 - 25466x_i \qquad (102)$$

and

$$\overline{P}_i = 6925 - 38990x_i \quad , \qquad (103)$$

which are represented in Figure 9 as a solid line and as alternate dots and dashes. The deviation from the theoretical limiting value seemed large enough to justify using equation (102) to calculate $\underline{\phi_L}$'s for the very dilute range. Integration of this equation yielded

$$\phi_L = 6230m^{\frac{1}{2}} - 12733m \quad . \qquad (104)$$

A least squares treatment, based on equation (86) and using the $\underline{\overline{\phi}_L}$'s of Table 12 and the value for 0.005 m from equation (104), gave the equation

Table 11. Heats of dilution of lanthanum nitrate solutions at 25° C.

Soln. No. m	Run	Sample	$q_E \cdot 10^3$	$q_D \cdot 10^3$	$q-q_o \cdot 10^3$	$n_2' \cdot 10^3$ $(n_2'+n_2'') \cdot 10^3$	$-\Delta H_{1,2}$	$-\Delta H_{1,3}$	$\bar{P}_i \cdot 10^3$
2	2	Inner I	116.8	-12.9	91.6	0.1891	484.4		
		Outer I	108.0	- 7.8	87.9	0.3783		474.5	1.65
0.02087		Inner II	131.0	-22.2	96.5	0.1890	510.2		
		Outer II	107.9	-10.4	85.2	0.3782		480.5	5.05
	6	Inner II	149.9	-37.3	100.3	0.1891	530.3		
		Outer II	103.3	- 4.8	86.2	0.3781		493.3	6.30
		Outer I	126.9	-15.9	98.7	0.1891	521.9		
		Inner I	101.9	- 8.3	81.3	0.3783		475.8	7.77
	9	Inner I	119.6	11.8	119.1	0.1892	629.5		
		Outer I	104.0	12.7	104.4	0.3784		590.7	6.57
		Outer II	120.6	-10.3	98.0	0.1892	518.1		
		Inner II	98.8	- 4.6	81.9	0.3783		475.6	7.19
	10	Outer I	120.6	5.8	114.1	0.1892	603.1		
		Inner I	105.5	9.8	103.0	0.3783		573.9	4.95
		Outer II	117.2	- 8.0	96.9	0.1892	512.3		
		Inner II	94.7	6.6	89.0	0.3784		491.2	3.53
						Average	538.7	506.9	5.37
						Standard Deviation	50.2	47.3	2.03

Table 11. (Continued).

Soln. No. m	Run	Sample	$q_E \cdot 10^3$	$q_D \cdot 10^3$	$q-q_o \cdot 10^3$	$n_2' \cdot 10^3$ $(n_2'+n_2'') \cdot 10^3$	$-\Delta H_{1,2}$	$-\Delta H_{1,3}$	$\bar{P}_i \cdot 10^3$
3	1	Outer I	245.2	-15.4	217.5	0.3705	587.1		
		Inner I	182.8	17.9	188.4	0.7411		547.7	4.74
0.04095		Outer II	229.3	10.8	227.8	0.3705	614.8		
		Inner II	187.5	20.3	195.5	0.7410		571.2	5.26
	7	Inner II	237.4	10.8	235.9	0.3703	637.0		
		Outer II	194.7	23.2	205.6	0.7409		595.9	4.89
		Outer I	237.1	16.4	241.2	0.3706	650.8		
		Inner I	202.6	2.4	192.7	0.7409		585.6	7.91
	11	Outer II	242.1	- 1.6	228.2	0.3702	616.4		
		Inner II	201.6	- 0.8	188.4	0.7407		562.5	6.48
	12	Inner II	242.8	0.5	231.0	0.3703	623.8		
		Outer II	200.4	4.7	192.8	0.7409		572.0	6.22
		Outer I	241.7	-12.0	217.4	0.3704	587.0		
		Inner I	202.7	4.4	194.8	0.7406		556.6	4.01
						Average	616.7	570.2	5.64
					Standard	Deviation	27.9	16.5	1.32

Table 11. (Continued).

Soln. No. m	Run	Sample	$q_E \cdot 10^3$	$q_D \cdot 10^3$	$q-q_o \cdot 10^3$	$n_2' \cdot 10^3$ $(n_2'+n_2'') \cdot 10^3$	$-\Delta H_{1,2}$	$-\Delta H_{1,3}$	$\bar{P}_i \cdot 10^3$
4	3	Outer II	475.7	-34.1	429.3	0.6492	661.3		
		Inner II	385.5	-21.1	352.1	1.299		601.6	5.41
0.07200		Inner I	437.3	20.4	445.4	0.6497	685.5		
		Outer I	375.0	- 1.8	360.9	1.299		620.5	5.92
	13	Inner I	442.6	10.9	441.2	0.6498	678.9		
		Outer I	378.4	- 2.9	363.2	1.300		619.0	5.47
		Inner II	436.9	4.3	428.9	0.6495	660.4		
		Outer II	369.2	3.5	360.4	1.299		607.8	4.80
						Average	671.5	612.2	5.40
					Standard	Deviation	12.6	9.1	0.22
5	5	Outer I	959.0	-22.9	923.8	1.298	712.0		
		Inner I	821.6	-87.3	722.0	2.595		634.2	5.01
0.1447		Outer II	913.4	26.3	927.4	1.298	714.7		
		Inner II	739.2	-11.3	715.6	2.594		633.4	5.26
	14	Inner I	937.4	1.5	926.6	1.298	714.0		
		Outer I	767.1	-28.6	726.2	2.594		637.1	4.98
						Average	713.6	634.9	5.08
					Standard	Deviation	1.4	2.2	0.16

Table 11. (Continued).

Soln. No. m	Run	Sample	$q_E \cdot 10^3$	$q_D \cdot 10^3$	$q-q_o \cdot 10^3$	$n_2' \cdot 10^3$ $(n_2'+n_2'') \cdot 10^3$	$-\Delta H_{1,2}$	$-\Delta H_{1,3}$	$\bar{P}_i \cdot 10^3$
6	8	Inner II	1307.1	10.6	1305.4	1.832	712.5		
		Outer II	1010.0	-24.0	973.7	3.663		622.2	4.92
0.2052		Inner I	1221.6	90.1	1299.4	1.831	709.8		
		Outer I	987.4	- 3.2	971.9	3.663		620.0	4.85
	14	Outer II	1300.6	16.1	1304.4	1.832	712.2		
		Inner II	1002.2	- 5.2	984.7	3.663		624.9	4.73
						Average	711.5	622.4	4.83
						Standard Deviation	1.5	2.5	0.10

Table 12. Short chord data and relative apparent molal heat content of lanthanum nitrate solutions at 25° C.

Soln. No.	$m_1^{\frac{1}{2}}$	$m_k^{\frac{1}{2}} \times 10^2$	$x_i \cdot 10^2$	$\overline{P}_i$	$E_{\overline{P}_i}$	$\phi_{L(m_k)}$	$-\Delta H_{1,k}$	$\phi_{L(m_1)}$	$\overline{\phi}_L$
2	0.14447	1.4571 2.0492	1.7532	5376	518	88.1 122.2	538.7 506.9	625.7 629.0	627.3
3	0.20236	2.0392 2.8680	2.4536	5644	335	121.7 168.2	616.7 570.2	738.4 738.4	738.4
4	0.26833	2.7007 3.7984	3.2496	5400	114	159.0 218.2	671.5 612.2	830.5 830.4	830.5
5	0.38043	3.8179 5.3689	4.5934	5083	60.8	219.3 297.8	713.6 634.9	932.9 932.7	932.8
6	0.45302	4.5366 6.3804	5.4585	4833	37.5	256.4 345.7	711.5 622.4	967.9 968.1	968.0

Table 13. Thermodynamic properties of lanthanum nitrate solutions at 25° C.

$m^{\frac{1}{2}}$	ϕ_L		$\bar{L}_2$	$-\bar{L}_1 \times 10^3$
	Derived	Eq. 104	Eq. 105	Eq. 106
0.01	61[a]	61	90	
0.03	175[a]	173	253	1
0.05	280[a]	274	394	5
0.0707	377[a]	368	519	14
0.1445	627	621	815	73
0.2024	738	748	925	131
0.2683	831	838	975	179
0.3804	933	920	1038	307
0.4530	968	973	1179	761

[a]Derived from equation (103).

$$\phi_L = 6206m^{\frac{1}{2}} - 15180m + 13735m^{3/2} \qquad (105)$$

for the concentration dependence of $\underline{\phi_L}$. The equations for $\underline{\bar{L}_2}$ and $\underline{\bar{L}_1}$ are

$$\bar{L}_2 = 9309m^{\frac{1}{2}} - 30360m + 34337m^{3/2} \qquad (106)$$

and

$$\bar{L}_1 = -55.90m^{3/2} + 273.48m^2 - 371.17m^{5/2} \quad . \qquad (107)$$

The data of Lange and Miederer (30) are presented in Figure 10 along with the $\underline{\phi_L}$ data from this work. Where the two sets of data overlap, the agreement is within three per cent. The limiting slope obtained by these men, who did not

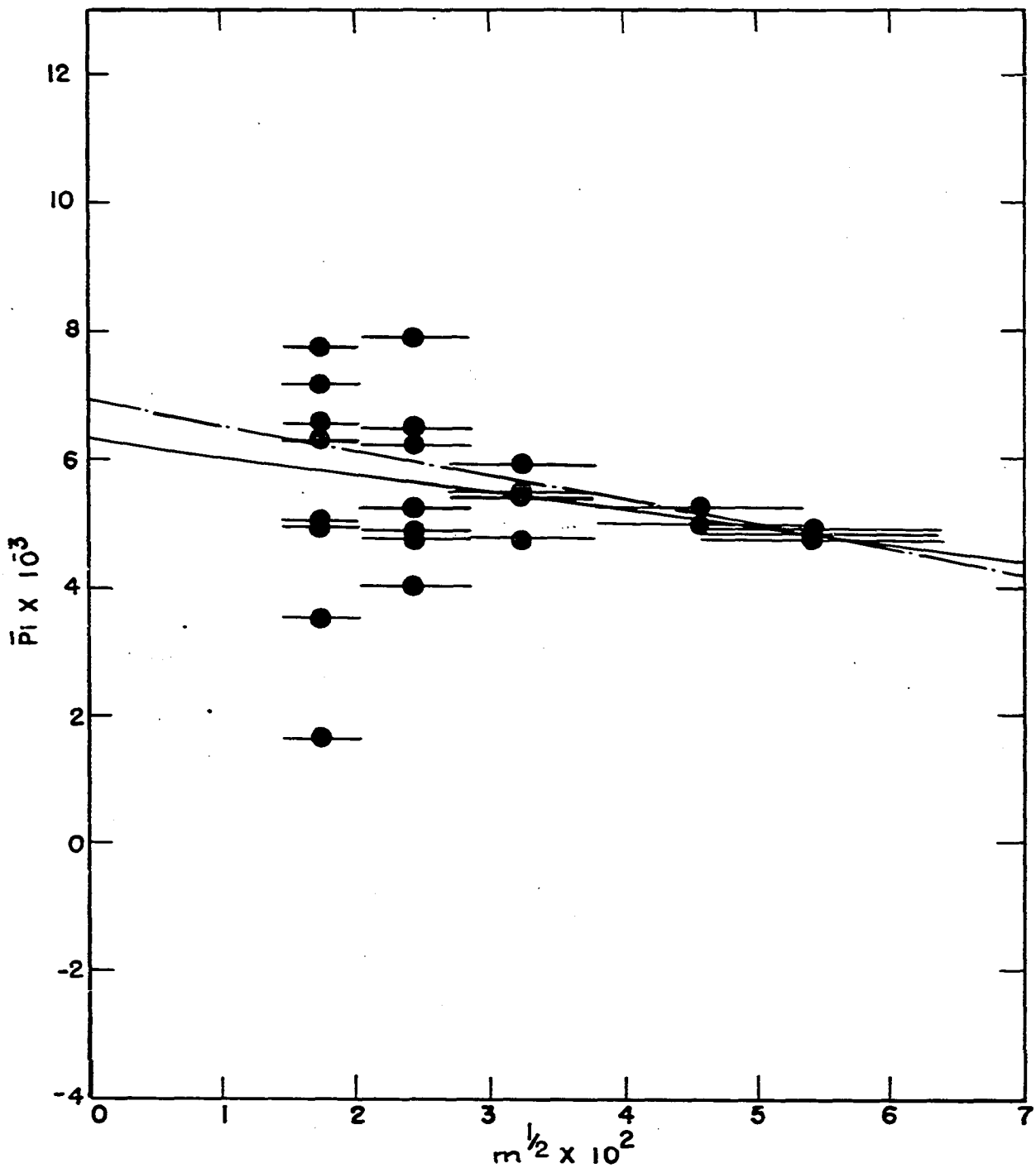

Figure 9. Short chord data for lanthanum nitrate solutions.

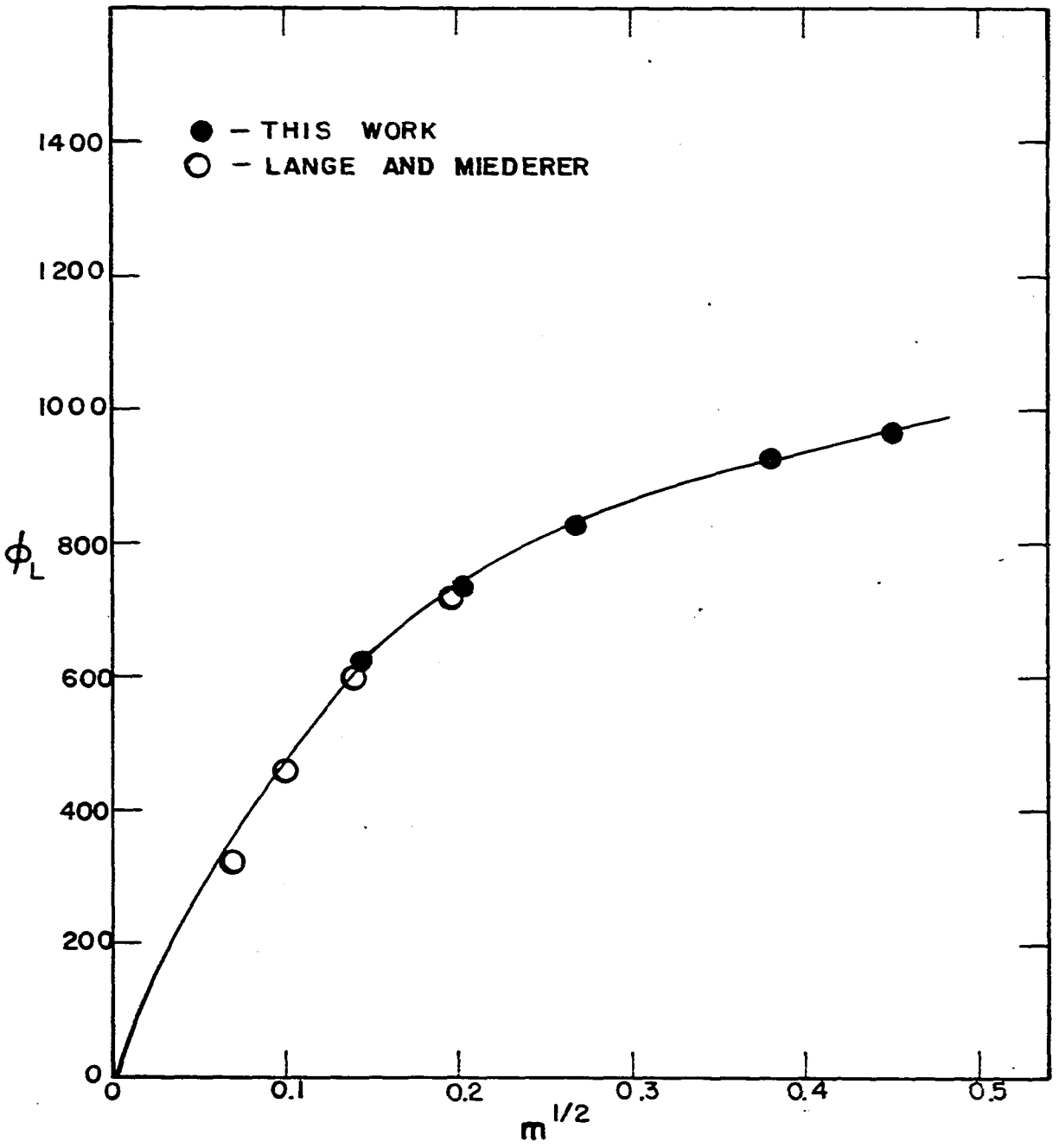

Figure 10. Relative apparent molal heat contents of lanthanum nitrate solutions at 25° C.

use the short chord method of treating the data, was 6100.

4. Ytterbium nitrate

The data for ytterbium nitrate solutions are tabulated in Tables 14, 15 and 16 and are plotted in Figures 11 and 12.

Because of the curvature present in the short chord plot (Figure 11), the concentration dependence of $\overline{P}_i$ was found by a least squares treatment using equation (84). The expression obtained was

$$\overline{P}_i = -1393 + 2.6700 \times 10^5 x_i - 2.9484 \times 10^6 (x_i^2 + \frac{\delta^2}{12}) \quad (108)$$

which was integrated to give

$$\phi_L = -1393 m^{\frac{1}{2}} + 1.3350 \times 10^5 m - 0.9828 \times 10^6 m^{3/2} \quad (109)$$

for the very dilute range.

The negative limiting value of equation (108) is not actually exhibited by the short chord plot. This case especially points out the difficulty in evaluating absolute values of ϕ_L. The methods depend upon an extrapolation to infinite dilution and thus assume that any trend in the data at the experimental concentrations continues to manifest itself at lower concentrations.

Again using equation (86), a least squares treatment gave

$$\phi_L = 3696 m^{\frac{1}{2}} - 5590.9m + 3468.7 m^{3/2} \quad (110)$$

for the concentration dependence of ϕ_L. The curve representing the concentration dependence of ϕ_L in Figure 12 was

Table 14. Heats of dilution of ytterbium nitrate solutions at 25° C.

Soln. No. m	Run	Sample	$q_E \cdot 10^3$	$q_D \cdot 10^3$	$q-q_\theta \cdot 10^3$	$n_2' \cdot 10^3$ $(n_2'+n_2'') \cdot 10^3$	$-\Delta H_{1,2}$	$-\Delta H_{1,3}$	$\bar{P}_i \cdot 10^3$
1	3	Inner II	127.1	-21.4	93.4	0.2009	465.0		
		Outer II	98.8	- 6.0	80.5	0.4016		432.9	5.27
0.02428		Outer I	125.2	-16.2	96.7	0.2010	481.2		
		Inner I	100.2	- 3.4	84.5	0.4019		450.9	4.98
	6	Outer II	137.9	-35.2	90.4	0.2009	450.0		
		Inner II	93.9	6.6	88.2	0.4017		444.6	0.90
		Outer I	140.7	-31.7	96.7	0.2008	481.6		
		Inner I	102.1	0.0	89.8	0.4017		464.3	2.82
	8	Inner II	117.9	- 9.1	96.5	0.2008	480.7		
		Outer II	99.3	6.4	93.4	0.4016		472.9	1.27
		Outer I	121.1	-28.5	80.3	0.2009	399.8		
		Inner I	96.1	- 2.9	80.9	0.4014		401.6	-0.24
	12	Inner II	124.1	-22.7	89.1	0.2009	443.6		
		Outer II	92.8	- 1.4	79.1	0.4017		418.7	4.08
		Outer I	122.5	-22.2	88.0	0.2009	438.0		
		Inner I	98.7	- 3.8	82.6	0.4016		424.8	2.20
						Average	455.0	438.8	2.66
					Standard	Deviation	28.4	23.9	2.06

Table 14. (Continued).

Soln. No. m	Run	Sample	$q_E \cdot 10^3$	$q_D \cdot 10^3$	$q-q_o \cdot 10^3$	$n_2' \cdot 10^3$ $(n_2'+n_2'') \cdot 10^3$	$-\Delta H_{1,2}$	$-\Delta H_{1,3}$	$\bar{P}_i \cdot 10^3$
2	1	Outer I	246.1	-12.3	221.5	0.3860	573.8		
		Inner I	193.7	20.6	202.0	0.7718		548.7	2.99
0.04680		Outer II	243.3	-13.4	217.6	0.3862	563.5		
		Inner II	195.9	15.0	198.6	0.7724		538.9	2.91
	7	Inner I	239.1	-15.6	211.2	0.3863	546.8		
		Outer I	206.4	- 2.3	191.8	0.7726		521.6	2.97
		Outer II	232.7	-13.9	206.5	0.3862	534.8		
		Inner II	202.7	- 1.1	189.3	0.7722		512.6	2.64
	11	Inner I	241.9	-12.5	217.1	0.3863	562.0		
		Outer I	213.6	-13.6	187.7	0.7725		524.0	4.50
		Outer II	242.5	-21.5	208.7	0.3864	540.1		
		Inner II	200.2	- 0.5	187.4	0.7726		512.7	3.26
	13	Inner I	229.2	- 3.8	213.1	0.3865	551.4		
		Outer I	200.0	1.8	189.5	0.7727		518.4	3.61
						Average	553.2	525.3	3.27
					Standard	Deviation	13.9	13.6	0.62

Table 14. (Continued).

Soln. No. m	Run	Sample	$q_E \cdot 10^3$	$q_D \cdot 10^3$	$q-q_o \cdot 10^3$	$n_2' \cdot 10^3$ $(n_2'+n_2'') \cdot 10^3$	$-\Delta H_{1,2}$	$-\Delta H_{1,3}$	$\bar{P}_i \cdot 10^3$
3	5	Inner II[a]	480.2	16.7	490.6	0.7504	653.8		
		Outer II[a]	421.9	0.2	415.8	1.501		604.0	4.22
0.09137		Inner I	465.1	42.1	494.9	0.7502	659.7		
		Outer I	431.6	0.2	419.5	1.501		609.3	4.25
	9	Inner II	499.3	- 6.0	481.0	0.7502	641.1		
		Outer II	437.5	-23.0	402.2	1.500		588.7	4.45
		Inner I	523.2	-20.0	490.9	0.7502	654.3		
		Outer I	454.2	-42.1	399.8	1.501		593.6	5.15
	13	Inner II	498.3	- 1.1	484.9	0.7501	646.4		
		Outer II	423.0	- 1.7	409.0	1.500		596.0	4.29
						Average	651.1	598.3	4.47
						Standard Deviation	7.3	8.3	0.39

[a]Only bottom disk of sample holder opened; $q_o = 6.3 \times 10^{-3}$ calories.

Table 14. (Continued).

Soln. No. m	Run	Sample	$q_E \cdot 10^3$	$q_D \cdot 10^3$	$q-q_o \cdot 10^3$	$n_2' \cdot 10^3$ $(n_2'+n_2'') \cdot 10^3$	$-\Delta H_{1,2}$	$-\Delta H_{1,3}$	$\bar{P}_1 \cdot 10^3$
4	4	Inner I	1050.9	- 0.5	1038.1	1.435	723.4		
		Outer I	882.4	-39.0	831.1	2.869		651.5	4.42
0.1763		Inner II	1035.2	9.2	1032.1	1.434	719.9		
		Outer II	871.3	-36.5	822.5	2.868		646.7	4.48
	10	Inner I	1032.0	38.9	1058.6	1.434	738.0		
		Outer I	875.1	-23.2	839.6	2.869		661.7	4.68
						Average	727.1	653.3	4.53
					Standard	Deviation	9.6	6.6	0.14
5	2	Outer II	1567.1	- 6.8	1548.0	2.047	756.3		
		Inner II	1229.0	4.2	1220.9	4.094		676.4	4.10
0.2538		Inner I	1561.4	- 2.8	1546.3	2.046	755.7		
		Outer I	1331.7	-101.1	1218.3	4.093		675.5	4.11
	10	Outer II	1590.5	-34.4	1544.8	2.047	754.6		
		Inner II	1215.9	13.1	1216.7	4.093		674.6	4.12
						Average	755.5	675.5	4.11
					Standard	Deviation	0.9	0.9	0.01

Table 15. Short chord data and relative apparent molal heat content of ytterbium nitrate solutions at 25° C.

Soln. No.	$m_1^{\frac{1}{2}}$	$m_k^{\frac{1}{2}} \times 10^2$	$x_i \cdot 10^2$	$\overline{P}_i$	$E_{\overline{P}_i}$	$\phi_{L(m_k)}$	$-\Delta H_{1,k}$	$\phi_{L(m_1)}$	$\overline{\phi}_L$
1	0.15581	1.5016	1.8066	2660	492	5.9	455.0	460.9	464.7
		2.1116				28.8	438.8	467.6	
2	0.21633	2.0825	2.5055	3269	159	20.0	553.2	573.2	573.8
		2.9284				49.0	525.3	574.3	
3	0.30227	2.9026	3.4924	4472	117	48.1	651.1	699.2	698.1
		4.0821				98.7	598.3	697.0	
4	0.41991	4.0144	4.8302	4527	53.0	95.6	727.1	822.7	823.0
		5.6459				170.0	653.3	823.3	
5	0.50375	4.7965	5.7712	4110	38.9[a]	131.8	755.5	887.3	887.3
		6.7458				211.8	675.5	887.3	

[a]Assigned probable error.

Table 16. Thermodynamic properties of ytterbium nitrate solutions at 25° C.

$m^{\frac{1}{2}}$	ϕ'_L		$\bar{L}_2$	$-\bar{L}_1 \times 10^3$
	Derived	Eq. 109	Eq. 110	Eq. 111
0.01	- 2[a]	(36)	(54)	
0.03	52[a]	(106)	(156)	(1)
0.05	141[a]	(171)	(250)	(4)
0.0707	222[a]	(235)	(339)	(10)
0.1558	465	453	625	75
0.2163	574	573	764	161
0.3023	698	702	894	315
0.4199	823	823	980	557
0.5038	887	887	1064	810

[a]Derived from equation (108).

constructed in the same manner as the one for the $YbCl_3$ solutions.

The relative partial molal heat contents were derived from equation (110) and are given by

$$\bar{L}_2 = 5544m^{\frac{1}{2}} - 11182m + 8671.7m^{3/2} \qquad (111)$$

and

$$\bar{L}_1 = -33.29m^{3/2} + 100.73m^2 - 93.737m^{5/2} \quad . \qquad (112)$$

Again the thermodynamic properties for low concentrations derived from equations (110), (111) and (112) are listed in

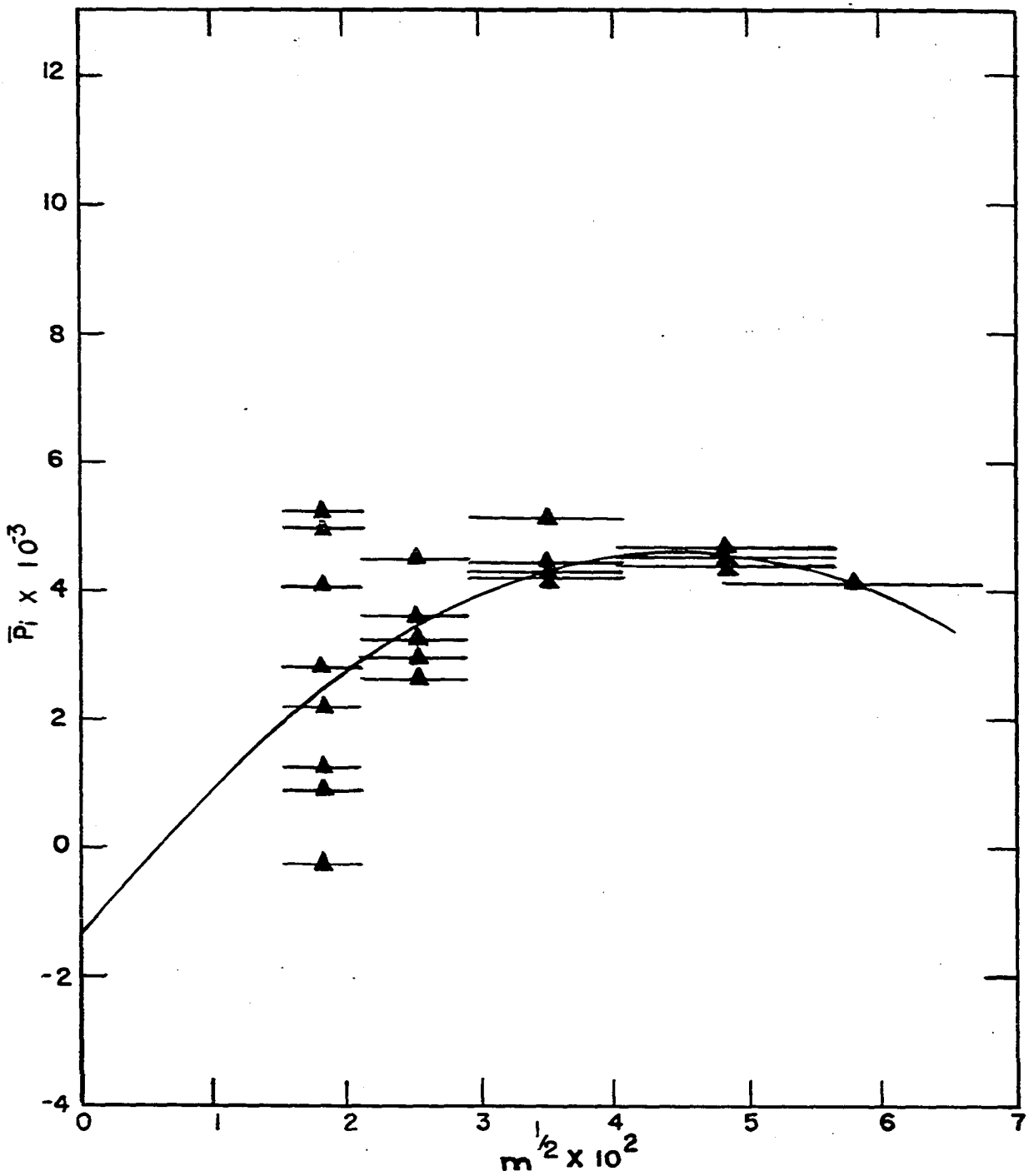

Figure 11. Short chord data for ytterbium nitrate solutions.

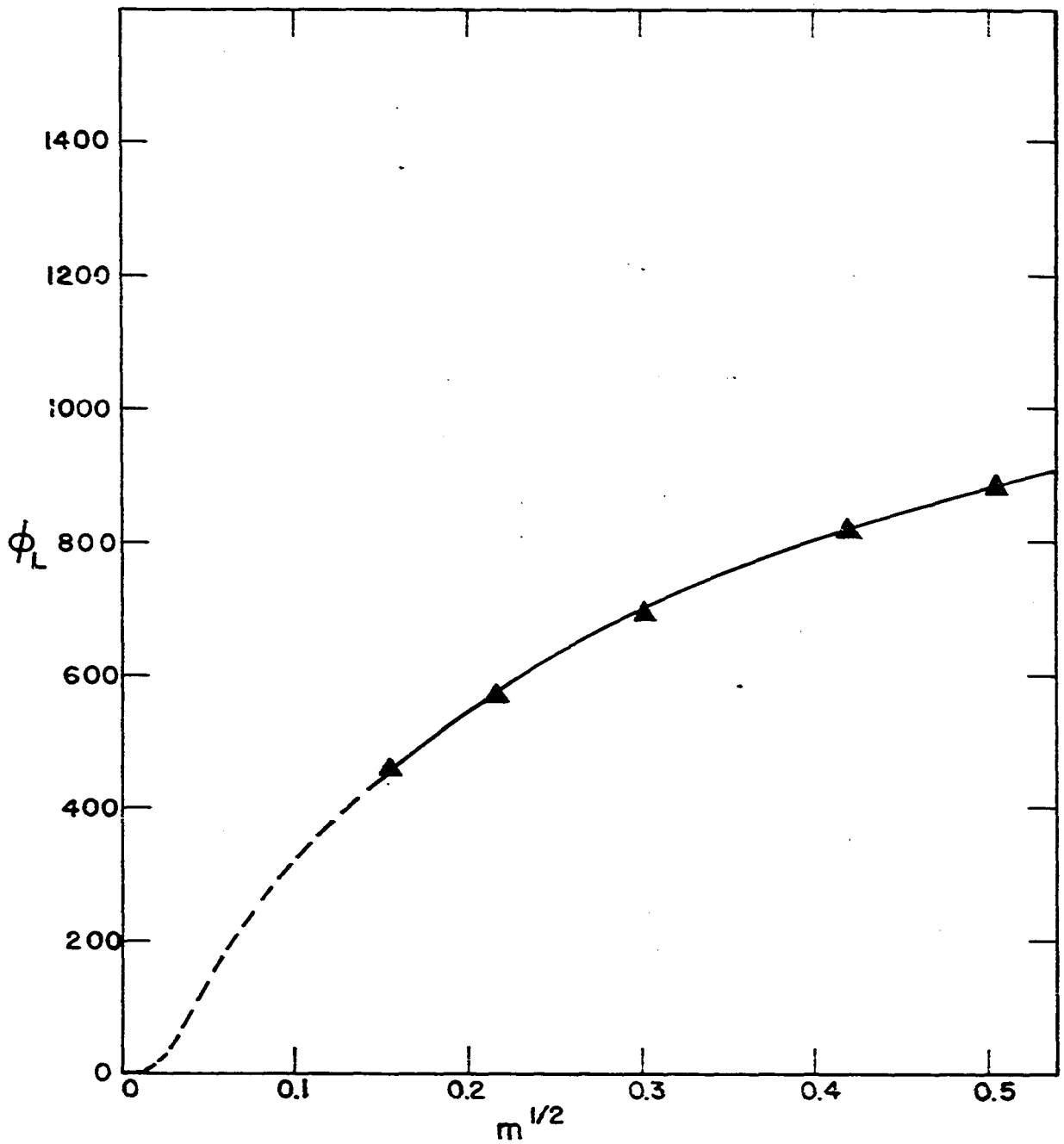

Figure 12. Relative apparent molal heat contents of ytterbium nitrate solutions at 25° C.

parentheses in Table 16 because of their doubtful validity.

H. Error Analysis

The method of propagation of precision indexes, as described by Worthing and Geffner (89), was used to estimate uncertainties in this work. In this method, the reliability of a derived quantity is estimated from the uncertainties in the directly measured quantities. If a derived quantity, $\underline{U}$, is some function of the independent and measurable quantities, $\underline{X_1, X_2, \ldots X_n}$, the probable error in the average value of $\underline{U}$ is calculated by the formula

$$E_{\overline{U}}^2 = \sum_{i=1}^{n} \left(\frac{\partial \overline{U}}{\partial \overline{X}_i}\right)^2 E_{\overline{X}_i}^2 \quad , \tag{113}$$

where $E_{\overline{U}}$ = probable error in $\overline{U}$,

$\overline{U}$ = average value of the derived quantity,

$\overline{X}_i$ = average value of the directly measured quantity $\underline{X_i}$.

$E_{\overline{X}_i}$ = probable error in $\overline{X}_i$.

The probable error in $\underline{\phi_L}$ was derived from the following equations:

$$\phi_{L(m_1)} = \phi_{L(m_k)} - \Delta H_{1,k} \tag{85}$$

$$\phi_{L(m_k)} = S^{\circ} m_k^{\frac{1}{2}} + \frac{B}{2} m_k + \frac{C}{3} m_k^{3/2} \tag{79}$$

$$\Delta H_{1,2} = - \frac{q_1 - q_o}{n'_2} \tag{66}$$

$$q_1 = q_{el} + q_{dis} \qquad (60)$$

It was found that the error in $\Delta H_{1,2}$ was slightly larger than that in $\Delta H_{1,3}$, so this quantity was used in the error analysis. The probable errors calculated for the least squares constants of equation (79) are listed in Table 17; the average values were used to determine the error in $\phi_{L(m_k)}$. The probable error in opening a sample holder was taken as 1.7 x 10^{-3} calories. Since the uncertainty in q_{el} contributed less than one per cent to the uncertainty in q_1, it was neglected in calculating the error in $\Delta H_{1,2}$.

Table 17. Probable errors of least squares constants of equation (79).

Salt	a	b	c
$LaCl_3$	680	5,300	
$YbCl_3$	610	1,500	22,500
$La(NO_3)_3$	510	6,300	
$Yb(NO_3)_3$	925	9,400	68,500
Average	700	5,600	45,500

The results of the error analysis are summarized in Table 18. The probable errors in $\Delta H_{1,k}$, which were obtained from the standard deviations of the average experimental values, are listed merely for comparison. As is evident, the largest contribution to the probable error in $\phi_{L(m_1)}$ arises

Table 18. Summary of error analysis for $\underline{\phi_L}$.

m	Probable error in n_2'[a]	q_{dis}[b] x 10^3	$\Delta H_{1,k}$ (exp)	$\Delta H_{1,2}$ (derived)	$\phi_{L(m_k)}$	$\phi_{L(m_1)}$
0.01	0.2	1.7	10	24	10	26
0.02	0.4	3.2	8	18	15	24
0.05	1.0	5.0	5	11	24	26
0.10	2.0	6.2	3	7	35	36
0.15	3.0	7.5	1	6	44	45
0.20	4.0	8.4	1	5	54	54
0.25	5.0	10.0	0	5	62	62

[a] n_2' given in moles x 10^6.

[b] All heat quantities given in defined calories.

from the uncertainty in the short chord data.

V. EXPERIMENTAL: HEATS OF SOLUTION

A. Apparatus

The calorimeter used in this work was similar to those of Maier (90) and of Southard (91). A schematic diagram of the apparatus is given in Figure 13 and of the electrical circuits in Figure 14.

A Precision Scientific Co., Model No. 162, 100 gallon constant temperature water bath, which could be controlled to 0.02° C, was used for the isothermal jacket of the calorimeter. The calorimeter vessel (13-A) was a two liter Dewar flask, which was sealed onto a heavy brass flange with Apiezon-W wax. A 1/4 inch soft rubber gasket fitted between the flange and the brass plate (13-B) which served as a lid. The flask was held against the lid by six large brass bolts. The lid was permanently fastened to an angle iron frame which held the apparatus in place in the water bath. Five brass tubes, which housed the stirrer shaft, the breaker assembly and the electrical leads, were mounted on the lid. The tubes extended out of the water bath to a second brass plate upon which a 1/4 inch Bakelite plate (13-C) was fastened. The electrical connections from the calorimeter to external leads were made at brass studs mounted on the Bakelite plate.

The internal parts of the apparatus were constructed of either copper or brass and were gold-plated to prevent corro-

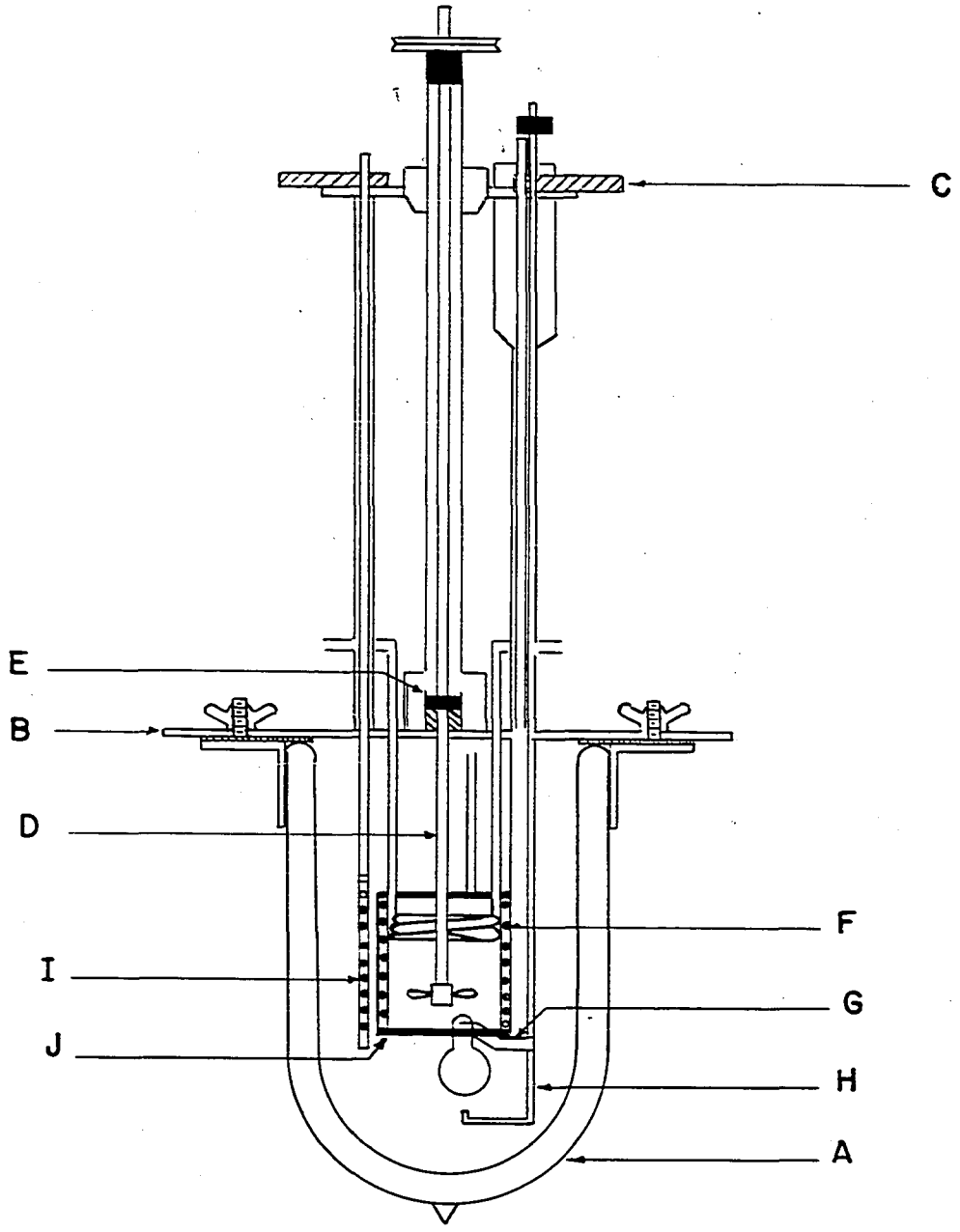

Figure 13. Schematic diagram of solution calorimeter.

sion. The heater and thermometer wells were filled with naphthalene to improve the thermal conductivity. In this way, the lag-time of the calorimeter was reduced to less than 10 seconds.

A multivane propeller (13-D) was soldered to the end of a 1/4 inch brass rod. The stirrer shaft was supported by a teflon gasket and a sealed bearing (13-E) located just above the lid and by a brass bearing at the top. An adjustable synchronous motor drove the stirrer at 575 r.p.m.

Water flowing through a coil (13-F) of 3/16 inch copper tubing was used to cool the calorimeter to the desired temperature before a run.

The samples for heat of solution experiments were contained in thin walled glass bulbs, which were blown from six mm Pyrex tubing. Three such bulbs could be fastened to the holder (13-G) with Apiezon-W wax. The sample bulbs were broken by a brass rod (13-H) with a crook at the bottom.

The calorimeter heater (13-I), used to calibrate the apparatus, consisted of a 100 ohm winding of 32 B and S gauge manganin wire. The wire was wound on a mica sheet and was enclosed in a thin-walled copper case. Two 30 B and S gauge copper lead wires from each end of the heater led out through a tube from the top of the case and up through the brass tube on the calorimeter lid. They were insulated from the tubes by a small polystyrene tube. The leads were joined to a four conductor shielded cable at the Bakelite plate. Since two

of the wires were used only for measuring the heater's resistance, the ends of these cable wires were ordinarily insulated with Scotch electrical tape.

The heater resistance was found by measuring the potential drop across the heater and across a standard resistor while current was flowing through the two in series. The 100 ohm standard resistor was calibrated by the National Bureau of Standards; the measurements were made with a White double potentiometer. The heater resistance at 25° C was 100.422 ohms.

A transposed bridge type thermometer (13-J), similar to that of Maier (92), was used to measure the temperature of the calorimeter. A circuit diagram of the thermometer is shown in Figure 14. It consisted of two 260 ohm, 36 B and S gauge nickel (14-N) and two 250 ohm, 38 B and S gauge manganin (14-M) arms. The wires were wound on a thin copper tube, which had rings soldered to its rims. Another copper tube was slipped over the rings and the joints were sealed with solder. Two small tubes extended up from opposite sides of the case to accommodate the four 30 B and S gauge copper lead wires. These wires were insulated and connected to a four conductor shielded cable in the same manner as the heater leads.

One half of a White double potentiometer was used to monitor the current passing through the thermometer by measuring the potential drop across a 10 ohm standard resistor

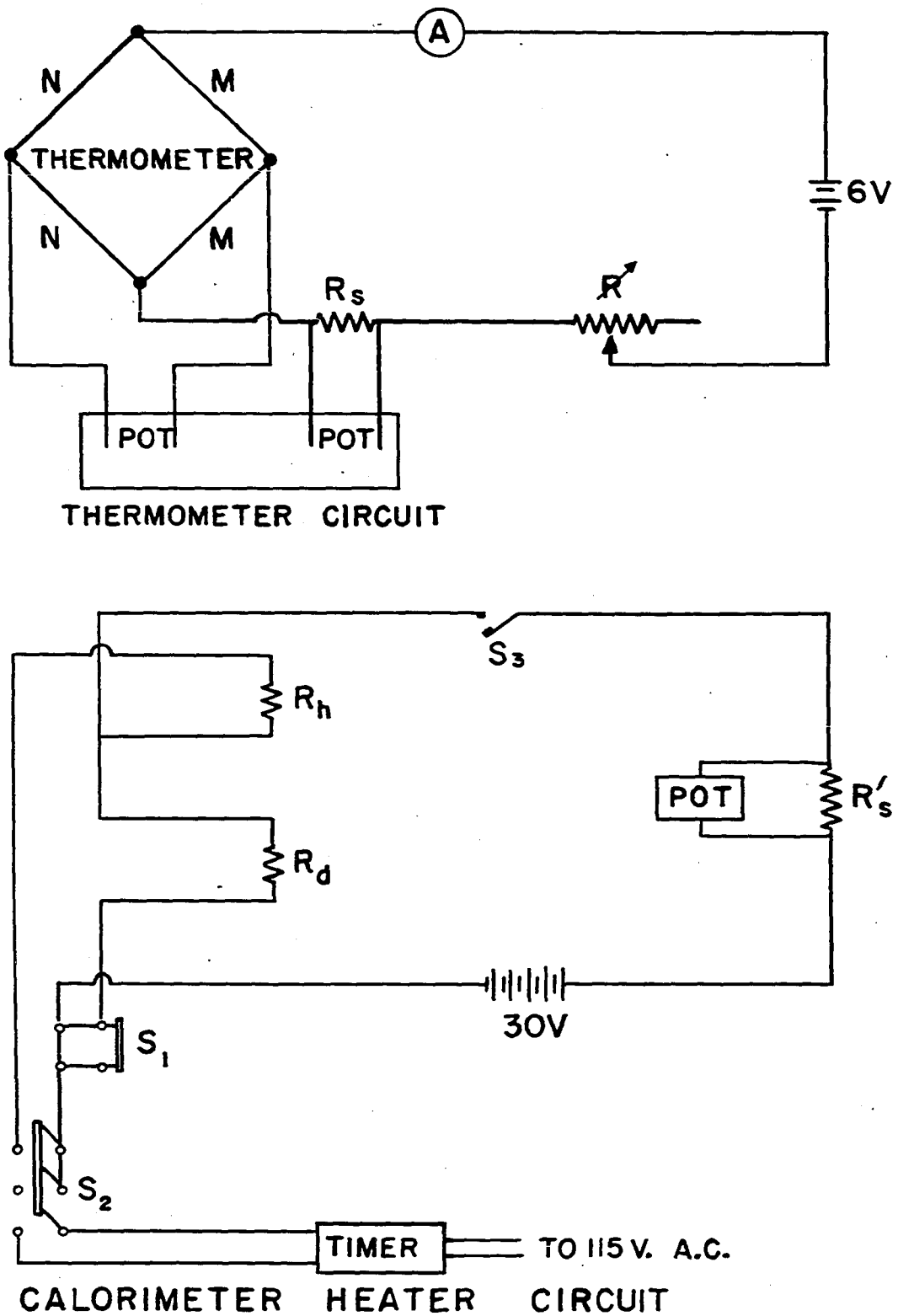

Figure 14. Schematic diagram of circuits for solution calorimeter.

(14-R_s). Current was supplied by two Willard, low discharge, six volt storage batteries connected in parallel and was maintained at five milliamperes by a variable resistance (14-R) in series with the thermometer. The other half of the double potentiometer was used to measure the potential drop across the thermometer. The potential was measured to 0.1 microvolt by using a Leeds and Northrup, Type HS, reflecting galvanometer with a sensitivity of 0.1 microvolt per mm deflection.

The transposed bridge thermometer was calibrated against a platinum resistance thermometer whose resistance was measured with a Müeller temperature bridge. The relationship between the temperature, T, and the potential across the thermometer, E, was derived by a least squares relationship and is given by the equation

$$T(^{\circ}C) = 14.9556 + 3.4724 \times 10^{-4}E - 2.3067 \times 10^{-10}E^2 . \quad (114)$$

B. Preparation of Neodymium Chloride Hexahydrate

The neodymium oxide used to prepare the salt was obtained from the rare earth separation group of the Ames Laboratory of the Atomic Energy Commission. The spectrographic analysis of the oxide is given in Table 1.

The oxide was dissolved in an excess of C. P. Baker and Adamson hydrochloric acid. The solution was boiled down until crystals just began to form; it was diluted with water; and then boiled down again. When crystals formed the second time, the beaker was placed in a vacuum desiccator, which was

evacuated frequently until a crop of crystals had formed in the beaker. The supernatent liquid was poured off into another beaker and returned to the desiccator to obtain more crystals. The crystals were rinsed off and then dissolved in water for recrystallization. The second crystallization was accomplished in the same manner as the first.

After the supernatent liquid was removed in the second crystallization step, the crystals were crushed and placed in a dessicator charged with fresh anhydrous calcium chloride. When the salt appeared quite dry, the crystals were powdered in a mortar and again placed in the desiccator for a final drying. The powder was left over the desiccant for two weeks before it was analyzed. An analysis for the neodymium content showed a slight excess of water, so the powder was desiccated for another two weeks. A second analysis gave almost identical results and the salt was used in this form. The analyses gave an $H_2O/NdCl_3$ ratio of 6.05 ± 0.01.

The powder was transferred to weighed glass sample bulbs in a dry box with a nitrogen atmosphere. After loading, the bulbs were stoppered, removed from the dry box, and reweighed. The stems of the bulbs were then sealed off with a torch. The weight of the salt was obtained by difference and corrected to weight <u>in vacuo</u>.

C. Experimental Procedure

In preparation for a run the sample bulbs were waxed to the sample holder, which was then inserted to its place in the calorimeter. A notched brass nob on the top of the breaker rod was set so as to position the breaker under the bulbs. About 1500 grams of conductivity water in a volumetric flask were weighed to the nearest milligram on a two kilogram analytical balance. The water was transferred to the Dewar flask, which was immediately bolted into place. The volumetric flask was reweighed and the weight of water obtained by difference. The calorimeter was lowered into the water bath, the electrical connections were made and stirring was begun. Switch (14-S_3) was closed to begin passing current through a 100 ohm dummy heater (14-R_d) to stabilize the battery current. The calorimeter was brought to the desired temperature either by passing cold water through the cooling coil or by electrical heating. The initial temperature was chosen so that the convergence temperature of the system would lie midway between the initial and final temperatures, thus reducing the amount of the heat leakage correction. The calorimeter was allowed to equilibrate for 15 to 30 minutes before measurements were begun.

Electrical calibration experiments were made before and after each solution experiment. A complete run consisted of four calibrations and three solution experiments. By measuring the temperature rise of the calorimeter due to a given

amount of electrical heating, the energy equivalent of the calorimeter was obtained. From the energy equivalent and the temperature rise, the heat evolved in a solution experiment could be obtained.

For an electrical calibration, readings of the temperature (in microvolts) were taken every 30 seconds for ten minutes to obtain a fore slope, $\underline{g_i}$. On a half minute interval the calorimeter heater (14-R_h) was placed in the battery circuit by closing switch (14-S_2). This switching action simultaneously turned on an electronic timer and opened switch (14-S_1), removing the dummy heater from the circuit. A second operator took readings of the potential across a 0.1 ohm standard resistor (14-R'_s) connected in series with the calorimeter heater. The first operator continued to follow the temperature of the calorimeter during the five minute heating period. After the switch (14-S_2) was opened to end the heating, readings were taken until the calorimeter temperature assumed a steady decrease or increase, depending upon whether the final temperature was above or below the convergence temperature. Measurements were then continued for ten minutes to obtain an after slope, $\underline{g_f}$.

A solution experiment was conducted in a very similar way. After the ten minute fore slope was taken, the sample bulb was broken. In this case the period of temperature rise lasted 10 to 20 minutes. The after slope was usually followed for a somewhat longer period of time to insure that the

system had come to equilibrium.

D. Theory of the Isothermal Calorimeter

The following outline of the evaluation of heat leakage correction was taken from the works of Coops, Van Ness, Kentie and Kienske (35), King and Grover (36), and Jessup (37). For a more complete derivation, the reader is referred to the original articles.

If an amount of heat is evolved in the calorimeter between an initial time, t_i, and a final time, t_f, a rise in temperature, $\theta_f - \theta_i$, is observed. The heat developed to cause the temperature change can be divided into

$$W(\theta_f - \theta_i) = Q_e + Q_r + Q_s + Q_t \quad , \tag{115}$$

where W = energy equivalent of the calorimeter,

Q_e = electrical or chemical energy,

Q_r = heat exchanged with the surroundings,

Q_s = heat due to stirring,

Q_t = heat liberated by passing current through the thermometer,

and where second order correction terms have been neglected. Since the stirring and thermometer current were kept constant during all the experiments, it was assumed that their contributions were effectively cancelled by calibration. This leaves the heat exchange with the surroundings to be evaluated.

During the steady state period, the change in the calorimeter temperature depends upon the difference between

the calorimeter temperature, θ, and the jacket temperature, θ_j, and is given by

$$\frac{d\theta}{dt} = g - G(\theta - \theta_j) \quad , \tag{116}$$

where g and G are constants and higher terms have been neglected. We define a convergence temperature, θ_k, for the calorimeter such that

$$\frac{d\theta}{dt} = - G(\theta - \theta_k) \quad . \tag{117}$$

During an experiment,

$$\theta_t = (\theta_f - \theta_i) + \theta_c \quad , \tag{118}$$

where θ_t = true temperature rise,

$\theta_f - \theta_i$ = observed temperature rise,

and θ_c = correction term for heat exchanged with the surroundings.

The correction term is found by integration of equation (117),

$$\theta_c = - \int_{t_i}^{t_f} G(\theta - \theta_k)\, dt. \tag{119}$$

To evaluate this integral, the temperature must be known as a function of time.

During an electrical heating the temperature rise is linear and the temperature can be expressed by

$$\theta = a + bt \quad . \tag{120}$$

The slope, b, is

$$b = \frac{\theta_f - \theta_i}{t_f - t_i} \quad , \tag{121}$$

and the constant $\underline{a}$ can be evaluated by choosing $\theta = \theta_f$ at $t = t_f$, that is,

$$\theta_f = \frac{\theta_f - \theta_i}{t_f - t_i} \; t_f + a \quad , \tag{122}$$

which gives

$$a = \frac{\theta_f \; (t_f - t_i) - (\theta_f - \theta_i) \; t_f}{t_f - t_i} \quad . \tag{123}$$

Equation (120) now becomes

$$\theta = \frac{\theta_f - \theta_i}{t_f - t_i} \; t + \frac{\theta_f \; (t_f - t_i) - (\theta_f - \theta_i) \; t_f}{t_f - t_i} \quad . \tag{124}$$

Using this function of $\underline{\theta}$ in equation (119) and performing the integration, one obtains for the correction term

$$\theta_c = - G \; (t_f - t_i) \left[\frac{\theta_f + \theta_i}{2} \quad - \theta_k \right] \quad . \tag{125}$$

The cooling constant $\underline{G}$ and the convergence temperature, $\underline{\theta_k}$, are evaluated from the fore slope and the after slope by equation (117). For the fore slope,

$$\left(\frac{d\theta}{dt}\right)'_{\theta_i} = g_i = - G \; (\theta_i - \theta_k) \tag{126}$$

and for the after slope,

$$\left(\frac{d\theta}{dt}\right)''_{\theta_f} = g_f = - G \; (\theta_f - \theta_k) \quad . \tag{127}$$

Solving these two equations simultaneously,

$$G = \frac{g_i - g_f}{\theta_f - \theta_i} \tag{128}$$

and

$$\theta_k = \frac{g_i\theta_f - g_f\theta_i}{g_i - g_f} \quad . \tag{129}$$

For a solution experiment, the temperature rise is not linear and the method of Dickinson (93) was used, in modification form, to evaluate the integral of the correction term. Equation (119) is evaluated by choosing a time, t_x, such that

$$G\int_{t_i}^{t_f} (\theta - \theta_k)\, dt = G\int_{t_i}^{t_x} (\theta - \theta_k)\, dt + G\int_{t_x}^{t_f} (\theta - \theta_k)\, dt \quad . \tag{130}$$

This condition is satisfied if, on a time versus temperature plot, the area between the curve, the extension of the fore slope and the line $\theta = t_x$ equals the area between the curve, the extension of the after slope and the line $\theta = t_x$.

Dickinson assumed the temperature rise to be exponential, in which case θ_x, the temperature at time t_x, equals $0.63\ (\theta_f - \theta_i)$. The solution experiments of this work did not give true exponential heat rises, so the time t_x was found by choosing it such that the area under and over the curve were equal. The correction term is given by

$$\theta_c = -\left[g_i(t_x - t_i) + g_f(t_f - t_x)\right] \quad . \tag{131}$$

E. Treatment of Data

The amount of heat liberated during a calibration experiment was calculated by

$$q_{el} = \frac{1}{4.184} \frac{R_h}{R_s^2} \int_0^t E_s^2 \, dt \qquad (132)$$

where q_{el} = electrical energy in defined calories,

R_h = heater resistance,

R_s = standard resistance,

E_s = potential across standard resistor,

t = time in seconds.

To evaluate the integral, a plot of E_s versus t was made and chords were drawn through the points. The midpoints of the chords were taken as the average potential for the time interval of the chords. The products $E_s^2 \Delta t$ for the chords were summed to obtain the total value for the integral.

To evaluate the temperature rise and the heat leakage correction, plots of E versus t were made. The slopes g_i and g_f were taken from the fore and the after periods. For a calibration experiment, the times t_i and t_f were taken from the graph at the intersections of the extrapolated lines of the fore period, the heating period and the after period. For a solution experiment, t_i, was taken as the time the bulb was broken and t_f as the time the calorimeter first reached a steady state in the after period. The thermometer potentials corresponding to these times were calculated from the slopes

and one temperature from the linear portions of the fore and the after periods.

The true temperature rise was calculated in terms of the change of the thermometer potential, ΔE_t, as described in the preceding section. At this point the change in thermometer potential was converted to the change in temperature, ΔT_t, by means of the thermometer equation. The energy equivalents, W_n, were determined from the calibration experiments according to

$$W = \frac{Q_{el}}{\Delta T_t} \tag{133}$$

The change in the energy equivalent between calibrations, ΔW_n, was a measure of the change in heat capacity for the reaction, i.e., the dissolution of salt.

To smooth the energy equivalent data, the values of ΔW_n for each solution experiment were plotted against the molalities of the final solutions and the best straight line was drawn through the points. Smoothed values of $\Delta W_n'$ were taken from the line and were added to the energy equivalents, W_n. The sum of these values was averaged to give a smoothed average value, W_o'', for the initial energy equivalent. The values of $\Delta W_n'$ were then successively subtracted from W_o'' to give final smoothed values, W_n'', for the energy equivalents.

The heat evolved in a solution experiment, q_i, was calculated by the formula

$$q_i = W_F \cdot \Delta T_t \quad . \tag{134}$$

The final energy equivalent of the calorimeter after the solution experiment, W_F, was used to calculate the heat and the temperature of the reaction was assigned as the initial temperature, T_i . Of the three combinations recommended by Rossini (94), the above assignment of energy equivalent and temperature was the simplest to apply to this work. The term to correct the experimental data to 25° C was calculated from the change in heat capacity during the experiment and the difference in the initial temperature from 25° C, that is,

$$\Delta q_i = (W_I - W_F)\ (T^{25} - T_i) \quad . \tag{135}$$

Then the heat of the reaction at 25° C is given by

$$q_i^{25} = q_i + \Delta q_i \quad . \tag{136}$$

The integral heat of solution, Q_M, is

$$Q_M = \frac{\sum q_i^{25}}{\sum n_i} \quad , \tag{137}$$

where n_i = moles of salt dissolved in a given experiment to give a final molality of m_i.

The final molality of the salt (on an anhydrous basis) was calculated from the formula

$$m_i = \frac{\sum n_i}{X + x_i} \tag{138}$$

where X = the weight of water originally added to the calorimeter,

and x_i = the water contributed to the solution when n_i moles of hydrated salt is dissolved.

Solutions, instead of water, were used at the beginning of some runs in order to attain higher final molalities. In these cases, a q_o^{25} was found from

$$q_o^{25} = \frac{Q_{M(m_o)}}{n_o} \quad . \tag{139}$$

The $Q_{M(m_o)}$ was taken from a plot of Q_M versus $m^{\frac{1}{2}}$ at the molality m_o. n_o was calculated to equal the moles of hydrated salt which needed to be added to X grams of water to give X_o grams of a solution having a molality m_o. Then the relation used to calculate integral heats of solution for the experiment became

$$Q_M = \frac{q_o^{25} + \sum q_i^{25}}{n_o + \sum n_i} \quad . \tag{140}$$

F. Results

The data and results of the heat of solution experiments are given in Table 19. All the symbols used have been previously defined. The heat quantities are given in defined calories. As can be seen, runs number two and five were made into solutions. To obtain an empirical expression for the experimental data, the least squares treatment was applied to an equation of the form

$$Q_M = a + bm^{\frac{1}{2}} + cm + dm^{3/2} \quad , \tag{141}$$

in which the constant b was given the Debye-Huckel limiting

Table 19. Heats of solution of neodymium chloride hexahydrate in water at 25° C.

Run	$m^{\frac{1}{2}}$	W_n''	ΔT_t	Δq_1	q_1^{25}	n_1	Q_M	ϕ_L [a]
1		1644.5						
	0.1225	1640.8	0.11599	0.09	190.40	0.022517	8456	644
2		1635.2						
	0.1284	1631.2	0.12675	0.46	207.22	0.024548	8441	658
	0.1885	1626.6	0.14086	0.04	229.17	0.028436	8236	863
	0.2327	1622.2	0.13646	0.04	221.40	0.027928	8130	969
3	0.2228	1664.9			622.70	0.076241	8168	
	0.2593	1660.8	0.12524	0.10	208.09	0.026482	8088	1011
	0.2926	1656.3	0.13399	0.05	221.97	0.028319	8034	1066
4		1634.3						
	0.1401	1629.7	0.15208	0.11	247.95	0.029291	8465	635
	0.1954	1625.0	0.13831	0.19	224.95	0.027791	8285	815
	0.2419	1620.0	0.14824	0.18	240.33	0.030548	8139	961
5	0.2628	1622.71			830.12	0.102776	8077	
	0.2957	1620.98	0.13160	0.06	213.38	0.130358	8005	1095
	0.3207	1619.47	0.10909	0.05	176.72	0.153599	7944	1156
	0.3479	1617.48	0.12960	0.07	209.69	0.181068	7897	1203

[a] Calculated using Q_M = 9100 at m = 0.

slope value of -6925. The equation for the integral heats of solution was

$$Q_M = 9103 - 6925\ m^{\frac{1}{2}} + 17987\ m - 24509\ m^{3/2} \qquad (142)$$

The curve defined by equation (142) has an inflection point at about $m^{\frac{1}{2}} = 0.3$, which causes it to deviate from the last two experimental points. However, the fit at the lower concentrations is quite good. Since the relative apparent molal heat content can be obtained by subtracting the integral heat of solution at a given molality from its value at infinite dilution, the equation for $\underline{\phi_L}$ is

$$\phi_L = 6925\ m^{\frac{1}{2}} - 17987\ m + 24509\ m^{3/2} \quad . \qquad (143)$$

In Figure 15 the values of the relative apparent molal heat content, $\underline{\phi_L}$, and of the integral heat of solution, $\underline{Q_M}$, are plotted against $\underline{m^{\frac{1}{2}}}$. To avoid confusion on the graph, a limiting heat of solution of 9100 was used to calculate the $\underline{\phi_L}$ values. The data from this work are compared to the curves obtained by Spedding and Miller (22) and by Naumann (26). This shows that the data is in agreement with that of Naumann. The fact that the experimental points from this work lie almost exactly on Naumann's curve should, however, be considered in the light of the following error analysis.

G. Error Analysis

The method of propagation of precision indexes, which has been described previously, was used to estimate the un-

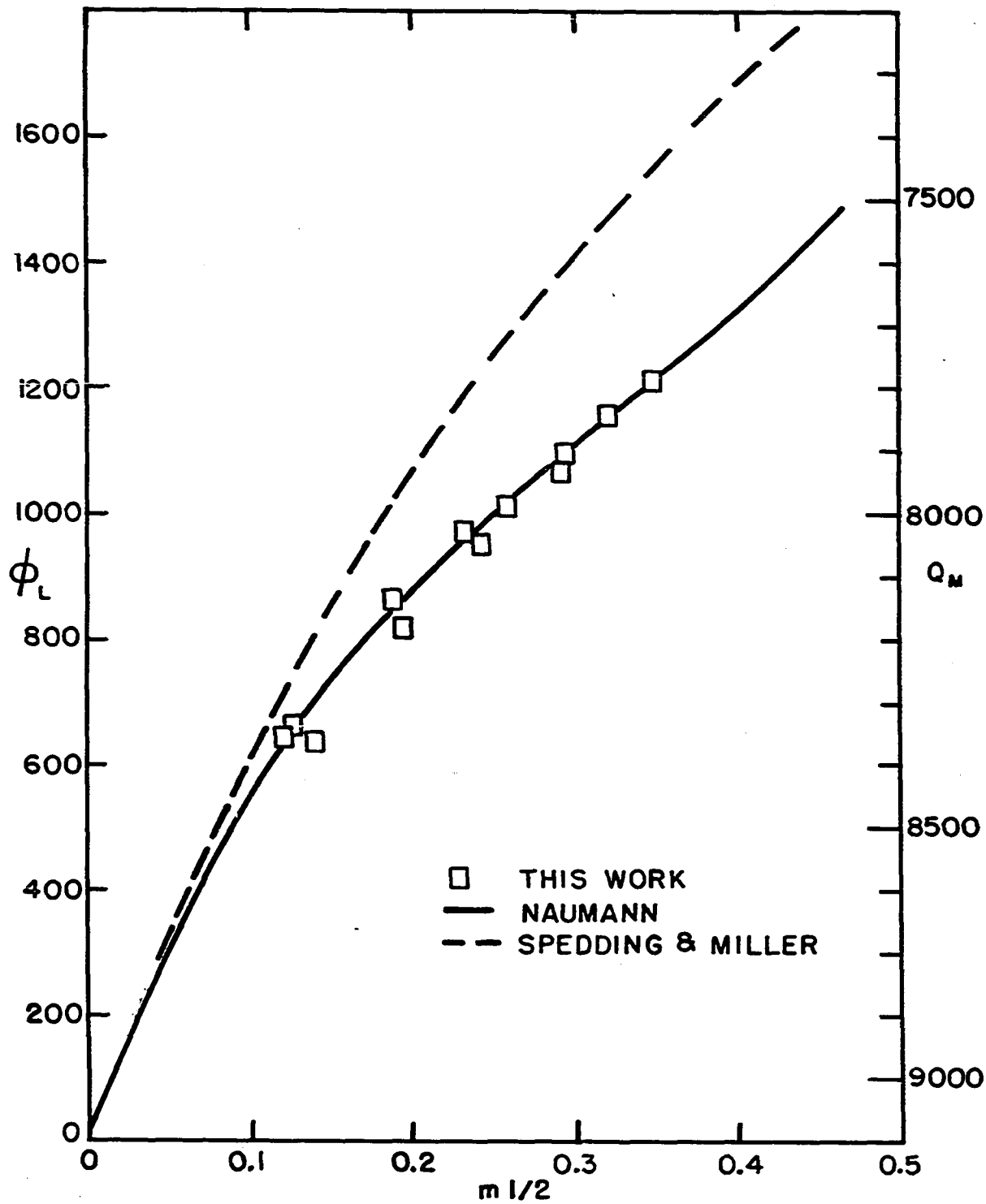

Figure 15. Relative apparent molal heat contents of neodymium chloride solutions at 25° C and integral heats of solution of $NdCl_3 \cdot 6H_2O$.

certainties in the integral heats of solution. The probable error in $\underline{Q_M}$ was derived from the following equations:

$$Q_M = \frac{q_o + \sum q_i}{n_o + \sum n_i} \quad , \tag{140}$$

$$q_i = W \cdot \Delta T_c + W \cdot \Delta T^{25} \quad , \tag{136}$$

$$W = \frac{Q_{el}}{\Delta T_c} \quad , \tag{133}$$

$$Q_{el} = \frac{1}{4.184} \frac{R_h}{R_s^2} E_s^2 t \quad . \tag{132}$$

The probable error in the energy equivalent, as derived from equation (133), was 0.2 calories/degree. However, it was known from the experiments that the error in $\underline{W}$ was about four calories/degree and this value was used. This difference arises from the fact that the dependence of the energy equivalent on the temperature of the experiment is not expressed in equation (133) .

The uncertainty in the values obtained for $\underline{Q_M}$ are summarized in Table 20. The error analysis showed that practically all the error in $\underline{Q_M}$ arises from the uncertainty in the energy equivalent.

The probable error in the constant $\underline{a}$ of equation (142) was calculated as 50 calories. Coupling this uncertainty with that in the value of $\underline{Q_M}$, the uncertainty in the values of $\underline{\phi_L}$ range from about 65 to 85 calories over the concentration range covered.

Table 20. Summary of error analysis.

Experimental point	Approx. $\bar{m^2}$	Probable error in n_i [a]	Probable error in q_i [b]	Probable error in Q_M [b]
1st sample into water	0.13	0.3	2	14
3re sample into water	0.24	0.5	6	21
Solution used	0.24	5.0	6	
1st sample into solution	0.27	5.3	8	25
3rd sample into solution	0.35	5.9	12	35

[a] n_i given in moles x 10^5.

[b] q_i and Q_M given in defined calories.

VI. DISCUSSION

Curves for the relative apparent molal heat contents of six rare-earth salt solutions are compared to theoretical predictions in Figure 16. The Debye-Huckel limiting law is represented as a dashed line, the extended Debye-Huckel law with $a^o = 5.7$ and $da^o/dT = 0$ as alternate dots and dashes, and the extended law with $a^o = 4.5$ and $da^o/dT = 0$ as a dotted line. The $\underline{a}^o$ values of 5.7 and 4.5 are averages of the mean distance of closest approach for rare-earth chlorides (15) and nitrates (19) respectively. The curve for neodymium chloride was taken from the work of Naumann (26); that for erbium chloride from the data of Naumann as revised in the appendix to this report.

The curves for the relative apparent molal heat contents fall in a regular order for the rare-earth chlorides. As might be expected, the $\underline{\phi}_L$'s show only a slight specificity for the various members. The crossing of the curves above $m^{\frac{1}{2}} = 0.4$ is a property of the empirical expressions and not of the experimental data. The experimental values for lanthanum and neodymium chlorides follow the theoretical curve only up to about 0.0005 molal. The values for erbium and ytterbium chlorides do not agree with the theory; in the very dilute concentration range the $\underline{\phi}_L$ curves for these salts have negative, instead of positive, slopes.

While the nitrate salts do show a slightly greater de-

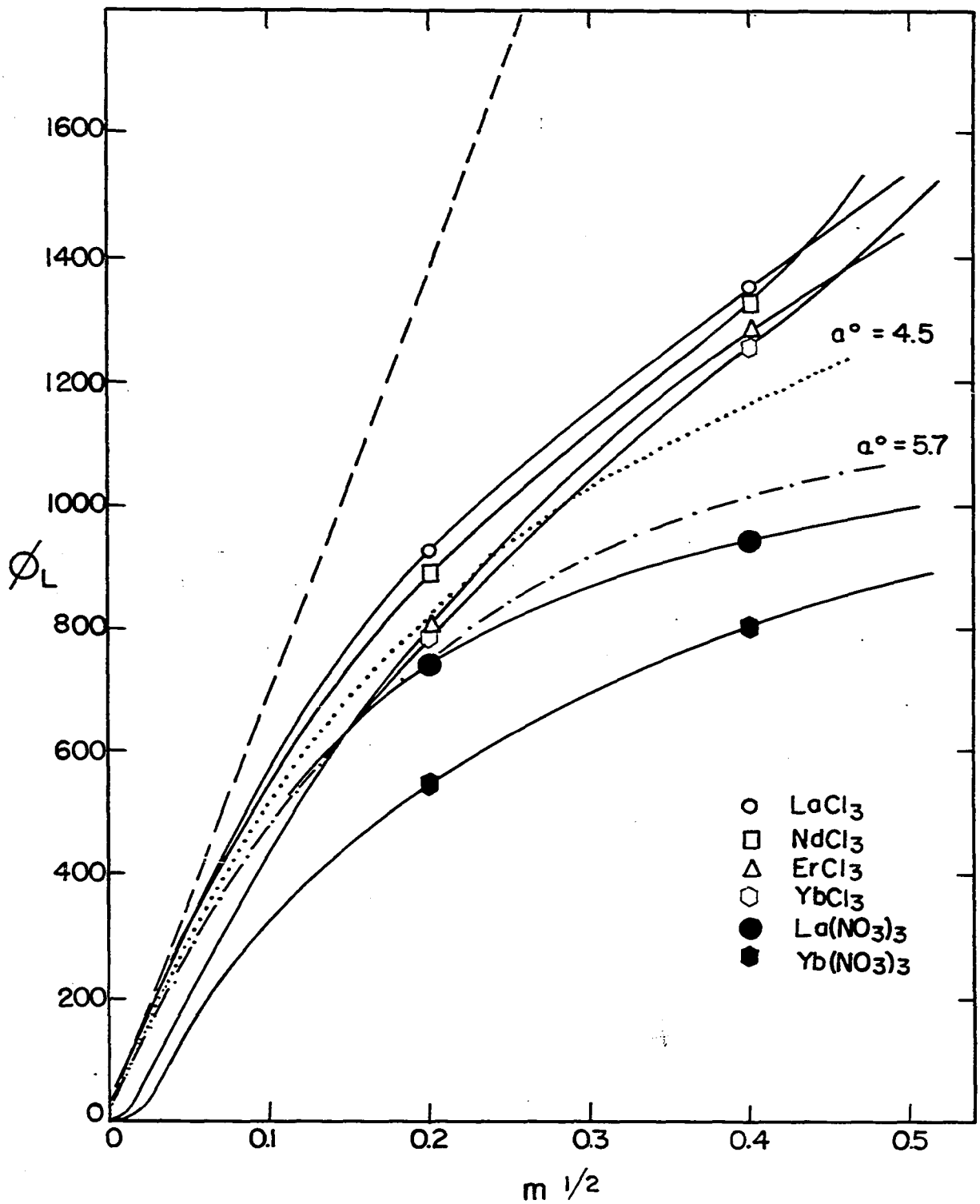

Figure 16. Relative apparent molal heat contents of rare-earth salt solutions at 25° C.

gree of specificity in $\underline{\phi_L}$, they seem to be approaching one another at higher concentrations. This is just the opposite of what has been observed for lower valence type salts, where the nitrate data tend to fan out as the concentration increases. The lanthanum nitrate data follow the theoretical curve up to about 0.005 molal; the curve for ytterbium nitrate is not in agreement with the theory. The nitrate curves lie below those for the chlorides, which is just the opposite of what would be expected from the a° values.

The short chord data for erbium chloride, ytterbium chloride and ytterbium nitrate exhibit maxima at about $m^{\frac{1}{2}} = 0.045$, dipping away from the theoretical value at lower concentrations. The behavior of these salts is unique, although the data of Lange and Miederer (30) for lanthanum ferricyanide might also show this behavior if analyzed in terms of the short-chord method. As was remarked earlier, the bivalent sulfates also have a maxima in $\underline{\overline{P}_i}$, but in these cases the values are approaching the theoretical value for the most dilute concentrations. While there is a possibility that the short chord data for these rare-earth salts may contain a minima, as well as the maxima, there is no evidence to indicate that this is the case.

An explanation of the short chord data for these salts must be somewhat tentative with the limited data that are available. Their anomalous behavior in the very dilute concentration range may be due to changes in the species present

in solution when the sample solution is diluted. To explain the data, the species formed would probably have to be some type of polymeric aggregate. This possibility is brought out by the pH data listed in Table 2. The very dilute solutions resulting from the dilution of the less concentrated sample solutions had pH's which approached or exceeded that of the water used, i.e., about 5.4 to 5.8 pH units. The fact that the pH's could exceed that of the water used is explained below. Atthese pH's hydrolysis can occur. The fact that the lanthanum and neodymium salts do not show the anomalous behavior can be attributed to their hydroxides being slightly more soluble.

Kendall (95) has pointed out that pure conductivity water, in equilibrium with air, has a pH of 5.7 to 5.8 due to the buffering action of the carbon dioxide present in the air. The fact that the water used in these experiments had a pH of 5.4 to 5.6 is undoubtedly due to the absorption of minute amounts of acid fumes which were present in the laboratory. Thus this water can be represented by

$$H_2O\ (lab) = H_2O + H^+ + OH^- + H_2CO_3 + H^+ + X^- \qquad (144)$$

$$H_2CO_3 \rightleftharpoons H^+ + HCO_3^- \rightleftharpoons 2H^+ + CO_3^=$$

where the H^+ and X^- are formed from the adsorbed acid. The rare earths are known to hydrolyse to some extent, so their solutions can be represented by

$$RCl_3\ (soln) = R^{+3}\ (aq) + Cl^-\ (aq) + R(OH)_n^{+3-n} + nH^+ \quad (145)$$

When the solution and the water are mixed

$$R(OH)_n^{+3-n} + H^+ + X^- \longrightarrow R^{+3} + X^- + H_2O \quad . \quad (146)$$

This last reaction would tend to raise the pH of the water to its CO_2 saturated value of 5.8.

Since the water used in the calorimetric measurements did contain dissolved carbon dioxide and hence carbonate ions, the possibility of a carbonate complex with the rare-earth ion must also be considered. In the very dilute solutions the concentrations of the rare-earth ion and the bicarbonate ion are of the same order of magnitude. With the rare-earth carbonates being insoluble, colloidal particles might be formed.

The possibility of polymeric aggregates being present in very dilute solutions is further confirmed by the work of Schweitzer and Jackson (96, 97) on radiocolloids. There is, however, some question as to whether the colloids they observe, at concentrations where the solubility product is not exceeded, may not be due to the radioactive tracers used in their work.

While the data reported here for the erbium and ytterbium salts are not in agreement with the predictions of the Debye-Huckel theory, it is not to be implied that the theory is at fault. Instead, the incomplete knowledge of the species present in solution is to be blamed. At the present time, however, it is a very formidable task, if not an impossible

one, to characterize the species present in the concentration range of interest.

Figure 15 shows conclusively that the $\underline{\phi_L}$ values for neodymium chloride obtained from the integral heats of solution of the hydrated salt are in agreement with the data of Naumann. The apparatus, procedure and method of calculation used in this work were similar to those used by Spedding and Miller, who calculated their $\underline{\phi_L}$ values from the integral heats of solution of the anhydrous salt. To agree with the data of Naumann, their heats of solution would have to be off by progressively larger amounts, reaching about 300 calories difference at $m^{\frac{1}{2}} = 0.3$. It should be noted that the integral heats of solution of the anhydrous salts are about 36,000 calories per mole and thus their data would need to be in error by about one per cent at the above concentration. It should also be remembered that the integral heat of solution is a function of the sum of the various experimentally determined heats and thus any error would tend to build up.

There are two possible explanations for the discrepancy in the data of Spedding and Miller. The first is based on the possibility of some slow-type reaction which might accompany the dissolution of the anhydrous salt. It is conceivable that the last chloride ion is held very energetically by the rare earth ion when the salt dissociates upon dissolution. If such were the case, the rare earth ion would be incompletely hydrated, in that one of the water molecules

in the hydration sphere would be replaced by the chloride ion. If the dissociation of the final chloride from the rare earth ion were to take the form of a slow reaction, the heat evolved by the reaction would not have been detected.

A second possibility involves the pH of the final solution. Spedding and Miller (98) have reported that their solutions had pH's of 6.3 to 6.6. At these high pH's the possibility of a hydrolysis reaction is ever present and the formation of a rare-earth hydroxide complex would be an endothermic reaction.

The data for this thesis were collected for salts of lanthanum and ytterbium, which lie at opposite ends of the rare-earth series. It would be of interest to measure heats of dilution for salts of the members near the middle of the series in order to determine just where and how abruptly the anomalous behavior in the very dilute concentration range begins to manifest itself. The fact that definite conclusions could not be reached from the data presented brings out what the author considers the most pressing need in the field of electrolytic solutions, that is, a method for determining just what species are present in the solutions.

VII. SUMMARY

An adiabatically jacketed differential calorimeter, with a sensitivity of about 5×10^{-4} calories per millimeter pen displacement of a recording potentiometer, was used to measure the heats of dilution of solutions of lanthanum chloride, ytterbium chlordie, lanthanum nitrate and ytterbium nitrate. The heats of dilution, which ranged from about 0.05 to 2.0 calories, were measured to within a few thousandths of a calorie. Empirical expressions were derived for the relative apparent molal heat content of solute, $\underline{\phi_L}$; the relative partial molal heat content of solvent, $\underline{\bar{L}_1}$; and the relative partial molal heat content of solute, $\underline{\bar{L}_2}$.

The "short-chord" method of treating the heat of dilution data was used for the very dilute concentration range. This treatment yielded limiting equations for the concentration dependence of $\underline{\bar{P}_i}$, which is the slope of a $\underline{\phi_L}$ versus $\underline{m^{\frac{1}{2}}}$ plot. Lanthanum chloride and nitrate gave limiting slopes of 6630 and 6230 respectively, compared to the theoretical limiting slope of 6925 as predicted by the Debye-Huckel interionic attraction theory. However, the ytterbium salts showed anomalous behavior in that the plot of $\underline{\bar{P}_i}$ versus $\underline{m^{\frac{1}{2}}}$ exhibited a maximum at about $m^{\frac{1}{2}} = 0.045$, dipping away from the theoretical limiting value below this concentration. The limiting slope was 247 for ytterbium chloride and -1393 for ytterbium nitrate. The anomalous behavior has been tentatively

explained by the presence of some polymeric type species which form when the sample solution is diluted.

The empirical expressions which were derived for the thermodynamic properties of the salts were as follows:

I. $LaCl_3$ - $\phi_L = 6925\ m^{\frac{1}{2}} - 14575 + 14178\ m^{3/2}$ (91)

$\bar{L}_i = -62.36\ m^{3/2} + 262.47\ m^2 - 382.98\ m^{5/2}$ (93)

$\bar{L}_2 = 10388\ m^{\frac{1}{2}} - 29150\ m + 35445\ m^{3/2}$ (92)

II. $YbCl_3$ - $\phi_L = 4783\ m^{\frac{1}{2}} - 5122\ m + 2644\ m^{3/2}$ (99)

$\bar{L}_1 = -43.09\ m^{3/2} + 92.278\ m^2 - 71.451\ m^{5/2}$ (101)

$\bar{L}_2 = 7175\ m^{\frac{1}{2}} - 10244\ m + 6610\ m^{3/2}$ (100)

III. $La(NO_3)_3$ - $\phi_L = 6206\ m^{\frac{1}{2}} - 15180\ m + 13735\ m^{3/2}$ (105)

$\bar{L}_1 = -55.90\ m^{3/2} + 273.48\ m^2 - 371.17\ m^{5/2}$ (107)

$\bar{L}_2 = 9309\ m^{\frac{1}{2}} - 30360\ m + 34337\ m^{3/2}$ (106)

IV. $Yb(NO_3)_3$ - $\phi_L = 3696\ m^{\frac{1}{2}} - 5590.9\ m + 3468.7\ m^{3/2}$ (110)

$\bar{L}_1 = -33.29\ m^{3/2} + 100.73\ m^2 - 93.737\ m^{5/2}$ (112)

$\bar{L}_2 = 5544\ m^{\frac{1}{2}} - 11182\ m + 8671.7\ m^{3/2}$ (111)

Comparing the data to the predictions of the Debye-Hückel theory, it was found that the lanthanum salts began deviating from the theoretical curves at a concentration of about 0.001 molal. The ytterbium salts did not agree with the theory due to their anomalous behavior in the very dilute concentration range.

An isothermally-jacketed calorimeter, utilizing a transposed bridge type thermometer with a sensitivity of about

3.5×10^{-4} degrees per microvolt, was used to measure the heat of solution of neodymium chloride hexahydrate. From the values of the integral heats of solution at various molalities, the relative apparent molal heat content was calculated for the neodymium chloride in the solutions. The $\underline{\phi_L}$ values obtained in this way were essentially in agreement with those of Naumann (26).

Two possible explanations have been offered for the discrepancy in the $\underline{\phi_L}$ data of Spedding and Miller (22). The first is based on a slow type reaction which might accompany the dissolution of the anhydrous salt; the second depends upon the hydrolysis of the rare earth ion when the salt is dissolved.

VIII. LITERATURE CITED

1. Spedding, F. H., A. F. Voigt, E. M. Gladrow, and N. R. Sleight, J. Am. Chem. Soc., 69, 2777 (1947).

2. Spedding, F. H., A. F. Voigt, E. M. Gladrow, N. R. Sleight, J. E. Powell, J. M. Wright, T. A. Butler, and P. Figard, J. Am. Chem. Soc., 69, 2786 (1947).

3. Spedding, F. H., E. I. Fulmer, T. A. Butler, E. M. Gladrow, M. Gobush, P. E. Porter, J. E. Powell, and J. M. Wright, J. Am. Chem. Soc., 69, 2812 (1947).

4. Spedding, F. H., E. I. Fulmer, B. Ayers, T. A. Butler, J. Powell, A. D. Tevebaugh, and R. Thompson, J. Am. Chem. Soc., 70, 1671 (1948).

5. Spedding, F. H., E. I. Fulmer, T. A. Butler, and J. E. Powell, J. Am. Chem. Soc., 72, 2349 (1950).

6. Spedding, F. H., E. I. Fulmer, J. E. Powell, and T. A. Butler, J. Am. Chem. Soc., 72, 2354 (1950).

7. Spedding, F. H., and J. L. Dye, J. Am. Chem. Soc., 72, 5350 (1950).

8. Spedding, F. H., E. I. Fulmer, J. E. Powell, T. A. Butler, and I. S. Yaffe, J. Am. Chem. Soc., 73, 4840 (1951).

9. Spedding, F. H., and J. E. Powell, J. Am. Chem. Soc., 74, 856, 857 (1952).

10. Wheelwright, E. J., and F. H. Spedding, J. Am. Chem. Soc., 75, 2529 (1953).

11. Spedding, F. H., J. E. Powell, and E. J. Wheelwright, J. Am. Chem. Soc., 76, 612, 2557 (1954).

12. Spedding, F. H., and J. E. Powell, J. Am. Chem. Soc., 76, 2545, 2550 (1954).

13. Spedding, F. H., P. E. Porter, and J. M. Wright, J. Am. Chem. Soc., 74, 2055 (1952).

14. Spedding, F. H., and I. S. Yaffe, J. Am. Chem. Soc., 74, 4751 (1952).

15. Spedding, F. H., and J. L. Dye, J. Am. Chem. Soc., 76, 879 (1954).

16. Spedding, F. H., and G. Atkinson, Ames, Iowa. "Conductances, Transference Numbers and Activity Coefficients of Some Rare Earth Halides at 25°". Mimeo. rept. To be published in J. Am. Chem. Soc. circa 1958.

17. Spedding, F. H., and S. Jaffe, J. Am. Chem. Soc., 76, 884 (1954).

18. Heiser, D. J., "A Study of Thermodynamic Properties of Electrolytic Solutions of Rare Earths". Unpublished Ph. D. Dissertation, Ames, Iowa, Iowa State College Library, circa 1957. In preparation.

19. Spedding, F. H., and S. Jaffe, J. Am. Chem. Soc., 76, 882 (1954).

20. Spedding, F. H., P. E. Porter, and J. M. Wright, J. Am. Chem. Soc., 74, 2778 (1952).

21. Spedding, F. H., P. E. Porter, and J. M. Wright, J. Am. Chem. Soc., 74, 2781 (1952).

22. Spedding, F. H., and C. F. Miller, J. Am. Chem. Soc., 74, 3158 (1952).

23. Spedding, F. H., and J. P. Flynn, J. Am. Chem. Soc., 74, 1477 (1954).

24. Ayers, B. O., "Apparent and Partial Molal Volumes of Some Rare Earth Salts in Aqueous Solutions", Unpublished Ph. D. Dissertation, Ames, Iowa, Iowa State College Library, 1954.

25. Atkinson, Gordon, "Compressibilities of Some Rare Earth Nitrates and Chlorides in Aqueous Solution", Unpublished Ph. D. Dissertation, Ames, Iowa, Iowa State College Library, 1956.

26. Naumann, A. W., "Heats of Dilution and Related Thermodynamic Properties of Aqueous Neodymium Chloride and Erbium Chloride Solutions", Unpublished Ph. D. Dissertation, Ames, Iowa, Iowa State College Library, 1956.

27. Spedding, F. H. and G. Atkinson, Ames, Iowa. "Properties of Rare Earth Salts in Electrolytic Solutions" Paper presented at the Symposium on the Structure of Solutions sponsored by the Electrochemical Society and the National Science Foundation. Washington, D. C. May 13, 1957. To be published circa 1958.

28. Debye, P., and E. Hückel, Physik Z., 24, 185 (1923).

29. Nathan, C. C., W. E. Wallace and A. L. Robinson, J. Am. Chem. Soc., 65, 790 (1943).

30. Lange, E. and W. Miederer, Z. Electrochem., 60, 362 (1956).

31. White, W. P., "The Modern Calorimeter", The Chemical Catalog Company, Inc., New York, 1928.

32. Sturtevant, J. M., "Calorimetry", In Weissberger, A., editor, "Technique of Organic Chemistry", 2nd ed., Volume 1, Part 1, page 731. Interscience Publishers, Inc., New York, 1949.

33. Swietoslawski, W., "Microcalorimetry", Reinhold Publishing Corporation, New York, 1946.

34. Rossini, F. D., "Experimental Thermochemistry", Interscience Publishers, Inc., New York, 1956.

35. Coops, J., K. Van Nes, A. Kentie, and J. W. Dienske, Rec. trav. chim., 66, 113 (1947).

36. King, A., and H. Grover, J. Appl. Phys. 12, 557 (1941).

37. Jessup, R. S., J. Appl. Phys., 13, 128 (1942).

38. Arrhenius, S., Z. physik. Chem., 1, 631 (1887).

39. van't Hoff, J. H., Z. physik. Chem., 1, 481 (1887).

40. Harned, H. S., and B. B. Owen, "The Physical Chemistry of Electrolytic Solutions", 2nd ed., Reinhold Publishing Corporation, New York, 1950.

41. Kirkwood, J. G., J. Chem. Phys., 2, 767 (1934).

42. Fowler, H., and E. A. Guggenheim, "Statistical Thermodynamics, Cambridge University Press, Cambridge, England, 1949.

43. Bjerrum, N., Kgl. Danske. Videnskab. Selskab. Mat. fgs. Medd. 1, No. 9 (1926). (Original available but not translated; cited in Harned, H. S., and B. B. Owen, "The Physical Chemistry of Electrolytic Solutions", 2nd ed., p. 42., Reinhold Publishing Corporation, New York, 1950.

44. Fuoss, R. M., and C. A. Kraus, J. Am. Chem. Soc., 55, 1019 (1933); 55, 2387 (1933); 57, 1 (1935).

45. Robinson, R. A., and R. H. Stokes, J. Am. Chem. Soc., 70, 1870 (1949).

46. Robinson, R. A., and R. H. Stokes, "Electrolyte Solutions", Butterworth's Scientific Publications, London, 1955.

47. Glueckauf, E., Trans. Faraday Soc., 51, 1235 (1955).

48. Bjerrum, N., Trans. Faraday Soc., 23, 445 (1927).

49. Debye, P., and L. Pauling, J. Am. Chem. Soc., 47, 2129 (1925).

50. Hückel, E., Physik. Z., 26, 93 (1925).

51. Hasted, J. B., D. M. Ritson, and C. H. Colle, J. Chem. Phys., 16, 1 (1948).

52. Ritson, D. M., and J. B. Hasted, J. Chem. Phys., 16, 11 (1948).

53. Haggis, G. H., J. B. Hasted, and T. J. Buchanan, J. Chem. Phys., 20, 1452 (1952).

54. Bagchi, S. N., J. Indian Chem. Soc., 21, 199, 204 (1950).

55. Dutta, M., and S. N. Bagchi, Indian J. Phys. 24, 61 (1950).

56. Dutta, M., Proc. Nat. Inst. Sci. India, 19, 183 (1953).

57. Eigen, M., and E. Wicke, Naturwissenshaften, 38, 456 (1951).

58. Wicke, E., and M. Eigen, Z. Electrochem., 56, 551 (1952).

59. Wicke, E., and M. Eigen, Z. Naturforschg., 8a, 161 (1953).

60. Wicke, E., and M. Eigen, Z. Electrochem., 57, 140 (1953).

61. Eigen, M., and E. Wicke, J. Phys. Chem., 58, 702 (1954).

62. Lange, E., and K. Möhring, Z. Electrochem., 56, 927 (1952).

63. Müller, H., Physik. Z., 28, 324 (1927); 29, 78 (1928).

64. Gronwall, T. H., V. K. LaMer, and K. Sandved, Physik. Z., 29, 358 (1928).

65. LaMer, V. K., T. H. Gronwall, and L. J. Greiff, J. Phys. Chem., 35, 2245 (1931).

66. Güntelberg, E., Z. physik. Chem., 123, 199 (1926).

67. Onsager, L., Chem. Rev., 13, 73 (1933).

68. Mayer, J. E., J. Chem. Phys., 18, 1426 (1950).

69. Poirier, J. C., J. Chem. Phys., 21, 965, 972 (1953).

70. Bjerrum, N., Z. physik. Chem., 119, 145 (1926).

71. Scatchard, G., J. Am. Chem. Soc., 53, 2037 (1931).

72. Richards, T. W., and A. W. Rowe, J. Am. Chem. Soc., 42, 1621 (1920).

73. Richards, T. W., and A. W. Rowe, J. Am. Chem. Soc., 43, 770 (1921).

74. Nernst, W., and W. Orthmann, Sitzb. ber. preuss. Akad. Wiss., p. 51, (1926). (Original not available for examination; cited in Nernst, W., and W. Orthmann, Z. physik. Chem., 135, 199 (1928).

75. Nernst, W., and W. Orthmann, Sitzb. ber. preuss. Akad. Wiss., p. 136 (1926). (Original not available for examination; cited in Nernst, W., and W. Orthmann, Z. physik. Chem., 135, 199 (1928).

76. Nernst, W., and W. Orthmann, Z. physik. Chem., 135, 199 (1928).

77. Naude, S. M., Z. physik. Chem., 135, 209 (1928).

78. Nernst, W., Z. Electrochem., 33, 428 (1927).

79. Lange, E. W., and G. Messner, Z. Electrochem. 33, 431 (1927).

80. Lange, E. W., and A. L. Robinson, Chem. Rev., 9, 89 (1931).

81. Young, T. F. and O. G. Vogel, J. Am. Chem. Soc., 54, 3030 (1932).

82. Young, T. F., and W. L. Groener, J. Am. Chem. Soc., 58, 187 (1936).

83. Gulbransen, E. A., and A. L. Robinson, J. Am. Chem. Soc., 56, 2637 (1934).

84. Young, T. F., and P. Seligmann, J. Am. Chem. Soc., 60, 2379 (1938).

85. Gucker, F. T., Jr., H. B. Pickard, and R. W. Planck, J. Am. Chem. Soc., 61, 459 (1939).

86. Wallace, W. E., and A. L. Robinson, J. Am. Chem. Soc., 63, 1582 (1941).

87. Young, T. F., Sci., 85, 48 (1937).

88. Willard, H. H., and N. H. Furman, "Elementary Quantitative Analysis", 3rd ed., D. Van Nostrand Company, Inc., New York, 1940.

89. Worthing, A. G., and J. Geffner, "Treatment of Experimental Data", John Wiley and Sons, Inc., New York, 1943.

90. Maier, C. G., J. Am. Chem. Soc., 52, 2160 (1930).

91. Southard, J. C., J. Ind. Eng. Chem., 32, 442 (1940).

92. Maier, C. G., J. Phys. Chem., 34, 2860 (1930).

93. Dickinson, H. C., Bull. Natl. Bur. Standards (U. S.), 11, 189 (1915).

94. Rossini, F. D., "Introduction: General Principles of Modern Thermochemistry", In Rossini, F. D., editor, "Experimental Thermochemistry", page 1. Interscience Publishers, Inc., New York, 1956.

95. Kendall, J., J. Am. Chem. Soc., 38, 2460 (1916).

96. Schweitzer, G. K., and M. Jackson, J. Chem. Ed., 29, 513 (1952).

97. Schweitzer, G. K., and W. M. Jackson, J. Am. Chem. Soc., 74, 4178 (1952).

98. Spedding, F. H., and C. F. Miller, J. Am. Chem. Soc., 74, 4195 (1952).

IX. ACKNOWLEDGMENTS

The author wishes to express his appreciation to Dr. F. H. Spedding for his helpful advice during the course of this work and in the preparation of this thesis. The writer also wishes to acknowledge the work of Dr. A. W. Naumann who originally assembled the differential calorimeter, of Mr. D. A. Csejka for his assistance in measuring the heats of solution, and of the members of the Ames Laboratory who prepared and analyzed the rare-earth oxides. In addition, the author would like to thank his wife, Louise, for typing this manuscript.

X. APPENDIX

A. Relative Apparent Molal Heat Contents of Erbium Chloride in Aqueous Solutions

Naumann derived three equations to represent the concentration dependence of the short chord data for erbium chloride. These are analogous to equations (95), (96) and (97), which were listed in this report for ytterbium chloride. He used the linear equation with a negative slope to calculate the thermodynamic properties. In the light of the very similar results which were obtained in this work for ytterbium chloride, the data have been recalculated on the basis of his parabolic equation,

$$\phi_L = 465\ m^{\frac{1}{2}} + 1.2105 \times 10^5\ m - 0.9557 \times 10^6\ m^{3/2} \qquad (147)$$

for the very dilute concentration range. The method of calculating the relative apparent molal heat content was the same as that used for the ytterbium chloride data. The results of the recalculation are given in Table 21 and are plotted in Figure 17. In this figure, Naumann's original curve is represented by alternate dots and dashes. The equation derived for the concentration dependence of $\underline{\phi_L}$ was

$$\phi_L = 4952\ m^{\frac{1}{2}} - 5077\ m + 1926\ m^{3/2} \quad , \qquad (148)$$

and the curve for this expression is represented by the solid

line. The experimental points shown are for the $\underline{\phi_L}$ values as recalculated here. The various type circles represent solutions prepared by different methods.

Table 21. Relative apparent molal heat content of erbium chloride solutions at 25° C.

Soln. No.	$m_1^{\frac{1}{2}}$	$m_k^{\frac{1}{2}}$	$\phi_{L(m_k)}$	$-\Delta H_{1,k}$	$\phi_{L(m_1)}$	ϕ_L Derived	ϕ_L Eq. 148
2	0.1050	1.110	19	436	455	461	463
		1.561	33	434	467		
7	0.1214	1.283	24	475	499	501	526
		1.804	42	461	503		
9	0.1389	1.468	30	546	576	585	591
		2.064	53	540	593		
12A	0.1432	1.514	31	611	642	641	608
		2.129	56	583	639		
12	0.1436	1.518	32	599	631	630	608
		2.135	56	573	629		
3	0.1489	1.574	34	599	633	636	627
		2.214	59	579	638		
8A	0.2005	2.119	55	769	824	821	799
		2.980	96	722	818		
8	0.2013	2.127	56	781	837	829	801
		2.991	97	724	821		
4	0.2134	2.255	61	773	834	836	838
		3.172	106	732	838		
10	0.2726	2.880	91	915	1006	1004	1004
		4.050	154	848	1002		
5	0.3024	3.196	107	956	1063	1066	1078
		4.494	179	889	1068		
11	0.3818	4.034	153	1099	1252	1252	1247
		5.673	242	1010	1252		
6	0.4293	4.533	181	1171	1352	1352	1331
		6.375	274	1077	1352		

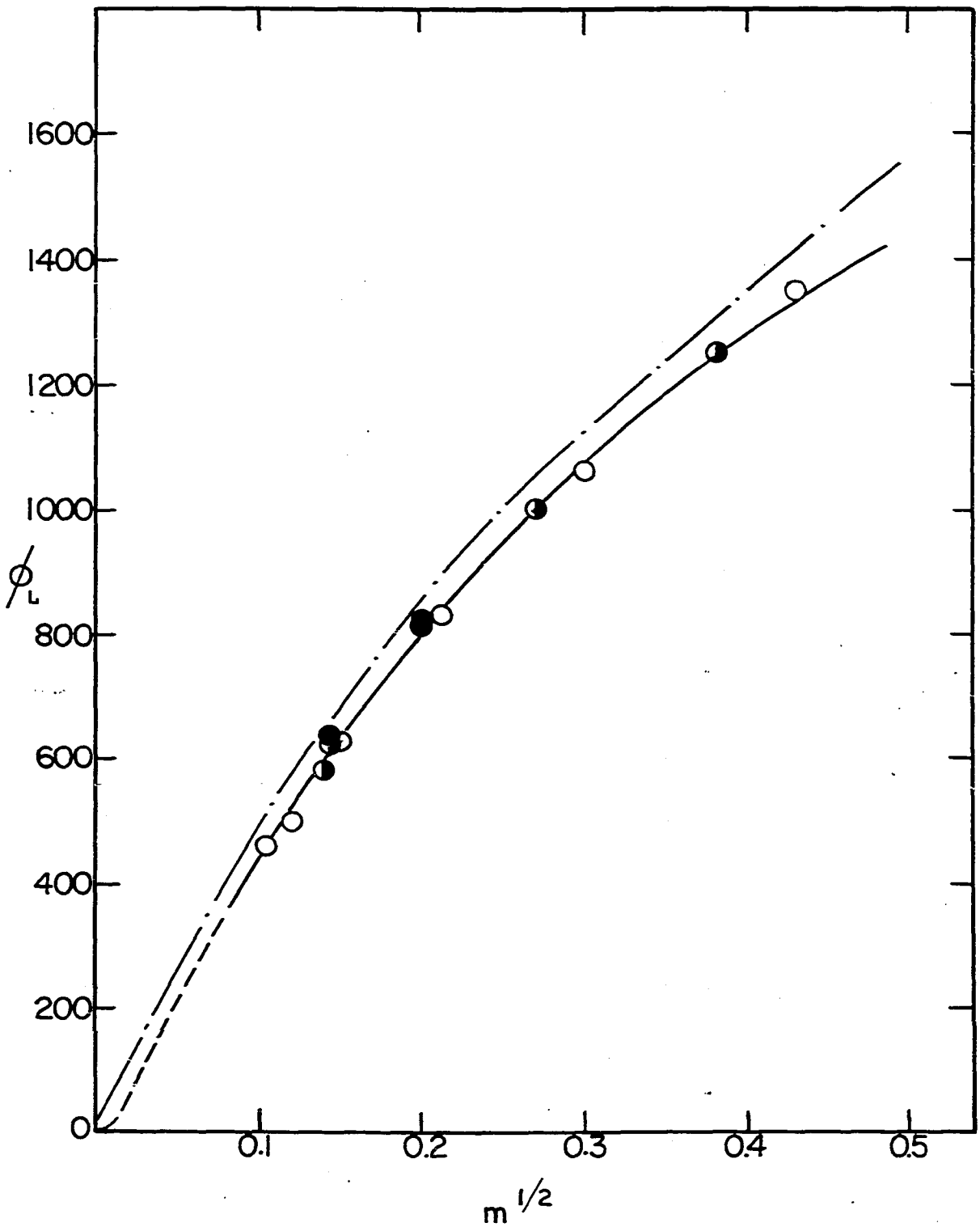

Figure 17. Relative apparent molal heat contents of erbium chloride solutions at 25° C.